APPENDIX A | INFORMATION QUALITY AND PEER REVIEW PROCEDURES

A.1 Ensuring Information Quality

The technical documentation, framework, underlying analyses, and associated R code were developed in accordance with EPA's Guidelines for Ensuring and Maximizing the Quality, Objectivity, Utility, and Integrity of Information Disseminated by the Environmental Protection Agency,[1] which follows Office of Management and Budget (OMB) guidelines[2] and implements the Information Quality Act (IQA) (Section 515 of Public Law 106–554).[3]

In accordance with OMB definitions, EPA defines the basic standard of information "quality" by its objectivity, integrity, utility, and transparency. For products meeting a higher standard of quality, like this product, the Agency requires an appropriate level of transparency regarding data and methods in order to facilitate the reproducibility of information by qualified third parties. The EPA uses various established Agency processes (e.g., the Quality System, peer review requirements and processes) to ensure the appropriate level of objectivity, utility, integrity, and transparency for its products, based on the intended use of the information and the resources available. Sections below describe how the technical documentation and associated R code meet each requirement.

Objectivity focuses on whether the disseminated information is being presented in an accurate, clear, complete, and unbiased manner, and as a matter of substance, is accurate, reliable, and unbiased. The technical documentation and associated R code meet this standard for objectivity, due to activities described in the following:

a) The information disseminated is determined to be complete, accurate, and reliable based on internal quality control measures adopted by the expert modeling teams. This includes quality checks throughout the chain of analytic steps, including developing and processing climate projections, calibrating and validating the sectoral impact models, and checking data to ensure that no errors occur in the process to compile and summarize results. The FrEDI R code package also includes a series of automatic quality control tests to ensure the code runs as expected and to flag changes to the FrEDI outputs relative to a benchmark run to assist in additional quality control review.

[1] EPA, 2002: Guidelines for ensuring and maximizing the quality, objectivity, utility, and integrity of information disseminated by the Environmental Protection Agency. United States Environmental Protection Agency, EPA/260R-02-008. Available online at http://www.epa.gov/quality/informationguidelines/documents/EPA_InfoQualityGuidelines.pdf

[2] OMB, 2002: Office of Management and Budget Information Quality Guidelines. Executive Office of the President, Office of Management and Budget. Available online at http://www.whitehouse.gov/sites/default/files/omb/inforeg/iqg_oct2002.pdf

[3] The IQA requires the Office of Management and Budget and federal agencies to issue guidelines that "ensur[e] and maximize[e] the quality, objectivity, utility, and integrity of information (including statistical information) disseminated by Federal agencies" (Public Law 106-554; 44 U.S.C. 3516, note). The IQA does not impose its own standard of "quality" on agency information; instead, it requires only that an agency "issue guidelines" ensuring data quality. Following guidelines issued by the Office of Management and Budget, EPA released its own guidelines to implement the IQA: "Guidelines for Ensuring and Maximizing the Quality, Objectivity, Utility, and Integrity of Information Disseminated by the Environmental Protection Agency."

b) The information disseminated is determined to be clear, complete, and unbiased based on multiple rounds of independent review. Consistent with guidelines described in EPA's Peer Review Handbook,[4] the underlying sectoral modeling methodologies are peer-reviewed through scientific journal publication processes. Citations for these publications can be found throughout the main technical documentation and its appendices. In addition, aspects of the FrEDI technical documentation and associated R package have also been subject to external journal publication processes (Sarofim et al., 2021, Hartin et al., 2023).
c) The FrEDI technical documentation and associated R code have been subject to both public review and external peer review. See Sections A.3 and A.4 for details about the peer and public reviews conducted in 2021 and 2024.

Integrity refers to security of information, such as the protection of information from unauthorized access or revision, to ensure that the information is not compromised through corruption or falsification. The technical documentation, framework, R code, and underlying analyses meet the standard for integrity due to the strategic steps taken to ensure that the data and information remained secure. These steps included the use of password protected data storage repositories, password protected data transfer technology, and multiple layers of data validation checks to ensure that the integrity was not compromised.

Utility is the usefulness of the information to the intended users. The technical documentation, framework, R code, and underlying analyses meet the standard for utility because the information disseminated provides insights (technical methods for quantifying physical and economic impacts) regarding the potential magnitude of the impacts of climate change. Understanding the risks posed by climate change can inform broader assessment reports and policy decisions designed to address these risks. See Chapter 1.2 of the technical documentation for a discussion of other example applications and intended uses.

Transparency ensures access to and description of (1) the source of the data, (2) the various assumptions employed, (3) the analytic methods applied, and (4) the statistical procedures used. The report and its underlying analyses meet the standard for transparency for the following reasons:

a) The underlying datasets, sectoral impact models, and the methods supporting the framework and associated R package have been published with open access in the peer-reviewed scientific literature and are cited throughout the report. These papers, along with their online supplementary materials, provide detailed information on the sources of data used, assumptions employed, the analytic and statistical methods applied, and important limitations regarding the approaches and/or how the results should be interpreted.
b) Appendix B for this Technical Documentation provides details on how results and output from each sectoral impact model (or impacts study) are formatted and adapted for usage in the framework and R code. This Appendix contains descriptions of the methodologies used in estimating impacts,

[4] EPA, 2015: Peer Review Handbook, 4th Edition, 2015. United States Environmental Protection Agency, Programs of the Office of the Science Advisor.

assumptions used, and citations to the underlying literature where the reader can go for more information.

c) The R package for FrEDI has been posted as a public repository on the USEPA GitHub website. Updates to the FrEDI R code are published as tagged releases, accompanied by release notes that summarize each update. See https://www.github.com/USEPA/FrEDI . Additional documentation on the R package components, as well as general information about downloading and running the FrEDI R package are posted on the following website: https://usepa.github.io/FrEDI.

d) The 2021 Technical Documentation was subject to a public comment period in 2021 to ensure interested stakeholders had a chance to review and provide input on the Framework and Tool methods. The 2024 Draft Technical Documentation is also subject to a public comment period.

e) Reponses to all comments received during the 2021 public comment period are publicly posted. See https://cfpub.epa.gov/si/. Search using the report title: *Technical Documentation on The Framework for Evaluating Damages and Impacts (FrEDI)*. Responses to the 2024 review period will be posted when completed.

f) Responses to all comments received during the 2021 independent, expert peer review have been posted on the report's website. See https://cfpub.epa.gov/si/. Search using the report title: *Technical Documentation on The Framework for Evaluating Damages and Impacts (FrEDI)*. During their review period, expert peer reviewers were provided a copy of all comments received from the public comment period. Responses to the 2024 review period will be posted when completed.

A.2 Consideration of Assessment Factors

When evaluating the quality, objectivity, and relevance of scientific and technical information, the considerations that EPA takes into account can be characterized by five general assessment factors, as found in *A Summary of General Assessment Factors for Evaluating the Quality of Scientific and Technical Information, and the Guidance for Evaluating and Documenting the Quality of Existing Scientific and Technical Information.*[5] The following section lays out how the assessment factors are considered to determine whether models and data in the technical documentation, framework, R code, and underlying analyses are acceptable for their intended use.

TABLE A-1. SUMMARY OF QUALITY ASSESSMENT FACTORS

Factor	Description	How the Factor was Considered
Soundness	The extent to which the scientific and technical procedures, measures, methods or models employed to generate	• Used publicly available (to the maximum extent practicable) data, reviewed for quality and accuracy with complete metadata available. • Used data included in peer-reviewed publications. Ensured evaluation of the scientific and technical procedures, measures, and methods employed to generate estimates produced by sectoral impact models.

[5] USEPA. 2003. A Summary of General Assessment Factors for Evaluating the Quality of Scientific and Technical Information, and the Guidance for Evaluating and Documenting the Quality of Existing Scientific and Technical Information. Science Policy Council U.S. Environmental Protection Agency Washington, DC. EPA 100/B-03/001

Factor	Description	How the Factor was Considered
	the information are reasonable for, and consistent with, the intended application.	• Considered the capabilities of integrated assessment, simple climate, and sectoral impacts models to examine changes in physical effects, economic damages, and changes in risk from climate change in a manner consistent with sound scientific theory and accepted approaches. • Considered the extent to which underlying models and data had been previously applied in projects of similar scope, such as the Climate change Impacts and Risk Analysis (CIRA) project. For example, the BenMAP model has been used in similar climate and health impact analyses, and the labor analysis has been employed in other multi-sector modeling projects (e.g., Hsiang et al. 2017). • Considered whether the data and code are available, made available by EPA, or determined to not be feasible as it is claimed as proprietary by a non-federal business. • Selected sectoral impacts models with the following criteria: sufficient understanding of how climate change affects the sector; the existence of data to support the methodologies; availability of modeling applications that could be applied in the FrEDI framework; based on peer reviewed literature and datasets; and the economic, iconic, or cultural significance of impacts and damages in the sector to the U.S.
Applicability and Utility	The extent to which the information is relevant for the Agency's intended use.	• Ensured that FrEDI uses applicable and relevant inputs and considers the capabilities of the integrated assessment, simple climate model, and sectoral impacts models to examine changes in physical effects, economic damages, and risk associated with climate change. • Ensured that FrEDI and its underlying analyses are relevant to their intended use so that the information disseminated provides insights and methods for quantifying the physical and economic impacts of climate change at national, regional, and state levels. • Ensured sectoral impacts models are reasonable for, and consistent with, the intended application by being sufficiently flexible to ensure consistency in inputs and monetizing physical impacts. • Ensured that models have been applied in peer-reviewed, published studies.
Clarity and Completeness	The degree of clarity and completeness with which the data, assumptions, methods, quality assurance, sponsoring organizations and analyses employed to generate the	• Ensured use of clear and complete inputs by considering the extent to which sectoral impacts models documented their key methods, assumptions, parameter values, limitations, sponsoring organizations/author affiliations, and funding information. • Ensured publications clearly and comprehensively describe analytic methods used and how they apply and build off existing bodies of research and underlying scientific and/or economic theories.

Factor	Description	How the Factor was Considered
	information are documented.	
Uncertainty and Variability	The extent to which the variability and uncertainty (quantitative and qualitative) in the information or in the procedures, measures, methods or models are evaluated and characterized.	• Ensured inputs that appropriately characterize uncertainty and variability by considering the capabilities of sectoral impacts models to evaluate and characterize key sources of variability and uncertainty. Results of these analyses are described in the underlying journal articles. • Reviewed the model documentation and peer-reviewed publications to determine if a model is sufficiently flexible and capable of evaluating important sources of uncertainty for climate change impacts analysis. • Documented outcomes of sensitivity and uncertainty analyses, where applicable, in the presentation of results using ranges and confidence intervals. • Addressed key sources of uncertainty by developing a flexible framework, as described in Chapter 2.
Evaluation and Review	The extent of independent verification, validation and peer review of the information or of the procedures, measures, methods or models.	• Ensured use of independently verified and validated inputs by considering the extent to which models have been independently peer reviewed. • Reviewed the documentation associated with each model and determined if they have been independently peer reviewed and published in scientific journals with procedures to ensure that the methods are technically supportable, properly documented, and consistent with established quality criteria. • Used scenarios and projections that have been independently verified and validated (e.g., scenarios and projections developed for the IPCC and its assessments, and then downscaled for the U.S. for used in the Fourth National Climate Assessment by the USGCRP Scenarios Working Group).

A.3 Review Process for the 2021 Technical Documentation

Consistent with guidelines described in EPA's Peer Review Handbook,[6,7] the 2021 Technical Documentation was subject to a public review comment period, and an independent, external expert peer review that concluded with the publication of the original Technical Documentation in October 2021. The peer and public review documentation is available at EPA's Science Inventory.

The 2021 Technical Documentation was subject to a public comment period to ensure that the information summarized by EPA was technically supported, competently performed, properly documented, consistent with established quality criteria, and communicated clearly. This public review period was also intended to provide feedback and comments on the framework's utility. Similarly, the purpose of the expert peer review by independent, qualified, and objective experts was to ensure that the information summarized by EPA was technically supported, competently performed, properly documented, consistent with established quality criteria, and communicated clearly. The sectoral impact models underlying the technical documentation, as well as the temperature binning approach used in the FrEDI framework were previously peer reviewed and published in the research literature.

Public Review Period

A 30-day public comment period was held from April 15th through May 17th, 2021. All comments received were carefully reviewed, considered, and responded to.

Expert Peer Review

The expert review was managed by a contractor (ICF International) under the direction of a designated independent EPA peer review leader, who prepared a peer review plan, the scope of work for the review contract, and the charge for the reviewers. Importantly, the EPA peer review leader played no role in producing any portion of the report. Reviewers worked individually (i.e., without contact with other reviewers, colleagues, or EPA) to prepare written comments in response to the charge questions. The reviewers were also provided with the public review comments for informational purposes.

The contractor identified, screened, and selected five reviewers who had no conflict of interest in performing the review, and who collectively met the technical selection criteria provided by EPA.

The peer review charge directed reviewers to provide responses to the following questions during the main review:

[6] EPA, 2015: Peer Review Handbook, 4th Edition, 2015. United States Environmental Protection Agency, Programs of the Office of the Science Advisor. Available online at https://www.epa.gov/osa/peer-review-handbook-4th-edition-2015

[7] EPA has determined that this report falls under the classification of "influential scientific information," as defined by OMB and further described in the EPA Peer Review Handbook. This product is for science dissemination and communication purposes only, and does not reflect analysis of nor recommendations regarding any particular policy.

1. Does the introductory chapter clearly explain the purpose of the report and provide appropriate context for the rest of the documentation? If not, please provide recommendations for improvement.
2. The report has been written for an educated and semi-technical audience. Are the writing level and graphics appropriate for these audiences?
3. Does the report adequately explain the overall analytic framework of the temperature binning approach?
4. Do the text, figures, and tables clearly communicate the framework's structure and design? Are the requirements for input data, and the options for output/results summaries, clearly stated?
5. Does the report clearly convey both the conceptual basis for temperature binning and the specific data processing and analytic steps taken to execute the concept? Is it clear how both the EPA-sponsored CIRA sector studies, and other non-CIRA studies, can be incorporated in the framework?
6. Is the sector-specific approach to account for the role of socioeconomic driver data clear? Is it reasonable and well-supported?
7. Is the approach to estimating sector-specific and aggregate economic impact (damages) of specified temperature trajectories reasonable and suitable for the stated purposes?
8. Does the report adequately inform the reader about how uncertainty is addressed in the framework, including how results should be interpreted and used given the limitations?
9. Has EPA objectively used, applied, and documented the underlying data of the temperature binning framework? Has the Agency appropriately described the sensitivity of the findings to analytic assumptions?
10. Is the draft technical documentation report missing important information based on your review of the report?
11. Report Format: Please comment on whether any aspects of the layout help or hinder the reader to understand the content and key messages of the report.

A.4 Review Process for the 2024 Technical Documentation

The 2024 Draft Technical Documentation is currently subject to a similar review process, including an independent, external peer review and a public comment period. Reviewers have been charged with focusing on the updates to the FrEDI Technical Documentation and associated R package since the 2021 document was reviewed. Key aspects include the addition of several new sectoral impact categories, additional state-level impact calculations, and two modules for extending the default FrEDI framework: one module that can be used to extend FrEDI to calculate impacts through 2300 and a second Social Vulnerability module that that extends the dimensionality of FrEDI to provide a distributional analysis of climate change impacts to different population groups within the U.S. through 2090.

Public Review Period

A 30-day public comment period is scheduled for February 23rd through March 25th, 2024. All comments received will be carefully reviewed, considered, and responded to.

Expert External Peer Review

The expert review is managed by a contractor (ICF International) under the direction of a designated independent EPA peer review leader, who prepared a peer review plan, the scope of work for the review contract, and the charge for the reviewers. Importantly, the EPA peer review leader played no role in producing any portion of the report. Reviewers will work individually (i.e., without contact with other reviewers, colleagues, or EPA) to prepare written comments in response to the charge questions.

The contractor identified, screened, and selected four reviewers who had no conflict of interest in performing the review, and who collectively met the technical selection criteria provided by EPA.

The peer review charge directed reviewers to provide responses to the following questions during the main review:

[*to be added upon expert review*]

All comments received will be carefully reviewed, considered, and responded to.

APPENDIX B | DETAILS OF SECTORAL IMPACT STUDIES

B.1 Sectoral Impact Category Data Overview

This appendix provides additional detail on the sectoral impact studies currently incorporated into the FrEDI framework, including the pre-processing steps required to prepare the sectoral study results for inclusion in the R code and the sector-specific run-time processes. This appendix will be updated over time as additional sectoral studies and their functions are incorporated into FrEDI.

-The main advantage of FrEDI is that it offers the unique flexibility to incorporate a wide range of peer-reviewed climate impact studies into a common analytical framework, as implemented by the FrEDI R package. While details of each study vary, there are a series of similar steps used to pre-process and format the study data into impact-by-degree damage functions for use in FrEDI. Common pre-processing steps often include: 1) the aggregation of underlying study impact data to the state or regional level, 2) the isolation of climate-driven impacts by subtracting baseline impacts, and 3) temperature binning the annual impacts (or impact rates) for each available GCM to calculate the final by-degree damage functions that are then used when the FrEDI R code is run.

Temperature binning has been described elsewhere (Sarofim et al., 2021), and in this Documentation refers to the process of averaging annual sectoral impact rates across the eleven-year windows where each GCM reaches integer degrees of warming relative to the baseline. **Figure B-1** shows the arrival years for 1 to 6 degrees C of warming in the contiguous U.S., as estimated by 6 GCMs from the 5th Coupled Model Intercomparison Project (CMIP). For example, the GFDL-CM3 model is projected to reach 2 degrees C of warming between 2027 and 2037 (centered on 2032) and 6 degrees between 2082 and 2092 (centered on 2087). In contrast, the GISS-E2-R model is only projected to reach 3 degrees C of warming before 2090.

FIGURE B-1. INTEGER DEGREE ARRIVAL WINDOWS AND YEARS FOR SIX CMIP5 GCMS

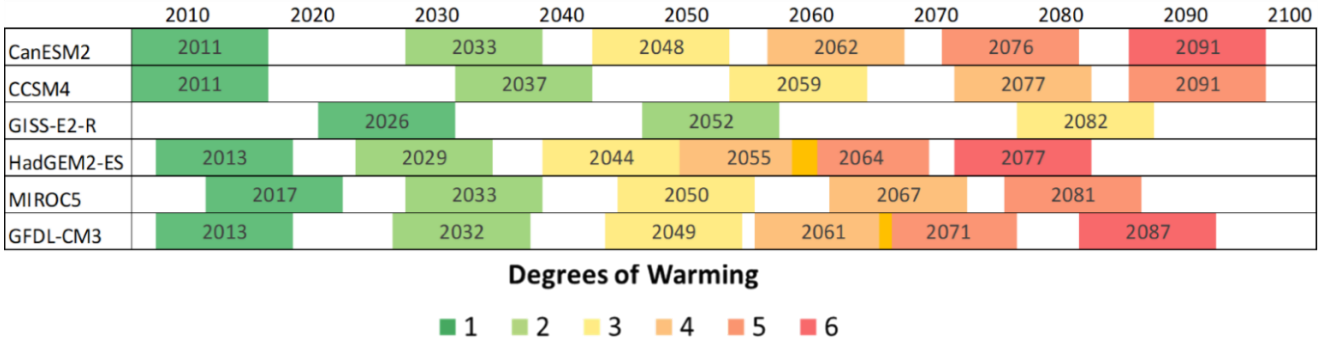

Arrival windows of each integer CONUS temperature change in six GCMs for RCP8.5. Arrival years, or the year at which the 11-year moving average reaches the given integer, are listed in each bin. The six CMIP5 GCMs are the suite used in the CIRA project, which represent many of the studies included within FrEDI.

Consistent with Chapter 3 in the Main Documentation, individual impact sectors are grouped into six aggregate categories: Health, Infrastructure, Electricity, Ecosystems & Recreation, Labor, and Agriculture. **Table B-1** lists each individual impact sector by aggregate group, summarizes the regional coverage of each impact within the Contiguous U.S. (CONUS), and lists the GCMs used in the underlying sectoral impact

models that form the basis of FrEDI's damage function. The last column identifies the geographic scale at which results are currently calculated in the FrEDI R code for each sector. **Table 2** (impact types, socioeconomic drivers, adaptation scenarios), **Table 4** (links to population and GDP inputs), **Table 5** (time dependent scalars), and **Table 6** (valuation measures) in the main text also provide summarized information about the 25 impact sectors.

TABLE B-1. REGIONAL COVERAGE AND GCMS USED BY SECTOR

		Regional Coverage							GCMs Used								Spatial Calculation Scale in FrEDI R code[d]
		Midwest	Northeast	Northern Plains	Northwest	Southeast	Southern Plains	Southwest	CanESM2	CCSM4	GFDL-CM3	GISS-E2-R	HadGEM2-ES	MIROC5	*Other*	*SLR Scenarios*	
Health	Climate-Driven Air Quality	■	■	■	■	■	■	■		■	■						State
	Extreme Temperature	■	■		■	■	■	■	■	■	■	■	■	■			Region
	CIL Temperature-Related Mortality	■	■	■	■	■	■	■	■	■	■	■	■	■			Region
	ATS Temperature-Related Mortality	■	■	■	■	■	■	■	■	■	■	■	■	■			State
	Southwest Dust							■	■	■	■	■	■	■			Region
	Valley Fever		■	■	■	■	■	■	■	■	■	■	■	■			Region
	Wildfire	■	■	■	■	■	■	■	■	■		■	■	■			State
	CIL Crime	■	■	■	■	■	■	■	■	■	■	■	■	■			Region
	Vibriosis	■	■	■	■	■	■	■	■	■	■	■	■	■			Region
	Suicide	■	■	■	■	■	■	■	■	■	■	■	■	■			State
Infrastructure	Coastal Properties		■		■	■	■	■								■	Region
	Transportation Impacts from HTF		■		■	■	■	■								■	State
	Rail	■	■	■	■	■	■	■	■	■	■	■	■	■			State
	Roads	■	■	■	■	■	■	■	■	■	■	■	■	■			Region
	Asphalt Roads	■	■	■	■	■	■	■							a		State
	Urban Drainage	■	■	■	■	■	■	■	■	■		■	■	■			State
	Inland Flooding	■	■	■	■	■	■	■							b		Region
	Hurricane Wind Damage		■			■	■			■	■		■	■	c		State
Electricity	Electricity Demand and Supply	■	■	■	■	■	■	■	■	■	■	■	■	■			State
	Electricity Transmission and Distribution	■	■	■	■	■	■	■	■	■	■	■	■	■			State
Ecosystems and Recreation	Water Quality	■	■	■	■	■	■	■	■	■		■	■	■			Region
	Winter Recreation	■	■	■	■	■		■	■	■	■	■	■	■			Region
	Marine Fisheries		■		■	■	■	■	■	■		■	■	■			Region
Labor	Labor	■	■	■	■	■	■	■	■	■	■	■	■	■			State
Agriculture	CIL Agriculture	■	■	■	■	■	■	■	■	■	■	■	■	■			Region

Notes: a. Asphalt Roads, a study not designed within the CIRA framework, utilized three GCMs in common with the CIRA2.0 set of scenarios (CanESM2, CCSM4, MIROC5) however, the climate data used in the underlying study was bias corrected and downscaled using a different process than the method used in CIRA. Therefore, although the GCMs are the same, the integer degree arrival times differ slightly for this sector.

b. The Inland Flooding sector used an ensemble of 14 GCMs (list provided in detailed write-up below), which includes four of the six GCMs from the CIRA2.0 set of scenarios (CanESM2, GFDL-CM3, HadGEM2-ES, MIROC5). The authors estimated arrival times and provided estimates of impacts by degree of warming for the mean of 14 GCM results.

c. The Hurricane Wind sector uses four of the six standard CIRA GCMs (CCSM4, GFDL-CM3, HadGEM2-ES, MIROC5) and MRI-CGCM3 to follow the underlying literature Marsooli et al. (2019). Similar to Asphalt Roads, the climate data used in the Hurricane Winds study was bias corrected and downscaled using a different process than the method used in CIRA. Therefore, although the GCMs are the same, the integer degree arrival times differ slightly for this sector. Unlike Marsooli et al. (2019), FrEDI does not include MPI5 due to data availability constraints.

d. As of 2/23/24, 12 sectoral impact categories are calculated in FrEDI at the state level. Using the same methodologies employed in this set, the remaining sectoral impacts will also be converted to state level upon review and final publication of the 2024 Technical Documentation.

Figure B-2 and **Figure B-3** present monetized damages by degree of warming for each temperature-driven impact category sector and by centimeter of Global Mean Sea Level (GMSL) rise for each sea level rise (SLR)-driven sector. These results are calculated using the default socioeconomic inputs for 2090. These figures show the relative magnitude of damages for each impact sector, by GCM, and the final shape of the CONUS damage functions after valuation scalars have been applied. Note that the GCMs in each underlying study do not all reach the same level of future warming. Therefore, FrEDI's sector-specific damage functions are derived from the range of warming degrees available from each GCM (e.g., Figure B1 and shown by solid lines in each impact-by-degree figure in this Appendix) and then linearly extrapolated (as described in Chapter 2.3 of the Main Documentation) to higher levels of warming (shown by markers in each impact-by-degree figure). Application of the framework is not limited to the current impact sectors. New sectors that meet the requirements outlined in Chapter 2 of the Main Documentation can be added to the framework following the process documented in Chapter 2. This expansion in sectoral scope remains a high priority for future updates.

FIGURE B-2. NATIONAL ECONOMIC IMPACTS BY DEGREE OF WARMING IN 2090 BY SECTOR

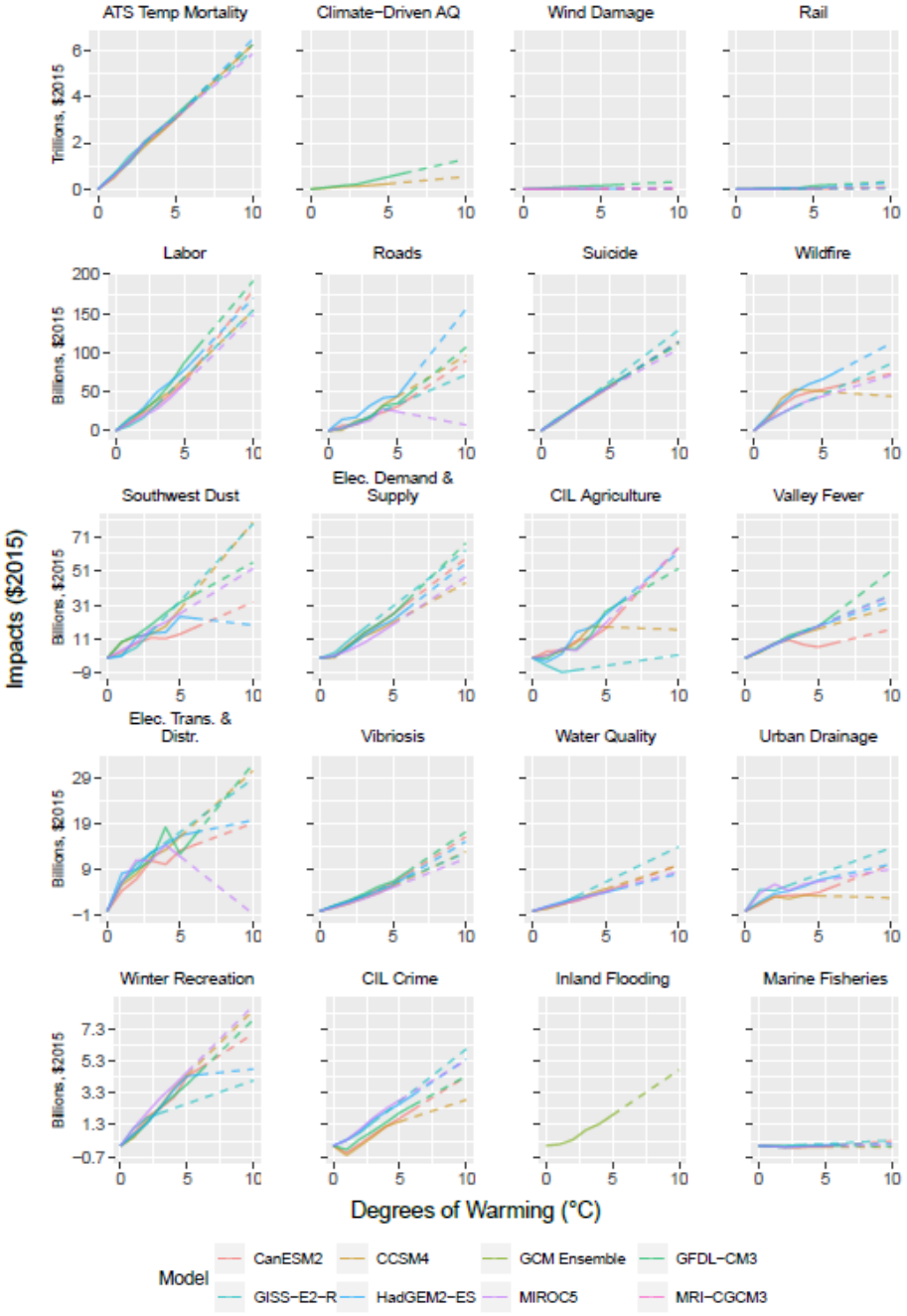

Impacts by CONUS degree of warming (Celsius) relative to the 1986-2005 average baseline, under 2090 socioeconomic conditions, in millions of $2015 U.S. Dollars (USD) for the default FrEDI sectors driven by temperature. Results for Roads, Rail, and Electricity Transmission and Distribution Infrastructure reflect the primary adaptation scenarios (see Section 2.2 of the Main Text). Each series represents the GCMs available in each underlying study where markers represent extrapolations above available integer degree warming. Sectors are ordered by their average 5-degree impacts. Not all sectors include estimates for all models listed in the legend—for details on which models are included by sectors, see the following sections of Appendix B. Note that the y-axis scalar varies by row. Figure produced using results from FrEDIv4.0.

FIGURE B-3. NATIONAL ECONOMIC IMPACTS BY CENTIMETER OF GMSL FOR SLR-DRIVEN SECTORS

Impacts by centimeter of GMSL rise relative to a year 2000 baseline, in millions of $2015 USD. Each data point represents an annual impact based on one of six GMSL rise scenarios from Sweet et al. (used in the underlying models). The two series show results by year each GMSL is reached. Results for Transportation Impacts from High Tide Flooding and Coastal Properties reflect the default adaptation scenarios (see Section 2.2 in the main report). Each series represents the underlying sea level rise scenario. Figure produced using results from FrEDIv4.0.

For each sectoral impact category, the following sections provide a description of the impacts considered, a reference to the underlying impact study, a description of the pre-processing steps used to derive sectoral damage functions, implementation in the FrEDI R package, and discussion of any limitations. To show GCM variability, impacts-by-degree of warming are shown for the GCMs used in each underlying study. In addition, for sectors that are projected to scale with temperature (or SLR) and socioeconomic conditions (i.e., population and GDP), impacts-by-degree are also provided for two example socioeconomic scenarios (e.g., 2010 and 2090) to illustrate the socioeconomic sensitivity.[8]

[8] Note that these sections will continue to be updated and standardized as all sectors are moved to state level processing upon final publication.

B.2 Health Sectors

Climate-Driven Changes in Air Quality

Summary

This sectoral study estimates mortality risk associated with climate-driven changes in air quality in the CONUS; specifically, ozone and fine particulate matter ($PM_{2.5}$) concentrations.

UNDERLYING DATA SOURCES AND LITERATURE

Fann, N. L., Nolte, C. G., Sarofim, M. C., Martinich, J., & Nassikas, N.J. (2021). Associations between simulated future changes in climate, air quality, and human health. JAMA Network Open, 4(1).

This analysis uses air quality surfaces (i.e., concentrations in response to changes in meteorology) and concentration-response functions employed by Fann et al. (2021) to future quantify $PM_{2.5}$- and ozone-attributable premature mortality. Air quality concentration changes are driven by changes in climate only and do not reflect time-varying changes in pollutant precursor emissions. Mortality is monetized using the value of statistical life (VSL). As the projected climate-driven changes will be sensitive to changes in pollutant precursor emissions (e.g., nitrogen oxides, sulfur dioxide, carbonaceous aerosol, ammonia, etc.), two simulated air pollutant emissions inventories are also considered as variants: a 2011 dataset that estimates unrestricted pollution burden from all sources as of that year, and a 2040 dataset that accounts for the implementation of a suite of regulatory policies on stationary and mobile emissions sources. For illustrative purposes, plots of resulting impacts by temperature degree for $PM_{2.5}$ (top) and ozone (bottom) are shown in **Figure B-4**, calculated using 2010 (A) and 2090 (B) socioeconomics (the end points of socioeconomics), and for each of the emission inventory variants**-**.

FIGURE B-4. AIR QUALITY IMPACTS BY TEMPERATURE BIN DEGREE

A. 2010 SOCIOECONOMICS

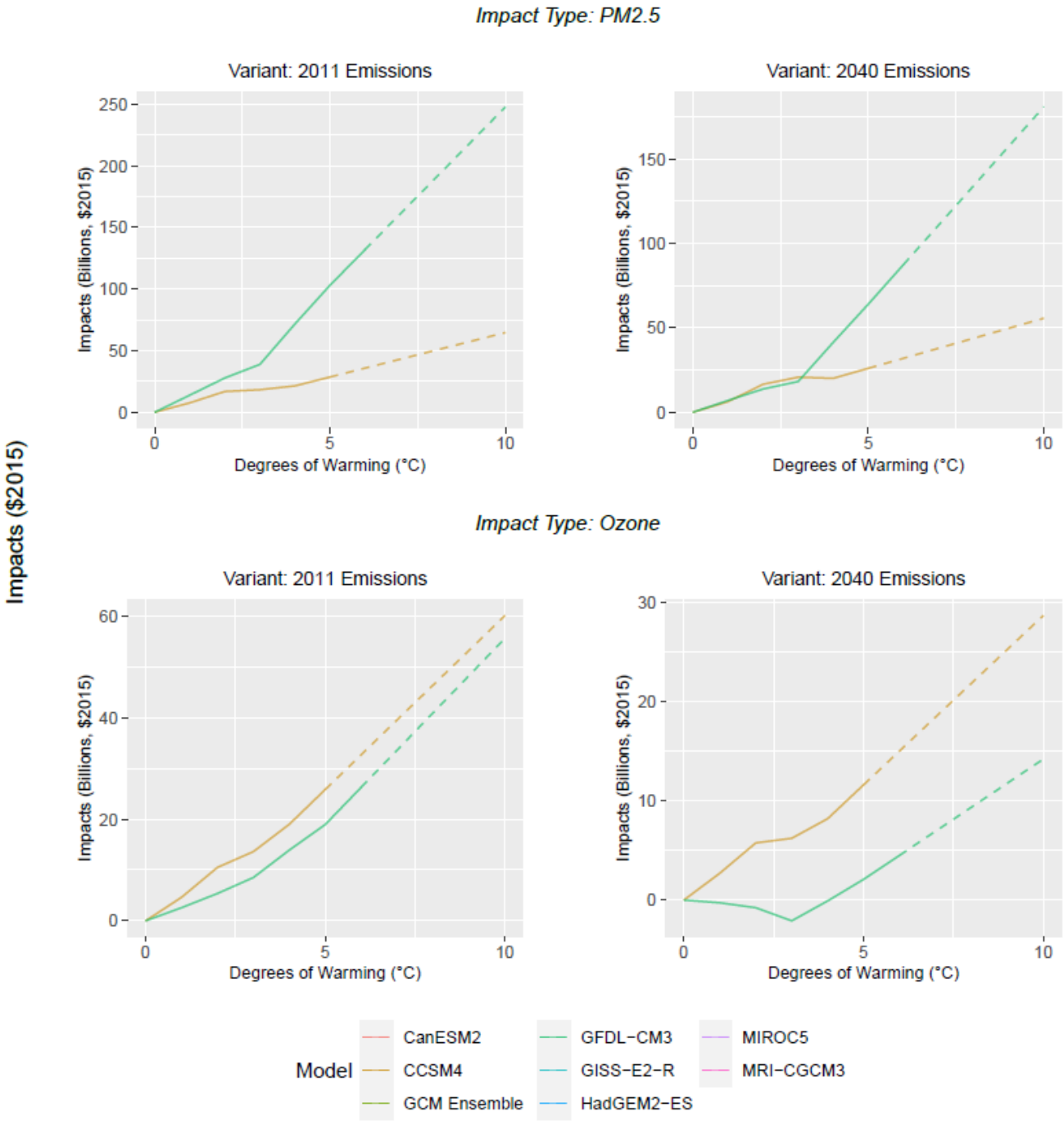

Note: Figure scale varies by impact type and variant

B. 2090 SOCIOECONOMICS

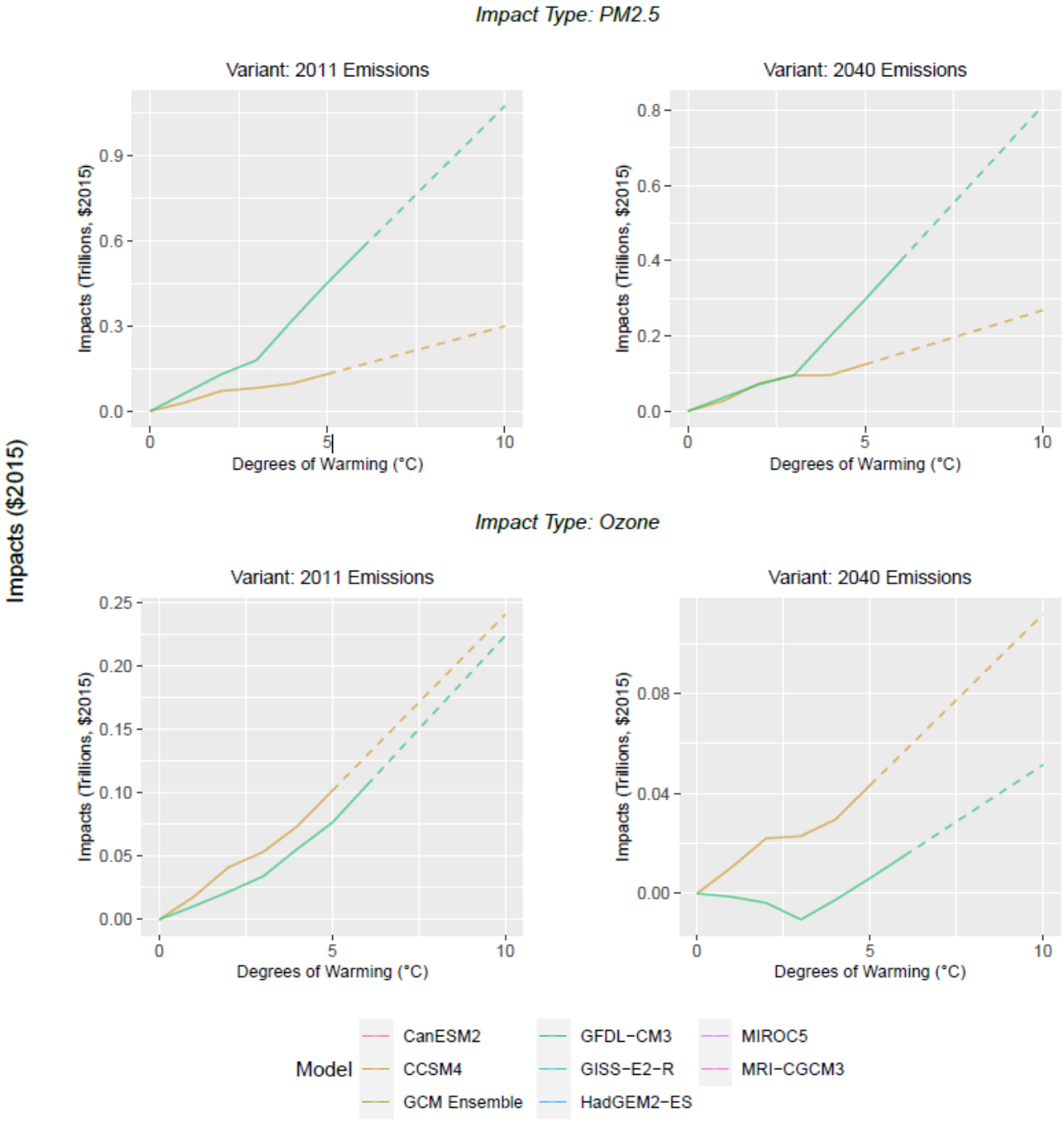

Note: Figure scale varies by impact type and variant

Processing steps

TABLE B-2. INPUT DATA CHARACTERISTICS: CLIMATE DRIVEN CHANGES IN AIR QUALITY

Data Features	Study Attributes
Evaluated Impacts	• Mortality: premature deaths per capita from Ozone and $PM_{2.5}$ (physical) • Value of premature mortality, Ozone and $PM_{2.5}$ (economic)
Variants	• 2011 Air Pollutant Emissions Level • 2040 Air Pollutant Emissions Level
Data Shape	• Four eras • Two GCMs (CCSM4 and GFDL-CM3) • 26-km grid cell • Two pollutants (ozone and $PM_{2.5}$)
Runs Provided	• With climate change and with population growth
Additional Data	• None

Processing steps are illustrated in **Figure B-5**. To derive impact-by-degree-damage functions, EPA's Benefits Mapping and Analysis Program – Community Edition (BenMAP-CE) is first used to generate total mortality results using the same data inputs as from Fann et al. (2021). For example, the air quality exposure data (for each 36-km CONUS grid cell) was provided by study authors by era, GCM, pollutant (ozone/$PM_{2.5}$), and emissions inventory (2011/2040). This exposure data is available for four eras (2030, 2050, 2075, 2095), derived from two climate models (CCSM4 and GFDL-CM3). Concentration-response functions used within BenMAP-CE to derive mortality counts from air pollutant exposure levels are also the same as those used in Fann et al. (2021), which are based on risk model information for those age 30-99 for $PM_{2.5}$ and those age 0-99 for ozone. Therefore, to derive total mortality estimates for FrEDI (1st pre-processing step), BenMAP-CE was used with these study data inputs to derive mortality impacts at the state level for each era, GCM, pollutant, and emissions inventory scenario.

In the second pre-processing step (second box) total state mortality counts are divided by dynamic state population from the Integrated Climate and Land Use Scenarios, v2 (ICLUSv2) dataset, to acquire per capita mortality estimates for each era and state. The original exposure levels provided in Fann et al., (2021) already accounted for baseline incidence and therefore no additional processing was needed to isolate climate impacts for use in FrEDI. In the last pre-processing step (fourth box), era-level per capita mortality impacts are assigned to the central year of the era (i.e., 2030, 2050, 2075, and 2095), and impacts for remaining years are derived by interpolating linearly between central era years. Finally, to bin the results by temperature degree and derive impact-by-degree functions, the yearly mortality per capita impacts for each pollutant impact type (ozone/$PM_{2.5}$) are averaged across the eleven-year windows where each GCM reaches each integer degree of CONUS warming relative to the baseline.

FIGURE B-5. CLIMATE-DRIVEN CHANGES IN AIR QUALITY PROCESSING FRAMEWORK

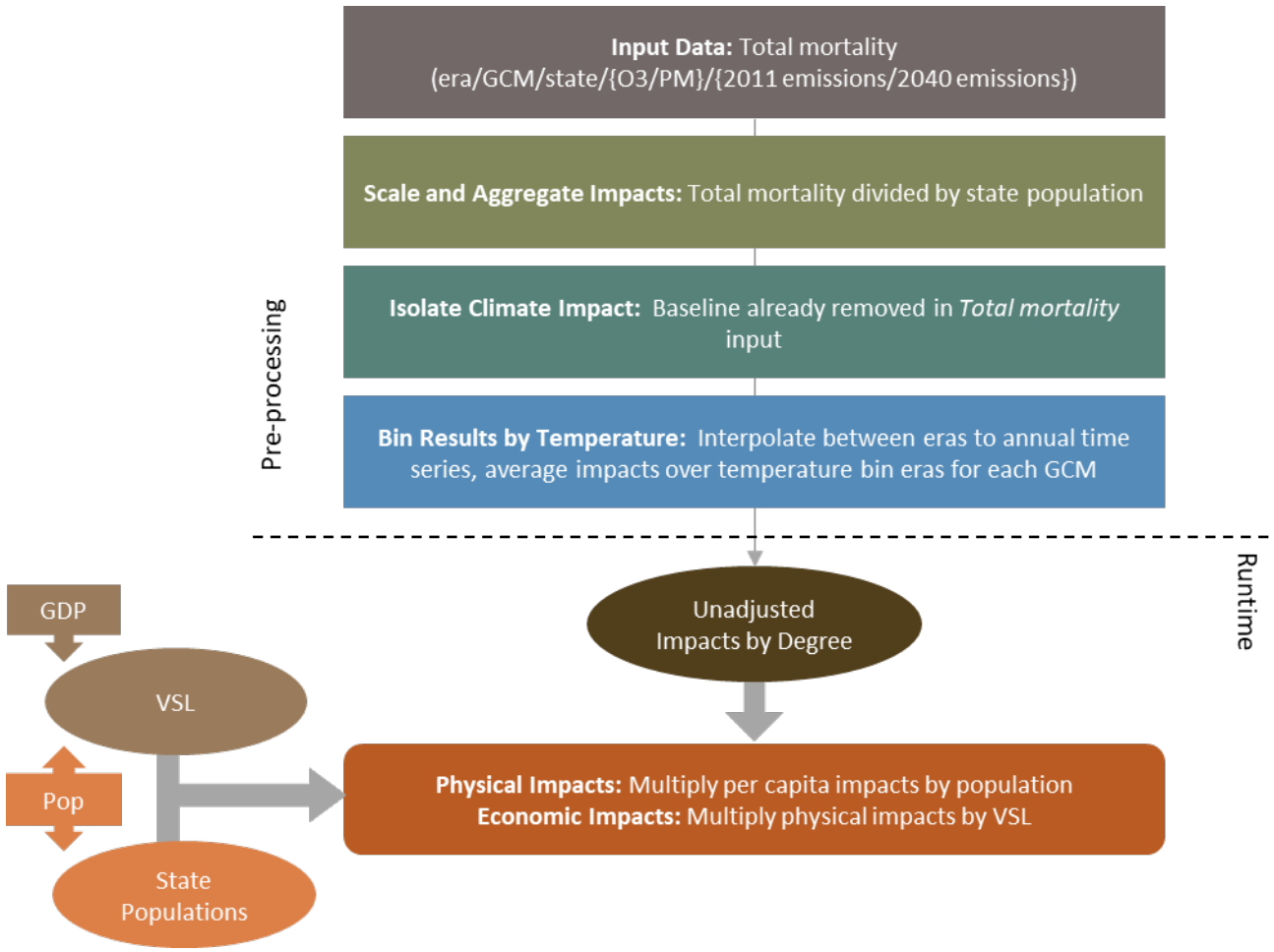

When FrEDI is run, the pre-processed by-degree per capita mortality functions are then applied to the input temperature scenario to calculate the unadjusted annual per capita impacts based on the level of warming in each year of the input scenario. The total annual physical mortality counts are then calculated by applying these annual per capita rates to the input population scenario. Lastly, annual mortality counts are monetized using the VSL, calculated at runtime from input GDP per capita. VSL is adjusted for changes in GDP per capita using an income elasticity function[9] (Eq. B-1):

$$VSL_t = VSL_{2010} \times \left(\frac{GDPcap_t}{GDPcap_{2010}}\right)^{elasticity} \qquad \text{(Equation B-1)}$$

Limitations and Assumptions

- $PM_{2.5}$-attributable premature mortality is quantified for those age 30 and older, and this analysis assumes the impacts for those under 30 to be zero. Doing so underestimates the risk of premature

[9] This is a generic elasticity function that can be used in a time-series fashion, as used here, or for cross-sectional benefits transfers, as in the example in Masterman and Viscusi (2018), "The Income Elasticity of Global Values of a Statistical Life: Stated Preference Evidence", Journal of Benefit-Cost Analysis, 9(3):407-434. Note that the current default elasticity is 1.0, but can be set by the user as an input to the R code.

mortality experienced by those under 30. Additionally, doing so assumes that age demographics remain proportional over the century.

- This analysis does not quantify morbidity effects associated with changes in $PM_{2.5}$ and ozone, which are likely to increase as temperature increases. Changes in air quality can provoke hospital admissions for respiratory diseases and worsen other conditions.
- For further discussion of the limitations and assumptions in the underlying sectoral modeling approach, see Fann et al. (2021).

Extreme Temperature

Summary

This sector addresses the impact of extreme temperature on premature mortality in 49 major U.S. cities. In the 2010 Census, the 49 cities accounted for 91.3 million of the total US population of 309.3 million, or nearly 30 percent. Economic damages are based on extreme heat and cold mortality rates, monetized by applying GDP per capita-adjusted VSLs.

UNDERLYING DATA SOURCES AND LITERATURE

Mills, D., Schwartz, J., Lee, M., Sarofim, M., Jones, R., Lawson, M., Duckworth, M., & Deck, L. (2014). Climate Change Impacts on Extreme Temperature Mortality in Select Metropolitan Areas in the United States. Climatic Change, 131, 83-95.

The underlying epidemiologic model from Mills et al., (2014) includes runs with 'adaptation' and with 'no additional adaptation' scenarios. The adaptation scenario does not reflect a benefit-cost calculation but an assumption that U.S. cities will gradually adapt to a hotter environment through physical acclimatization of their residents, infrastructure replacement with more heat suitable shading and air conditioning, and behavioral changes, so that the stressor-response will look like that of the current Dallas context.[10] The original estimates are provided for 49 cities. For illustrative purposes, **Figure B-6** shows the resulting damages by degree of warming for both the heat and cold related mortality variants (top and bottom panels), both adaptation scenarios (left and right plots), and six GCMs, calculated using 2010 (figure A) and 2090 (figure B) socioeconomics (i.e., the endpoints of the socioeconomic scenarios).

[10] The adaptation scenario was considered in Mills et al. (2014) and U.S. EPA (2017). More refined adaptation scenarios for this sector, including the costs and efficacy of increased air conditioning market penetration, are the subject of active and ongoing research. Some research has found the efficacy of cooling centers can be high in preventing extreme heat mortality, but surveys and current experience suggest that many residents are unwilling to use formal cooling centers. For at least some of the cities evaluated in Mills et al. (2014), the empirical data reflects the availability, if not the widespread use, of cooling centers to residents.

FIGURE B-6. EXTREME TEMPERATURE IMPACTS BY TEMPERATURE BIN DEGREE

A. 2010 SOCIOECONOMICS

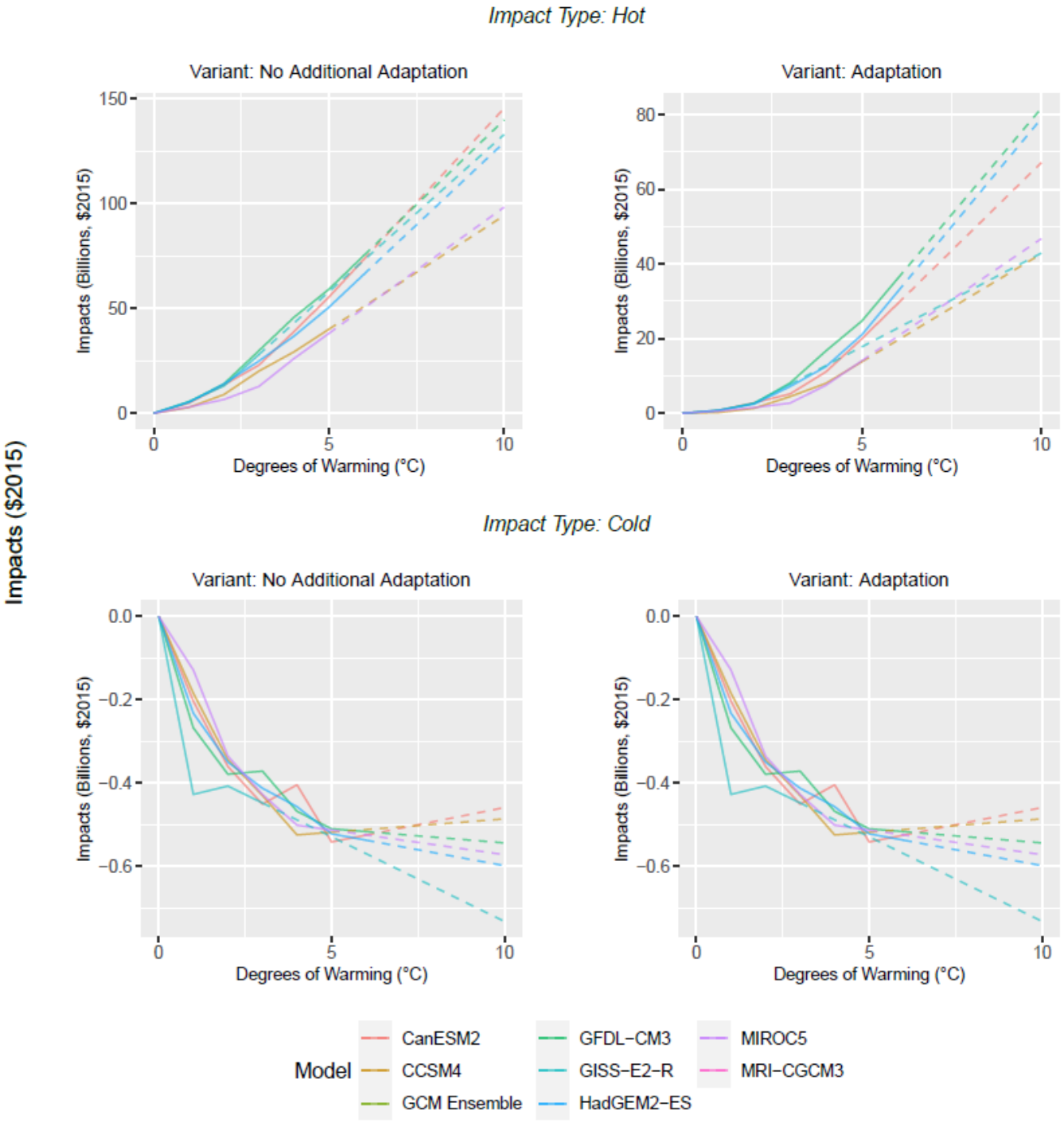

Note: Figure scale varies by impact type and variant

B. 2090 SOCIOECONOMICS

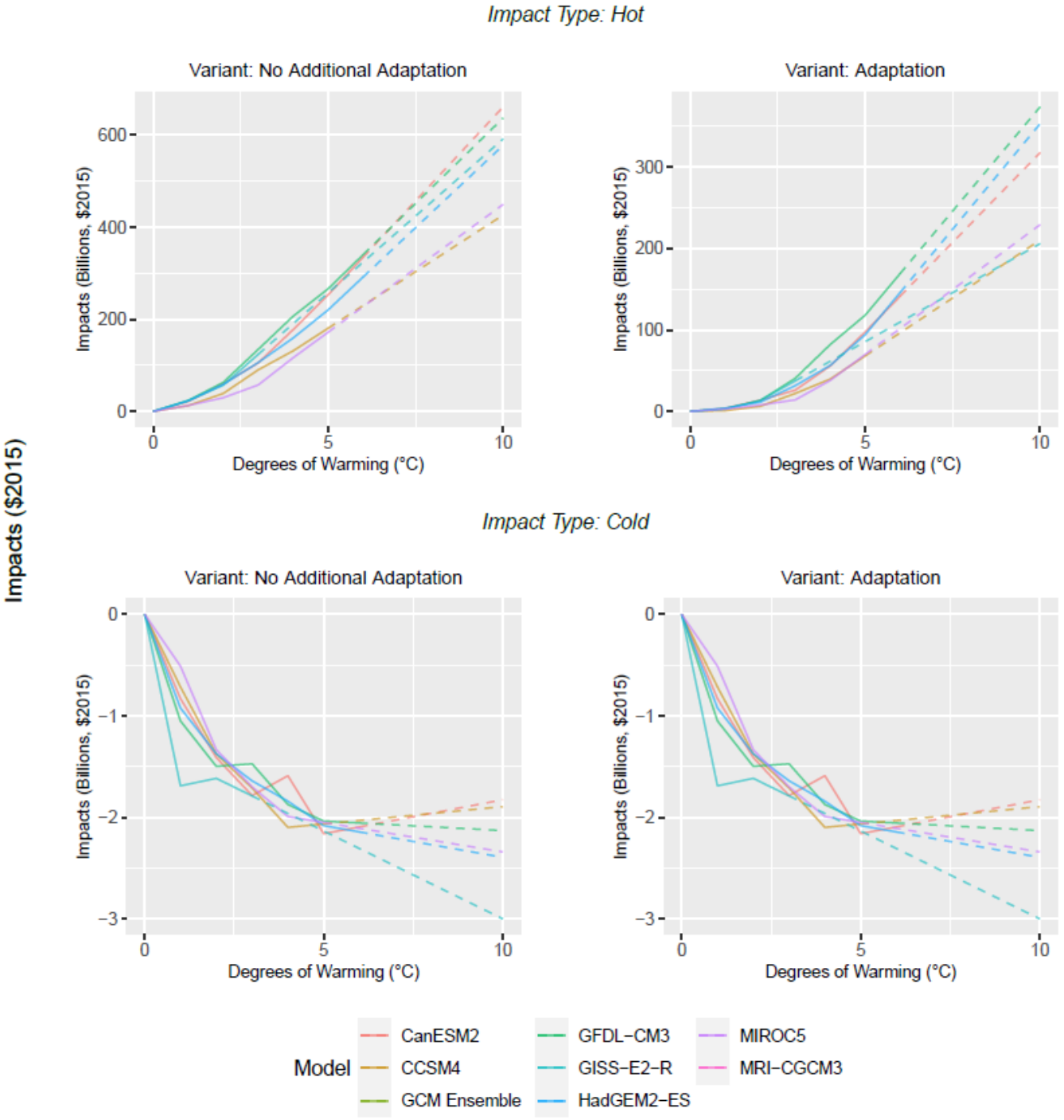

Note: Figure scale varies by impact type and variant

Processing steps

Processing steps are shown in **Figure B-7**. Total mortality data are provided by the study authors by *degree, GCM, city, damage type (heat/cold mortality), and base population (2010/2090)*. These original city-level mortality counts are then summed to counts for each CONUS region. In the next pre-processing step, the incremental impacts of climate change are then isolated by subtracting mortality counts from the 0-degree bin from those in each subsequent warming bin. The original model in Mills et al., (2014) was run under two constant population assumptions: 2010 and 2090 estimates from ICLUSv2 (EPA 2017; Bierwagen et al., 2010), which vary in total population and the distribution of population across modeled cities. Therefore, in the third pre-processing step, regional mortality counts from the two population scenarios (and for hot and cold impacts and two adaptation scenarios) are divided by the total population (for the 49 modeled cities) to obtain a mortality per capita estimate for each population scenario (2010/2090), by GCM, adaptation variant, and hot and cold impact types. The last step is to calculate a population scalar to account for the fraction of the CONUS population living in the 49 study cities, by taking the ratios of the regional populations from ICLUSv2 (i.e., FrEDI default population scenario) and the sum of modeled city populations per region.

FIGURE B-7. EXTREME TEMPERATURE DATA PROCESSING FRAMEWORK

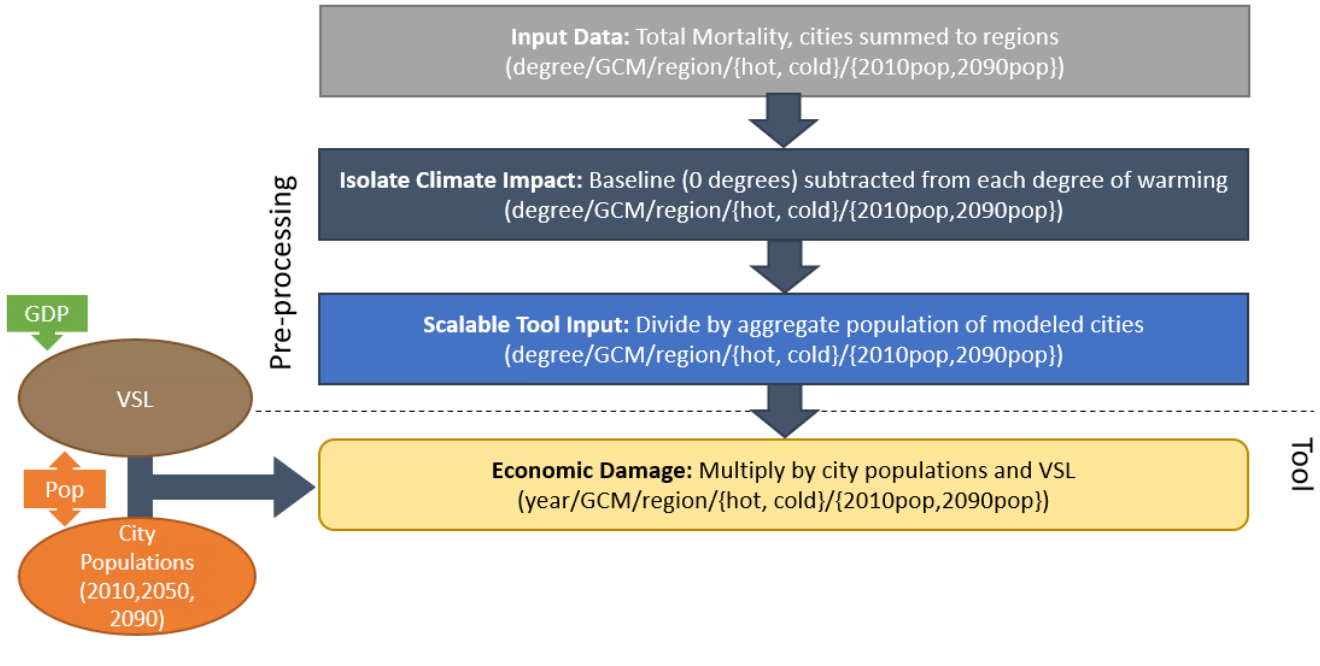

When FrEDI is run, the pre-processed by-degree per capita mortality functions are then applied to the input temperature scenario to calculate the unadjusted annual per capita impacts based on the level of warming in each year of the input scenario. The total annual physical mortality counts are then calculated by applying these annual per capita rates to the input population scenario. Regional population inputs are translated to city populations using the population scalars derived from the ICLUSv2 population scenarios in

2010, 2050, and 2090, and interpolated for years in between. Lastly, annual mortality counts are monetized using the VSL, calculated at runtime from input GDP per capita (Eq. B-1).

Limitations and Assumptions

- National per capita averages are based on the total population of modeled cities with heat and cold impacts. There are certain cities in the Southeast (Atlanta, Broward-Ft. Lauderdale, Miami, Orlando), Southern Plains (Austin, Dallas), and Southwest (Albuquerque, Los Angeles, Phoenix, San Diego) regions that are modeled for adaptation to heat but are not modeled for adaptation to extreme cold. It is assumed that these cities have minimal extreme cold damages, and therefore their populations are included in the denominator as part of the total population over which cold damages are averaged.
- This analysis only covers considers health impacts to individuals living in 49 cities within the CONUS and therefore omits a large fraction of the population vulnerable to extreme temperatures.
- Cities that only experienced extreme cold in the historic period, notably those in the Northwest region, do not show an increase in extreme-temperature related mortality in this analysis. This result is an artifact of the methodology, which relies on observed temperature thresholds based on a historic period. With increased temperatures, it is likely that many of these Northwestern cities could experience heat-related mortality as well, which might be reflected if a different impact estimation methodology had been applied.
- For further discussion of the limitations and assumptions in the underlying sectoral model, please see Mills et al. (2014) and EPA (2017).

CIL Temperature-Related Mortality

Summary

This sector addresses the impact of climate-driven temperature changes on premature mortality across all the CONUS, using an alternative method to that based on Mills et al. (2014) and Cromar et al., (20212. The Climate Impact Lab (CIL) Temperature-Related Mortality estimates rely on the development of a function linking extreme heat to excess mortality incidence, using a method first established in Deschenes and Greenstone (2011), updated in Barreca et al. (2016), and refined to develop projections of future impacts by GCM and RCP through the 21st century in Hsiang et al. (2017).

UNDERLYING DATA SOURCES AND LITERATURE

Deschênes, O., Greenstone, M. (2011). Climate Change, Mortality, and Adaptation: Evidence from Annual Fluctuations in Weather in the US. American Economic Journal: Applied Economics 3(4): 152–185.

A. Barreca, K. Clay, O. Deschênes, M. Greenstone, J. S. Shapiro, (2016). Adapting to Climate Change: The Remarkable Decline in the US Temperature-Mortality Relationship over the Twentieth Century. J. Polit. Econ. 124, 105–159 (2016).

S. Hsiang, R. Kopp, A. Jina, J. Rising, M. Delgado, S. Mohan, D. J. Rasmussen, R. Muir-Wood, P. Wilson, M. Oppenheimer, K. Larsen, T. Houser. (2017) Estimating economic damage from climate change in the United States Science 356: 1362–1369

Economic damages are based on the net effect of extreme heat and cold mortality rates, monetized by applying the VSL. Although the original Hsiang et al. (2017) application held VSL constant through time, the VSL used in FrEDI changes as a function of annual per capita income. The spatial domain of the study is all the CONUS, and as a result this work addresses temperature-related mortality for a population approximately three times larger than the Mills et al. (2014) work. As shown in Hsiang et al. (2017), consideration of the net effect of changes in both cold and heat related mortality results in a net increase in mortality rates attributed to temperature changes in southern areas of CONUS, and a net decrease in mortality rates in northern areas of CONUS. As in Hsiang et al. (2017), we rely on the premature mortality estimates dose derived from survival function components of the Deschenes and Greenstone (2011) paper (i.e., the mortality dose response function with respect to temperature) and apply a VSL consistent with the FrEDI framework (Eq. B-1). The willingness-to-pay valuation component in Deschenes and Greenstone (2011) was not adopted for this work.

To date, the CIL study authors have shared data for the "without additional adaptation" scenario, which is currently included in FrEDI. FrEDI results from this sector study therefore reflect damages when considering current rates of air conditioning penetration. We anticipate that future revisions of FrEDI could incorporate a "with adaptation" variant from this sector study, based in part on the findings of Barreca et al. (2016) that show a large impact of air conditioning in reducing the rate of heat-related mortality in the historical (1900-2004) period, with extensions to forecast air conditioning penetration rates. The CIL study authors also shared results from uncertainty modeling in the underlying work, which were used to develop two additional damage functions for FrEDI that reflect the 90 percent confidence interval of the damages. Therefore, physical and economic damage from this study in FrEDI are available for the low and high end of the confidence interval (5^{th} and 95^{th} percentile values) as well as a central estimate which corresponds to the median result (50^{th} percentile).

For illustrative purposes, **Figure B-8** shows a summary of the damages by degree of warming for the median and low and high confidence intervals, by GCM and for both 2010 (figure A) and 2090 (figure B) socioeconomics (i.e., the endpoints of the socioeconomic scenarios).

FIGURE B-8. CIL TEMPERATURE-RELATED IMPACTS BY TEMPERATURE BIN DEGREE

A. 2010 SOCIOECONOMICS

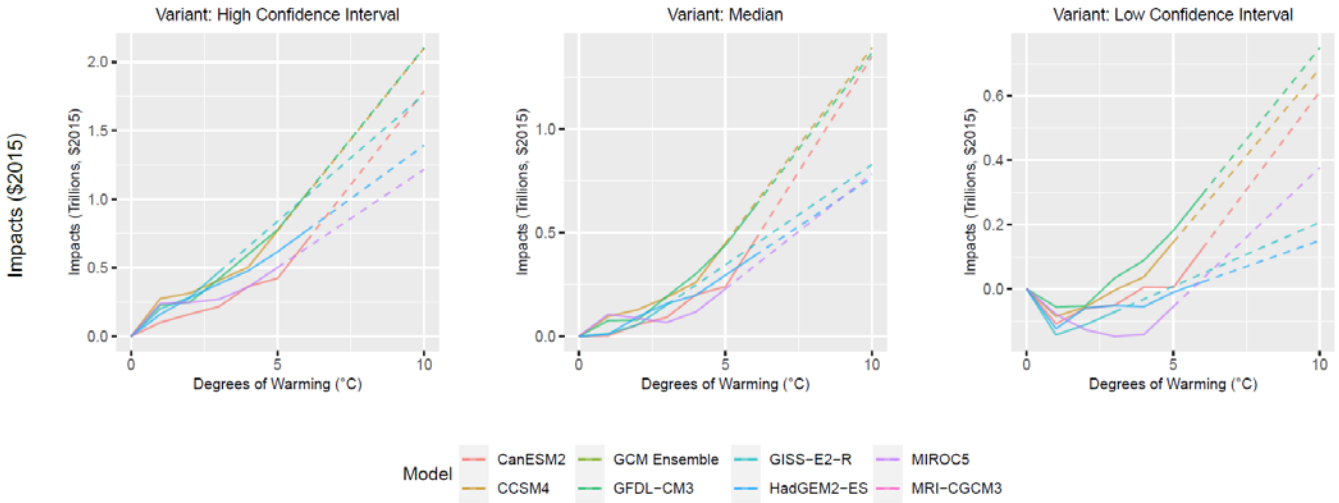

Note: Figure scale varies by variant

B. 2090 SOCIOECONOMICS

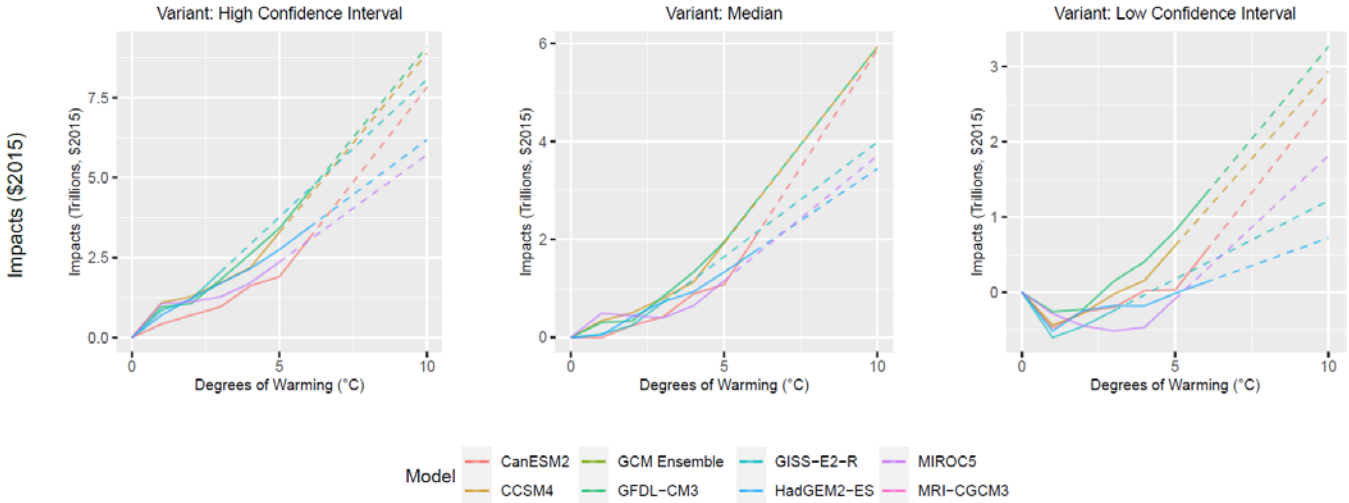

Note: Figure scale varies by variant

Processing steps

Processing steps are shown in **Figure B-9**. The Hsiang et al., (2017) study authors provided data on the incremental net change in per capita mortality under the RCP 8.5 scenario, by *GCM, year, and state*. These results reflect a single base socioeconomic scenario in 2012. In the first pre-processing step, annual incremental per capita mortality rates are then converted to total annual incremental mortality counts using 2010 state populations from ICLUSv2, which are then summed to total mortality counts per region. In the second step, these region-level annual incremental deaths are then binned by temperature by averaging across the eleven-year windows where each GCM reaches each integer degree of CONUS

warming relative to the baseline. Lastly, temperature-binned total incremental deaths are converted back to incremental per-capita mortality rates by dividing by regional baseline populations from ICLUSv2.

FIGURE B-9. CIL EXTREME TEMPERATURE DATA PROCESSING FRAMEWORK

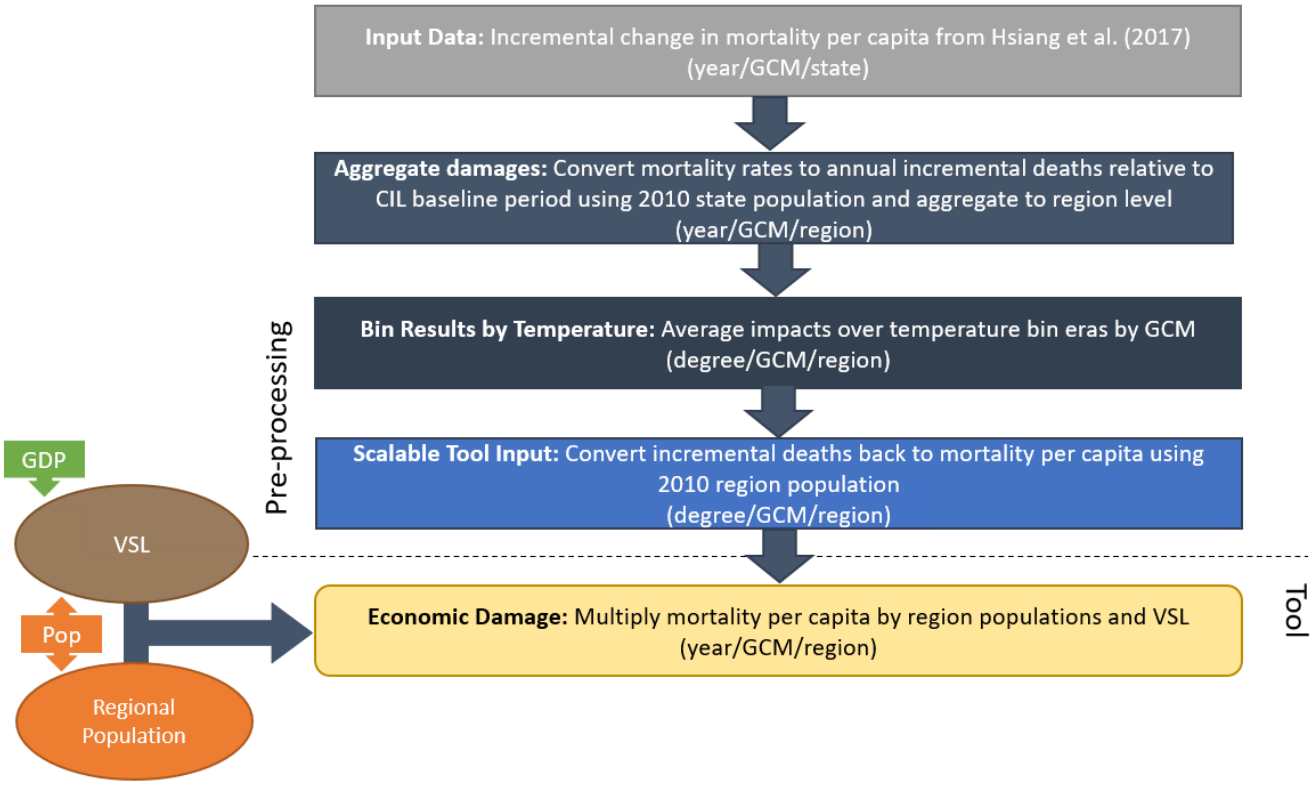

When FrEDI is run, the pre-processed by-degree per capita mortality functions are then applied to the input temperature scenario to calculate the unadjusted annual per capita impacts based on the level of warming in each year of the input scenario. The total annual physical mortality counts are then calculated by applying these annual per capita rates to the input population scenario. Lastly, annual mortality counts are monetized using the VSL, calculated at runtime from input GDP per capita (Eq. B-1).

Limitations and Assumptions

- The estimates included in FrEDI reflect a scenario of current air conditioning penetration rates, without expansion of air conditioning to mitigate health risks, consistent with the results initially shared by the study authors. When results that reflect additional adaptation effort are shared, results for enhanced adaptation will be incorporated in future revisions of the tool.
- The underlying studies focus on extreme temperature mortality impacts, and as noted in Deschenes and Greenstone (2011) excludes impacts of extreme temperature on morbidity, so likely underestimates the full effect of temperature on health.
- The Hsiang et al. (2017) work includes adjustments to climate damages associated with general equilibrium impacts. While the general equilibrium effects estimate in that paper shows a lower economic impact for mortality when compared to the direct impact included in FrEDI, as the

authors note the general equilibrium approach omits the large component of willingness to pay to avoid mortality risk that is captured in the VSL. For this reason, as in the underlying study, we omit the general equilibrium adjustment for mortality impacts.

- For further discussion of the limitations and assumptions in the underlying sectoral model, please see Deschenes and Greenstone (2011) and Hsiang et al. (2017).

ATS Temperature-Related Mortality

Summary

This sector provides a measure of the impact of climate-driven change in temperature on premature mortality across all the CONUS, using an alternative method to that based on Mills et al. (2014) and the Hsiang et al., (2017) CIL study. While users can select to analyze impacts from any of the temperature-related mortality studies, the default FrEDI results use this ATS study to assess climate-driven damages associated with changes in temperature-related mortality.

UNDERLYING DATA SOURCES AND LITERATURE

K. Cromar, S.C. Anenberg, J.R. Balmes, A.A. Fawcett, M. Ghazipura, J.M Gohlke, M. Hashizume, P.Howard, E. Lavigne, K. Levy, J. Madrigano, J.A. Martinich, E.A. Mordecai, M.B. Rice, S. Saha, N.C. Scovronick, F. Sekercioglu, E.R. Svendsen, B.F. Zaitchik, and G.Ewart. (2022). Global Health Impacts for Economic Models of Climate Change: A Systematic Review and Meta-Analysis. Annals of the American Thoracic Society. 19(7): 1202-1212. DOI: 10.1513/AnnalsATS.202110-1193OC

K. Rennert, F. Errickson, B.C. Prest, L. Rennels, R.G. Newell, W. Pizer, C. Kingdon, J. Wingenroth, R. Cooke, B. Parthum, D. Smith, K. Cromar, D. Diaz, F.C. Moore, U.K. Müller, R.J. Plevin, A.E. Raftery, H. Ševčíková, H. Sheets, J.H. Stock, T. Tan, M. Watson, T.E. Wong & D. Anthoff. (2022), Comprehensive evidence implies a higher social cost of CO_2. Nature. 610:687–692. https://doi.org/10.1038/s41586-022-05224-9

The American Thoracic Society (ATS) Temperature-Related Mortality study developed a mortality impact function using meta-analysis of seven previously published US studies of the connection between temperature change and excess mortality incidence, as well as other non-US studies for other results of the globe. The result of the meta-analysis is a set of globally applicable impact functions calibrated to changes in average annual temperature – based on discussion with the lead author, we interpret the relevant average annual temperature to be a locally experienced exposure (i.e., CONUS temperature), which is also consistent with the relevant exposure metric applied in the seven US studies to which the USA region results are calibrated. For this work, we rely on the estimates for the USA region only.

Economic damages are based on the net effect of heat and cold-related mortality rates, monetized by applying the VSL. The original work did not attempt to project damages for any climate scenarios, or attempt valuation, but the VSL in FrEDI is applied as a function of per capita income (Eq. B-1). The spatial domain of the study is all of CONUS. As recommended by communication with the study's lead author, we apply an aggregated net function that reflects both reductions in cold-related mortality and increases in

heat-related mortality as temperatures increase.[11] We use county-scale estimates, and then aggregate to a net total effect by state.

The ATS study also provides a standard error on the impact function relative risk coefficient, which was used to develop two additional damage functions that represent a 90 percent confidence interval around the excess risk parameter. As a result, the final physical and economic impacts from this sector study in FrEDI are available for the low and high end of the confidence interval (5th and 95th percentile values) as well as a central estimate which corresponds to the mean result.

For illustrative purposes, **Figure B-10** shows the resulting damages by degree of warming for the mean and high and low confidence intervals, by GCM, calculated using 2010 (figure A) and 2090 (figure B) socioeconomics (i.e., the endpoints of the socioeconomic scenarios).

FIGURE B-10. ATS TEMPERATURE-RELATED IMPACTS BY TEMPERATURE BIN DEGREE

A. 2010 SOCIOECONOMICS

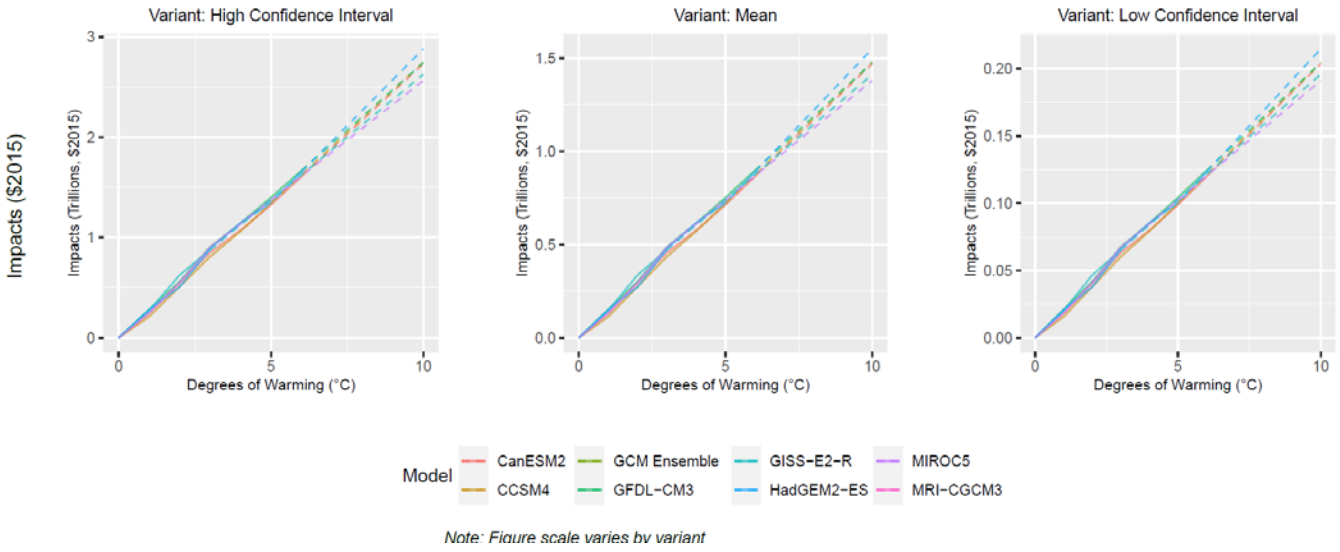

Note: Figure scale varies by variant

[11] See Table 3 in Cromar et al. (2022) – the valued used is the mean estimate for the USA and Canada region. Note that the table shows a mean beta value of 0.0046 (0.46%) – we chose to apply the value reported in the Supplemental Information of Rennert et al. (2022) of 0.464% - confirmed as reasonable by the study lead author.

B. 2090 SOCIOECONOMICS

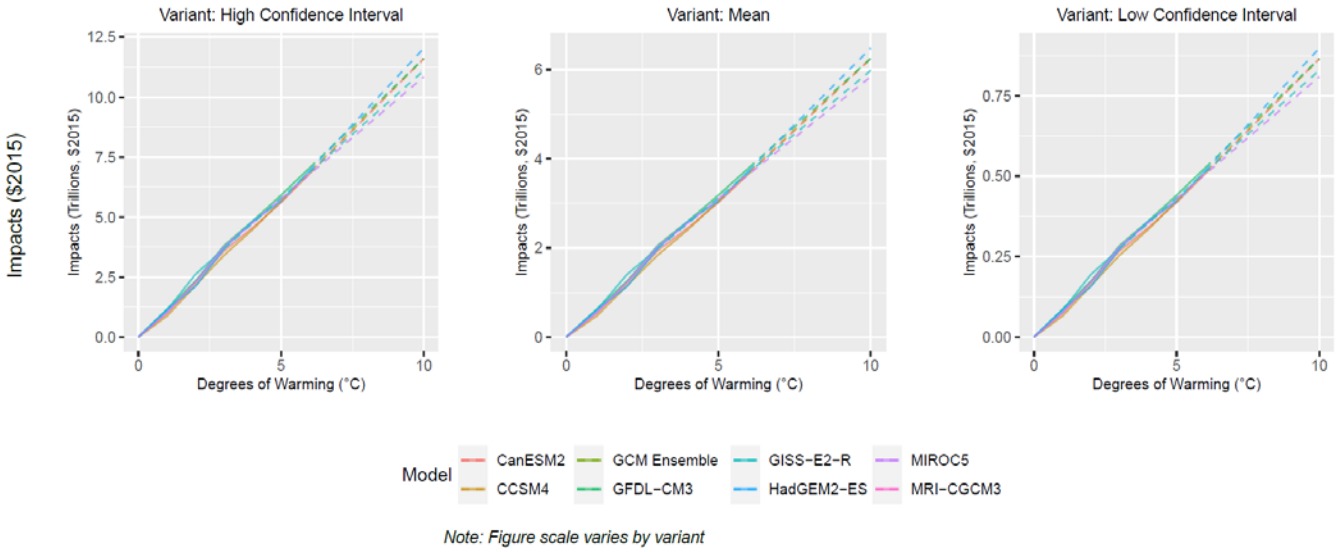

Note: Figure scale varies by variant

Processing steps

TABLE B-3. INCOMING DATA CHARACTERISTICS: ATS TEMPERATURE-RELATED MORTALITY

Data Features	ATS Temperature-Related Mortality Attributes
Evaluated Impacts	• Mortality: premature deaths per capita (physical) • Value of premature mortality (economic)[a]
Variants	• Mean estimate • High confidence interval • Low confidence interval
Data Shape	• Integer degree (1-6) • Six GCMs (standard CIRA set) • County-level
Runs Provided	• With socioeconomic growth and with climate change
Additional Data	• None

Notes:
a. The underlying Cromar et al. and Rennert et al. studies provide a mean and 90 percent confidence interval beta coefficient for excess relative risk associated with temperature changes (see Eq. 2). FrEDI pre-processing steps develop the projected county level mortality incidence and rates for each GCM, consistent with the data shape stated in this table.

Processing steps are shown in **Figure B-11**. Unlike most sectoral impacts where the underlying study provides either damages by degree or a trajectory of damages over time, the input 'data' from Cromar et al. (2022) are relative excess risk functions. Specifically, FrEDI uses the US-specific relative risk functions (Eq B-2) for incremental annual mortality associated with the net effect of heat and cold-related mortality for each incremental change in annual average temperature (β= 0.464%, from Table 3 of Cromar et al. 2022), and the standard errors of estimation for these functions.

$$\Delta Y = \left(1 - e^{-\beta \Delta Temp}\right) * Y_0 * Pop \qquad \text{(Equation B-2)}$$

Where $\Delta Temp$ is the temperature change; Y_0 is the baseline mortality rate or incidence (at county scale); Pop is the county level population; β is as stated above, taken from the underlying study; and ΔY is the change in mortality (rate or incidence).

Therefore, in the first and second pre-processing steps, the relative risk function is used with annual county-level mean temperatures (relative to the 1986-2005 baseline) for each temperature bin and GCM, county-level baseline mortality rates forecasted through the 21st century from EPA's BenMAP model[12], and default county-level populations from ICLUSv2 to calculate the net change in county-level mortality by degree and by GCM. The by-degree total county-level mortality counts are then aggregated to the state level, and converted to mortality rates (i.e., mortality per capita) by degree by dividing by the ICLUSv2 state population for each era of GCM integer degree of warming. This sector does not utilize any sector-specific scalars beyond FrEDI GDP and population inputs. Therefore, no scalar extensions are necessary to run the 2300 extension module.

FIGURE B-11. ATS EXTREME TEMPERATURE DATA PROCESSING FRAMEWORK

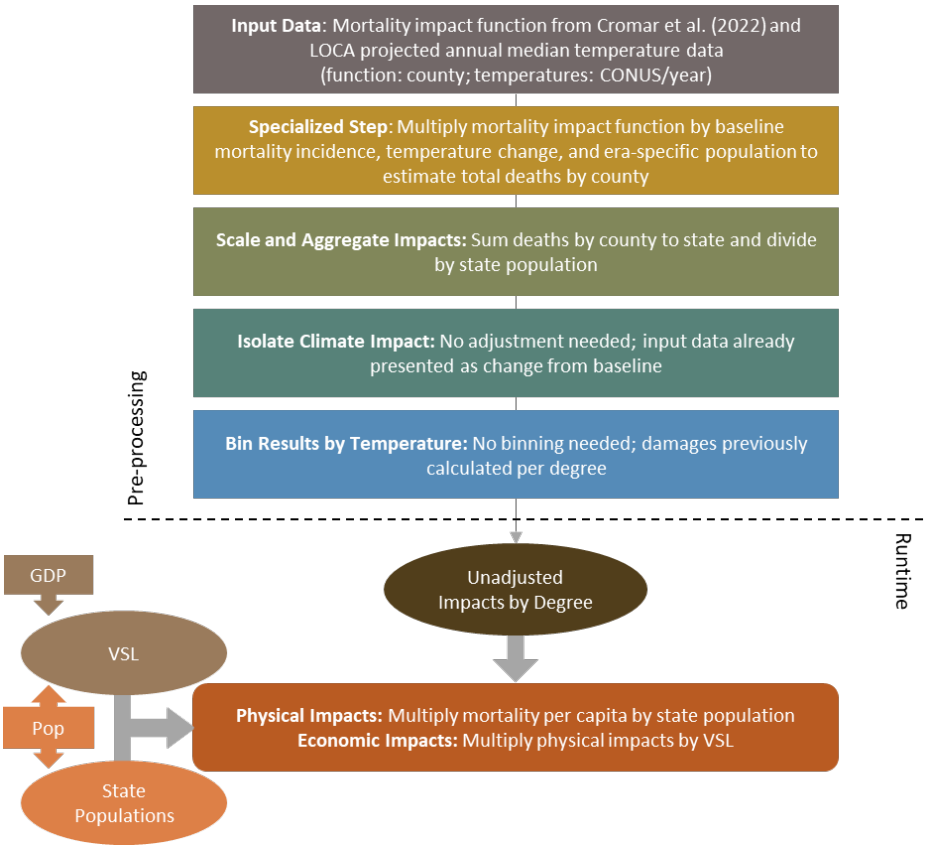

[12] EPA 2022, Environmental Benefits Mapping and Analysis Program – Community Edition, User's Manual. January 2022, Updated for BenMAP-CE Version 1.5.8. Available at: https://www.epa.gov/sites/default/files/2015-04/documents/benmap-ce_user_manual_march_2015.pdf

When FrEDI is run, the pre-processed by-degree per capita mortality functions are then applied to the input temperature scenario to calculate the unadjusted annual per capita impacts based on the level of warming in each year of the input scenario. The total annual physical mortality counts are then calculated by applying these annual per capita rates to the input population scenario. Lastly, annual mortality counts are monetized using the VSL, calculated at runtime from input GDP per capita (Eq. B-1). In addition to the mean results, this sector includes additional variants that reflect the 5th and 95th percentile results for the net impacts of cold and heat mortality. These estimates reflect statistical estimation uncertainty in the underlying Cromar et al. (2022) study, reported as the standard error on the health impact function relative risk result (see underlying study, Table 3 for detail).

Limitations and Assumptions

- The estimates added to the FrEDI tool for this revision do not incorporate adaptations to temperature changes beyond measures reflected in current practices, as established in the seven underlying studies of the Cromar et al. (2022) meta-analysis.
- The underlying studies focus on extreme temperature mortality impacts, and exclude impacts of extreme temperature on morbidity, so the Cromar et al. (2022) meta-analysis likely underestimates the full effect of temperature on health.
- For further discussion of the limitations and assumptions in the underlying sectoral model, please see Cromar et al. (2022).

Southwest Dust

Summary

This sectoral study estimates the health burden and associated economic value of that burden resulting from changes in exposure to fine and coarse airborne dust due to climate change in the Southwest.

UNDERLYING DATA SOURCES AND LITERATURE

Achakulwisut, P., Anenberg, S. C., Neumann, J. E., Penn, S. L., Weiss, N., Crimmins, A., Fann, N., Martinich, J., Roman, H. A., & Mickley, L. J. (2019). Effects of increasing aridity on ambient dust and public health in the U.S. southwest under climate change. GeoHealth, 3(5), 127-144. Doi:10.1029/2019GH000187

Damages are based on the change in incidence of multiple physical morbidity and mortality outcomes, including all Cardiovascular, Respiratory, and Mortality, as well as Emergency Department visits due to Asthma, and Acute Myocardial Infarction. These are monetized using direct hospitalization costs, indirect loss of income from hospitalization, costs of emergency department visits, and (for premature mortality) the VSL.

For illustrative purposes, **Figure B-12** shows the resulting damages by degree of warming for each of the five health endpoints (or impact types) by GCM, calculated using 2010 (figure A) and 2090 (figure B) socioeconomics (i.e., the endpoints of the socioeconomic scenarios).

FIGURE B-12. SOUTHWEST DUST IMPACTS BY TEMPERATURE BIN DEGREE

A. 2010 SOCIOECONOMICS

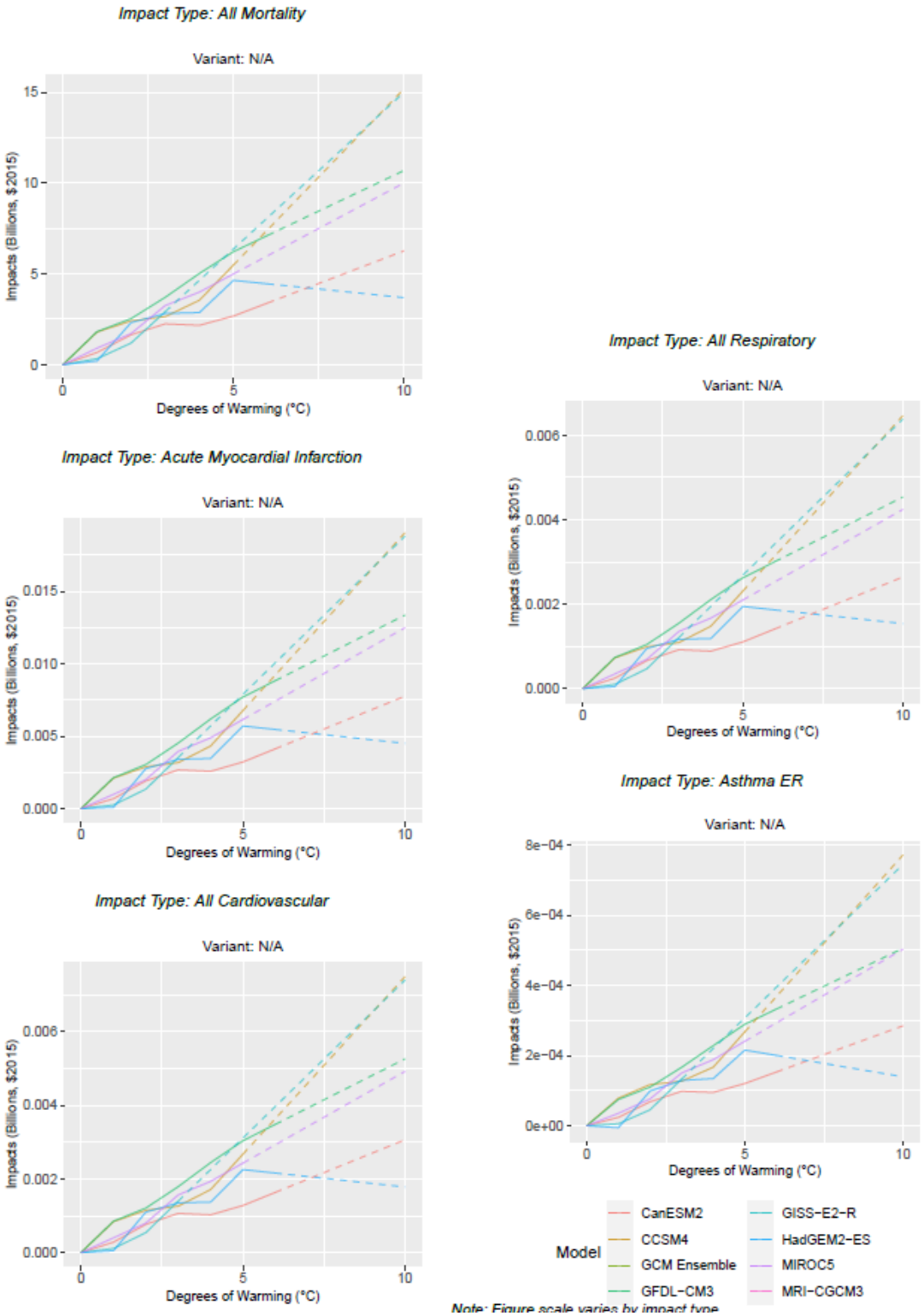

Note: Figure scale varies by impact type.

B. 2090 SOCIOECONOMICS

Impact Type: All Mortality

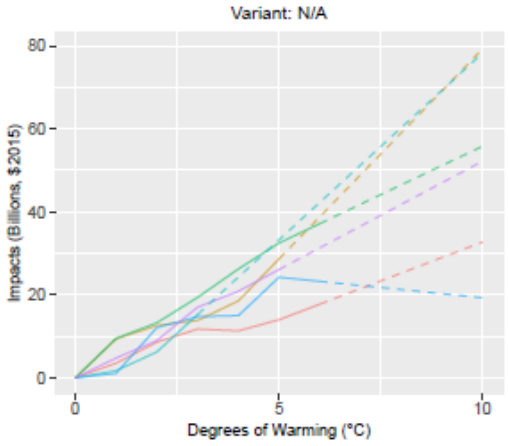

Impact Type: Acute Myocardial Infarction

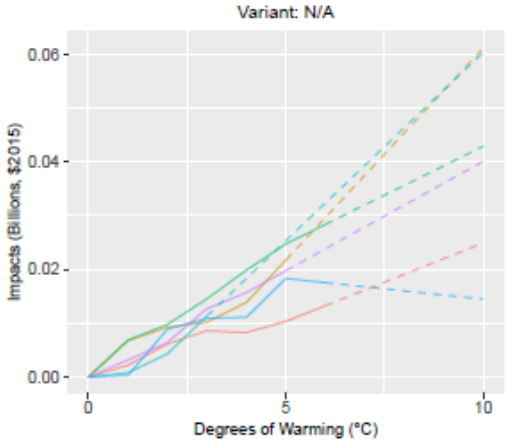

Impact Type: All Cardiovascular

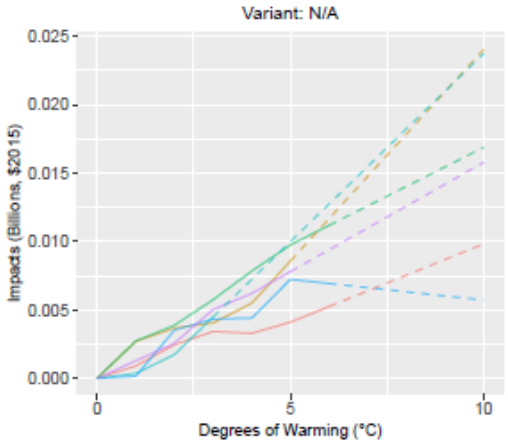

Impact Type: All Respiratory

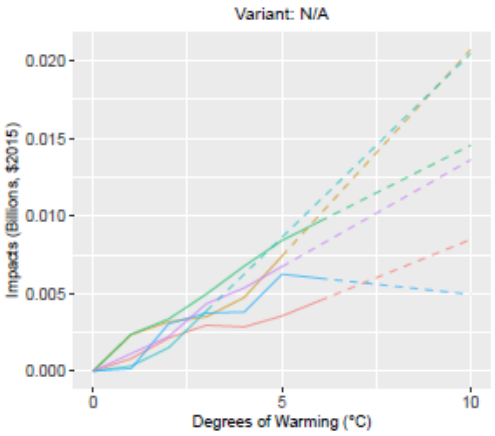

Impact Type: Asthma ER

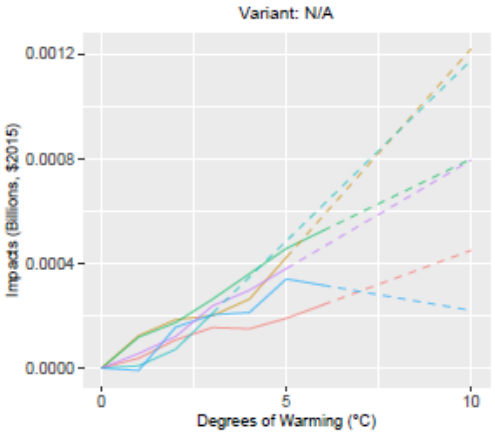

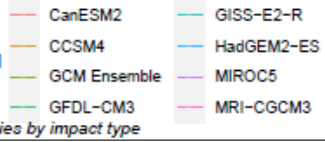

Note: Figure scale varies by impact type

Processing steps

Processing steps are illustrated in **Figure B-13**. Original results from Achakulwisut et al., (2019) are presented as percentage increases in the incidence of health impacts relative to baseline levels for affected populations — for example, percent increase in cardiovascular disease incidence for people over 65. These results already account for baseline incidence; therefore, no additional processing is needed to isolate climate impacts for use in FrEDI. Therefore, the last pre-processing step is to bin the average percentage increases in incidence of each health endpoint by degree of CONUS temperature change for each GCM by averaging across the eleven-year windows where each GCM reaches each integer degree of CONUS warming relative to the baseline. These by-degree incidence rates are then multiplied by the regional populations specific to each health endpoint (e.g., 65+ for cardiovascular disease) in the years 2010 and 2090 from ICLUSv2, and then divided by the total regional population (using 2010 and 2090 populations) to derive by-degree per capita incidence for each health endpoint (i.e., impact type) by GCM.

FIGURE B-13. SOUTHWEST DATA PROCESSING FRAMEWORK

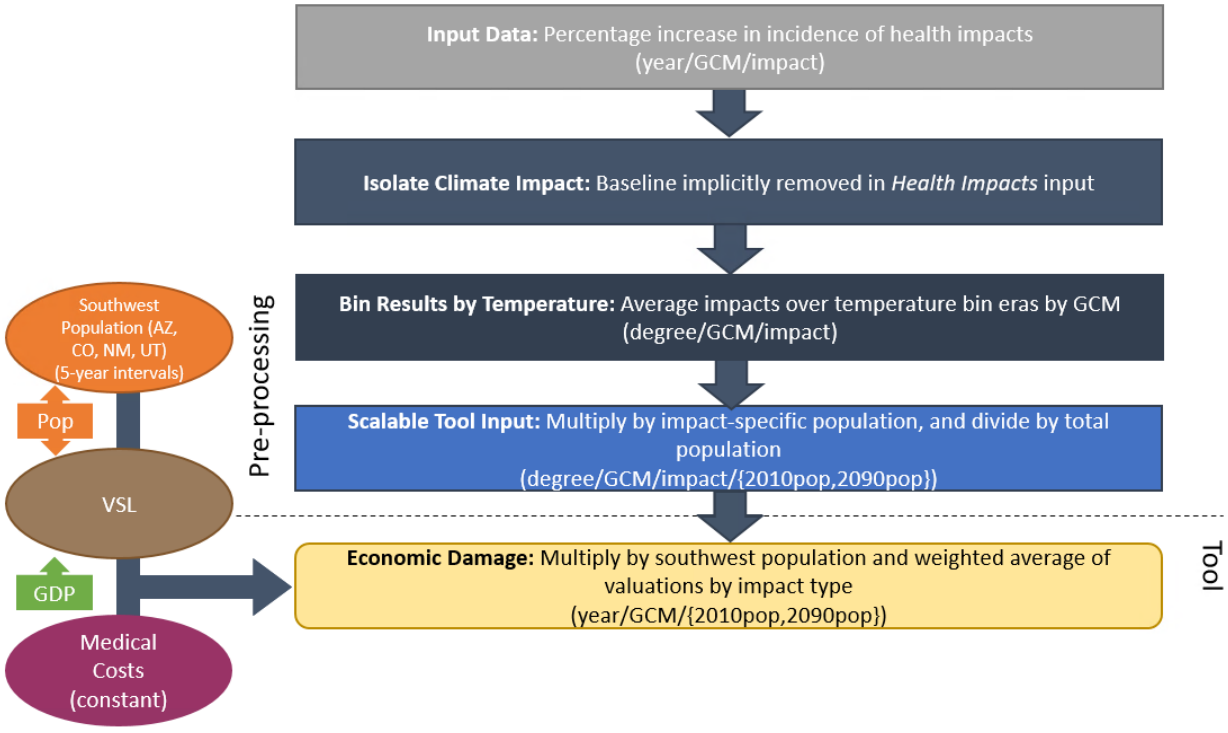

When FrEDI is run, the pre-processed by-degree per capita incidence functions for each health endpoint are then applied to the input temperature scenario to calculate the unadjusted annual per capita impacts based on the level of warming in each year of the input scenario. The total annual physical counts are then calculated by applying these annual per capita rates to the input population scenario. Lastly, physical impacts are monetized by multiplying these impacts by the average medical costs. Medical costs are variable across health impacts and constant overtime. Annual mortality counts are monetized using the VSL, calculated at runtime from input GDP per capita (Eq. B-1).

Limitations and Assumptions

- While dust exposures are known to be large in the southwestern U.S., this analysis does not consider health effects from coarse and fine dust in other regions of the U.S.
- This sector relies on population for a section of the Southwest region (Arizona, Colorado, New Mexico, Utah) to calculate damages across impact types. The scaling of damages by this population allows for custom inputs of socio-economic estimates but may introduce error if the age demographics of the population are not roughly constant over the simulation period.
- For further discussion of the limitations and assumptions in the underlying sectoral model, see Achakulwiset et al. (2019).

Valley Fever

UNDERLYING DATA SOURCES AND LITERATURE

Gorris, M. E., Neumann, J. E., Kinney, P. L., Sheahan, M., & Sarofim, M. C. (2020). Economic Valuation of Coccidioidomycosis (Valley Fever) Projections in the United States in Response to Climate Change. Weather, Climate, and Society, 13(1), 107-123. Doi:10.1175/WCAS-D-20-0036.1

Summary

This sectoral study estimates the health burden and economic value associated with climate change-related Valley fever incidence. Valley fever is a prevalent disease in the hot and dry Southwest region of the U.S. but is expected to expand in geographic scope with warming. Therefore, this analysis quantifies Valley fever impacts across the CONUS, with most of the burden in the Southwest.

Impacts are based on the change in number of Valley fever cases and the probability of a range of morbidity outcomes. These outcomes are monetized using direct hospitalization costs, costs of emergency department visits, costs of physician visits, indirect cost of lost productivity from hospitalization, and the VSL (for premature mortality).

For illustrative purposes, **Figure B-14** shows the resulting damages by degree of warming for mortality, all morbidity, and lost wage end points, by GCM, calculated using 2010 (figure A) and 2090 (figure B) socioeconomics (i.e., the endpoints of the socioeconomic scenarios).

FIGURE B-14. VALLEY FEVER IMPACTS BY TEMPERATURE BIN DEGREE

A. 2010 SOCIOECONOMICS **B. 2090 SOCIOECONOMICS**

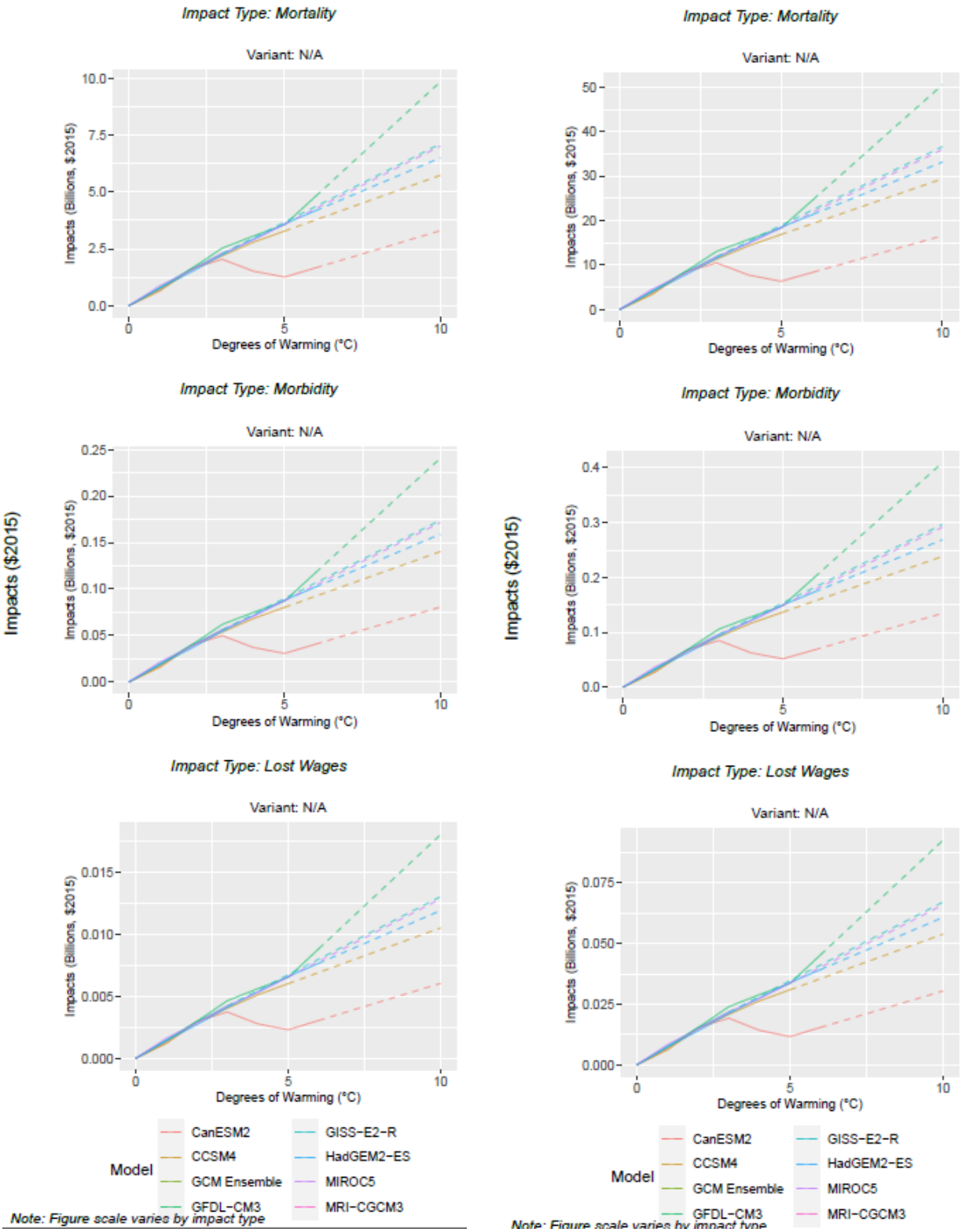

Processing steps

Processing steps are illustrated in **Figure B-15**. The Gorris et al. (2020) study authors provided the projected number of Valley fever cases at the county-level for 10-year eras centered on the years 2030, 2050, 2070, and 2090, for six GCMs. In the first pre-processing step, the impacts from climate change are isolated by subtracting the baseline incidence by county, for those Southwest counties that met an endemicity threshold for Valley fever in the baseline period (112 Southwest counties out of 216). A baseline of zero is assumed for all other counties with projected incidence.[13] To ensure that changes in incidence are relative to the FrEDI baseline (e.g., 1986-2005), the baseline incidence used in this pre-processing step are based on results derived from LOCA weather data instead of the baseline used in the underlying study[14]. In the next pre-processing step, the number of cases in each county are summed to the regional level, resulting in a total counts of Valley fever cases per region. These total impacts are then divided by dynamic ICLUSv2 regional population to calculate the cases per capita for each era, GCM, and region. Lastly, cases per capita for each era are interpolated to construct an annual timeseries of cases per capita, which are then binned by degree of CONUS temperature change for each GCM by averaging across the eleven-year windows where each GCM reaches each integer degree of CONUS warming relative to the baseline.

[13] Note that climate-attributed excess cases are estimated by comparison of the modeled future climate to the model baseline, using the two-stage approach developed in the paper. Incidence is only calculated in counties that meet an endemicity threshold. Therefore, there are two ways that cases can be attributed to climate change: 1. Endemicity thresholds are met in both the baseline and future climate, and so excess cases are the difference between the calculated incidence in future minus baseline; 2. Climate change causes a county to cross the endemicity threshold, in which all future cases are attributed to climate change. This approach is consistent with the current understanding of Valley fever incidence, which is that the fungus must first be established in the soil before a case attributed to exposure in the county can be inferred.

[14] Baseline incidence from the Gorris et al., (2020) study are from the Precipitation-Elevation Regressions on Independent Slopes Model (PRISM). The PRISM baseline provides total regional incidence, but does temporally align with the FrEDI baseline period and therefore impacts are re-based during this pre-processing stage.

FIGURE B-15. VALLEY FEVER PROCESSING FRAMEWORK

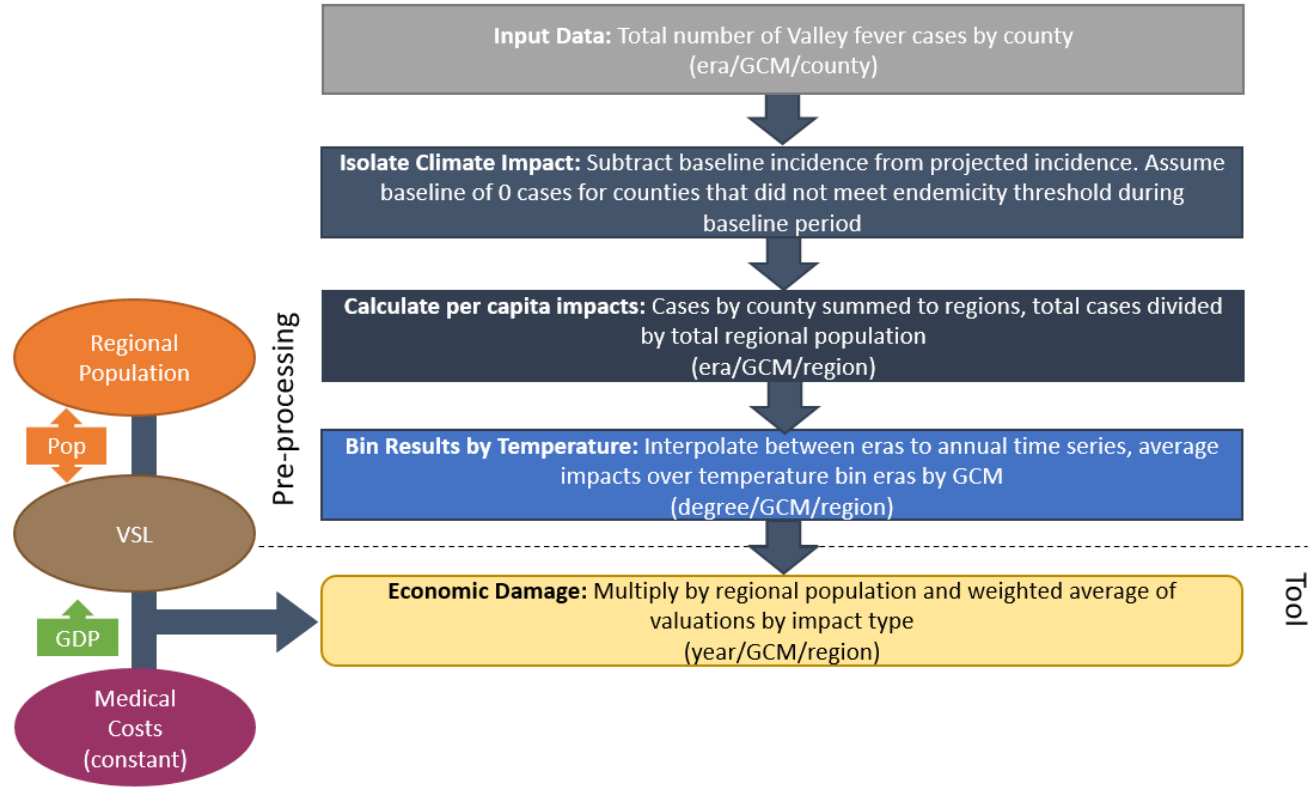

When FrEDI is run, the pre-processed by-degree per capita incidence functions for each endpoint are then applied to the input temperature scenario and weighted by the occurrence rates of each to calculate the unadjusted annual per capita impacts based on the level of warming in each year of the input scenario. For example, based on prior literature, morbidity outcomes are expected to occur in 96 percent of Valley fever cases. The annual totals for each endpoint are then calculated by applying these annual per capita rates to the input population scenario. Lastly, direct morbidity impacts (direct hospitalization, emergency room visit with discharge, emergency room visit with hospitalization, and physician visit) are monetized based on an incidence-weighted average morbidity outcome, with the weights applied to the cost of illness value for each of the four mutually exclusive outcomes. Lost productivity costs in the form of lost wages associated with hospitalizations are monetized using likelihood of outcome and wage rate, scaled by user-input GDP per capita. Mortality is also expected to occur in four percent of Valley fever cases and these physical impacts are monetized using the VSL, calculated at runtime from input GDP per capita (Eq. B-1).

Limitations and Assumptions

- This analysis assumes a baseline of zero cases for counties that did not meet the endemicity threshold in the Southwest region during the baseline period and all counties with projected Valley fever cases outside of the Southwest region.
- For further discussion of the limitations and assumptions in the underlying sectoral model, see Gorris et al. (2020).

Wildfire

Summary

This sectoral study estimates health impacts from wildfire emissions and response costs from wildfire suppression. Neumann et al. (2021) models change in wildfire activity for the western region of CONUS. As such, response costs are limited to this area, but this study models health impacts of the particulate matter from western wildfires across the CONUS (as these emissions typically travel eastward across the continent).

UNDERLYING DATA SOURCES AND LITERATURE

Neumann, J. E., Amend, M., Anenberg, S., Kinney, P. L., Sarofim, M., Martinich, J., Lukens, J., Xu, J., & Roman, H. (2021). Estimating PM2.5-related premature mortality and morbidity associated with future wildfire emissions in the western US. Environmental Research Letters, 16(3). Doi:10.1088/1748-9326/abe82b

Health impacts are based on the change in incidence of a range of morbidity and mortality outcomes, which are monetized using direct hospitalization costs, costs of emergency department visits, lost productivity, and (for mortality) the VSL. Response costs are estimated based on average wildfire response costs per acre burned, by state. For illustrative purposes, **Figure B-16** shows the resulting damages by degree of warming all mortality, response costs, and morbidity impact types by GCM, calculated using 2010 (figure A) and 2090 (figure B) socioeconomics (i.e., the endpoints of the socioeconomic scenarios).

FIGURE B-16. WILDFIRE IMPACTS BY TEMPERATURE BIN DEGREE

A. 2010 SOCIOECONOMICS **B. 2090 SOCIOECONOMICS**

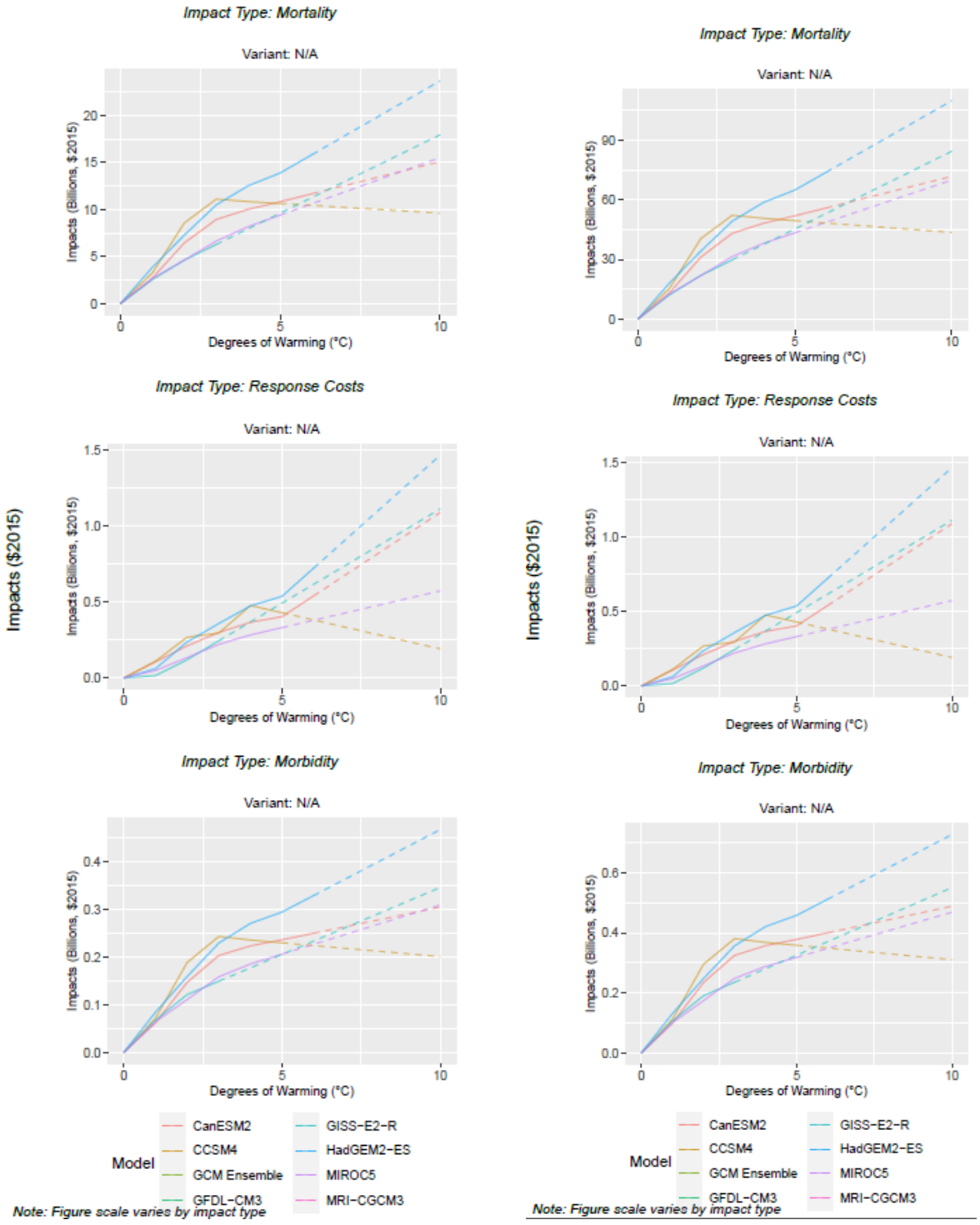

Processing steps

TABLE B-4. INPUT DATA CHARACTERISTICS: WILDFIRE

Data Features	Wildfire Attributes
Evaluated Impacts	• Mortality: premature deaths per capita (physical) and value of premature mortality (economic) • Morbidity: value of morbidity incidence (economic) • Response cost: acres burned (physical) and response costs (economic)
Variants	• No additional adaptation
Data Shape	• Annual • GCMs (standard CIRA set) • State level
Runs Provided	• With climate change, with and without population growth
Additional Data	• None

Processing steps are illustrated in **Figure B-17**. Data for each impact type (mortality, morbidity, and response costs) are each processed separately.

For mortality, the Neumann et al., (2021) study authors provided state-level mortality incidence attributable to climate change-related changes in $PM_{2.5}$ concentrations resulting from wildfires, for two 10-year eras centered on 2050 and 2090 and five GCMs. This analysis considers mortality estimated using a concentration-response function based on risk model information specific to those age 30 and older. In the first pre-processing step, the excess health burden associated with climate-induced changes in wildfire activity is isolated by subtracting incidence from a synthetic "no wildfires" mortality scenario (using the Localized Constructed Analogs, or LOCA data) from the projected incidence with wildfires. This technique allows identification of air quality and health effects associated solely with wildfire. In the next pre-processing step, climate change-related mortality incidence is then divided by dynamic ICLUSv2 state-level population for each era to calculate mortality per capita for each era/GCM/state scenario. Finally, an annual time series of incidence per capita is constructed by linearly interpolating between era values, and yearly impacts are binned by degree of CONUS temperature change for each GCM by averaging across the eleven-year windows where each GCM reaches each integer degree of CONUS warming relative to the baseline.

For morbidity, the Neumann et al., (2021) study authors provided state-level morbidity incidence and valuation for the same 10-year eras centered on 2050 and 2090 and five GCMs. To represent this morbidity impact type in FrEDI, the valuation is summed across a set of health endpoints to determine one value associated with all morbidity impacts, representing cost of illness and lost productivity for each era/GCM/state scenario.[15] In the first pre-processing step, the baseline valuation is subtracted from the

[15] Full list of health endpoints includes: acute bronchitis, nonfatal acute myocardial infarction, asthma exacerbation (cough, wheeze, shortness of breath), asthma emergency room visits, cardiovascular hospital admissions, asthma hospital admissions, chronic lung

2050 and 2090 projected valuation to isolate the impact of climate change on wildfire-related morbidity. In the following steps, the morbidity valuation for each era is then divided by state-level population, interpolated to construct an annual timeseries, and temperature binned by GCM-specific eleven-year windows to generate state-level morbidity damages per capita by degree damage functions.

For the response costs, the Neumann et al. (2021) study authors provided data on the acres burned by year, GCM, and state (excluding states within the Midwest, Northeast, and Southeast regions). In the first pre-processing step, acres burned in the baseline is subtracted from the projected acres burned values. As this endpoint is not dependent on population, the next step temperature bins the acres burned per state across the GCM-specific eleven-year windows to derive acres burned per state per degree damage functions. For this impact type, state-level response costs per acre from the original study are also input as an economic scalar in FrEDI. Response costs per acre remain constant across the century.

FIGURE B-17. WILDFIRE PROCESSING FRAMEWORK

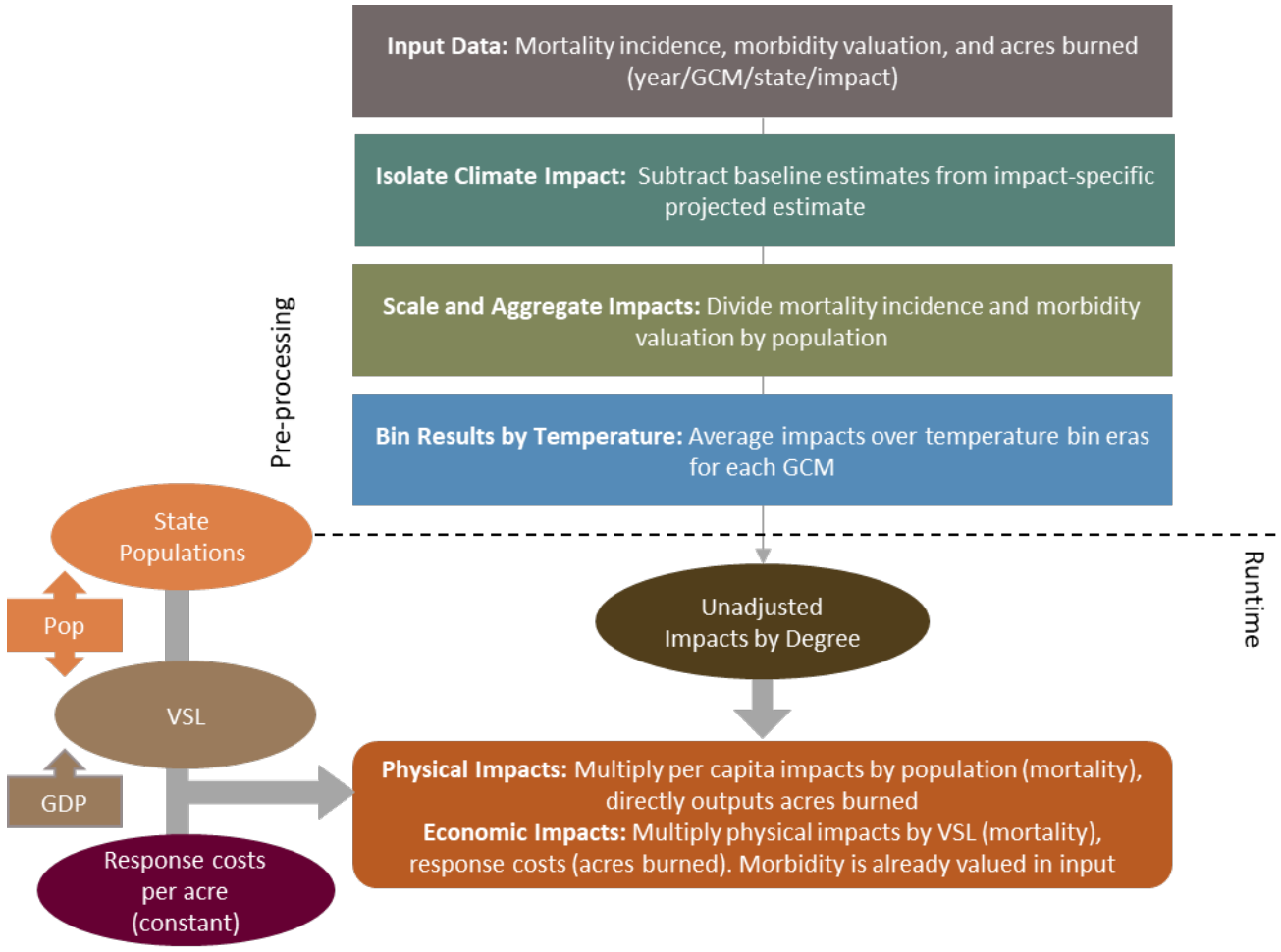

disease hospital admissions (less asthma), respiratory hospital admissions, lower respiratory symptoms, upper respiratory symptoms, work loss days, and minor restricted activity days.

When FrEDI is run, the pre-processed by-degree per capita impact (morbidity and mortality) and acres burned functions are then applied to the input temperature scenario to calculate the unadjusted impacts based on the level of warming in each year of the input scenario. The total annual physical mortality counts, and the total value of morbidity damages are then calculated by applying these annual per capita rates to the input population scenario. Lastly, annual mortality counts are monetized using the VSL, calculated at runtime from input GDP per capita (Eq. B-1) and suppression costs are monetized by scaling the acres burned by the response cost per acre burned economic scalar. Morbidity impacts are already valued.

Limitations and Assumptions

- Mortality incidence is quantified for those age 30 and older, and this analysis assumes the impacts for those under 30 to be zero. Doing so underestimates the risk of premature mortality experienced by those under 30. Additionally, doing so assumes that age demographics remain proportional over the century.
- Similarly, the morbidity health endpoints included in this analysis are associated with various age distributions. Total valuation is divided by state population, assuming the health burden outside of included age ranges is zero.
- For further discussion of the limitations and assumptions in the underlying sectoral model see Neumann et al. (2021).

CIL Crime

Summary

This sector addresses the impact of climate change on incidence of property and violent crime across all of CONUS. The Climate Impact Lab (CIL) Crime projections are drawn from a temperature response function derived from Jacob, Lefgren, and Moretti (2007), refined and tuned to data from Ranson (2014), and applied in Hsiang et al. (2017) to generate projected future climate impacts on crime occurrence by GCM and RCP through the 21st century.

UNDERLYING DATA SOURCES AND LITERATURE

Hsiang, S., Kopp, R., Jina, A., Rising, J., Delgado, M., Mohan, S., Rasmussen, D.J., Muir-Wood, R., Wilson, P., Oppenheimer, M., Larsen, K., and Houser T. (2017). Estimating economic damage from climate change in the United States, *Science*, 356, 1362–1369.

Jacob, B., Lefgren, L., and Moretti, E. (2007). The dynamics of criminal behavior, *J. Hum. Resour.*, 42, 489–527.

Ranson, M. (2014). Crime, weather, and climate change, *J. Environ. Econ. Manage.*, 67, 274–302.

Heaton, P. (2010). Hidden in Plain Sight: What Cost-of-Crime Research Can Tell Us About Investing in Police, RAND Corporation.

Data on costs of crime from Heaton (2010) and baseline incidence data from Hsiang et al. (2017) are used to construct region-specific costs for two categories of crime: property (robbery, burglary, larceny, and motor vehicle theft) and violent (murder, rape, and assault). For each category, the cost of crime is calculated as the incidence-weighted average of the costs of the included crimes.

The currently available results account for adaptation approaches only to the extent that they have been previously implemented within the studied populations. We anticipate that future revisions of FrEDI may incorporate a "with adaptation" variant that includes modelling of projected future adaptations. For illustrative purposes, **Figure B-18** shows the resulting damages by degree of warming violent and property crime, by GCM.

FIGURE B-18. CIL CRIME IMPACTS BY TEMPERATURE BIN DEGREE

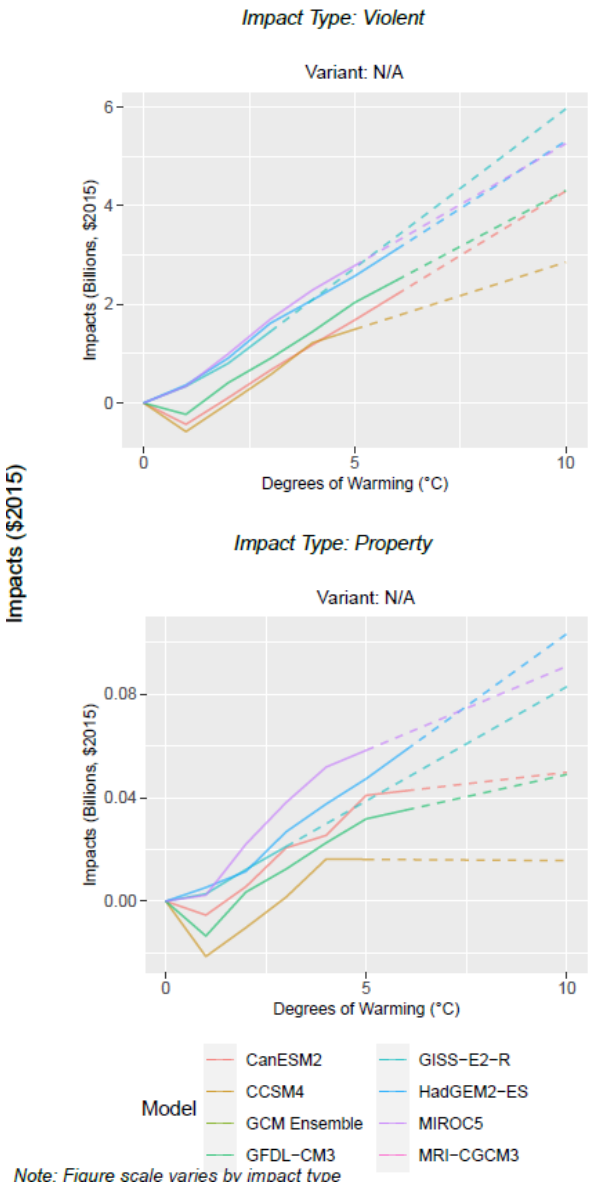

Note: Figure scale varies by impact type

Processing steps

Processing steps are shown in **Figure B-19**. The Hsiang et al., (2017) study authors provided data on the percent change in crime under RCP 8.5 as a function of GCM, year, state, and crime type, along with

baseline incidence by state and region for each category of crime averaged over the 2000-2005 period. While the authors provided a full distribution of impact results, FrEDI currently only accounts for the median estimate. In the first pre-processing step, the percent changes and baseline data by state are converted to incremental changes in the number of crimes and summed to the region level. In the second pre-processing step, the region-level annual incremental changes in crime are binned by degree of CONUS temperature change for each GCM by averaging across the eleven-year windows where each GCM reaches each integer degree of CONUS warming relative to the baseline. Region-specific incidence-weighted cost of crime estimates are also derived from the original study data and input as an economic scalar in FrEDI. These cost of crime estimates are drawn from the baseline incidence data and remain static for all projected years as the available documentation does not provide information on how or whether crime would scale with population, GDP, GDP per capita, or other socioeconomic driver data.

FIGURE B-19. CIL CRIME DATA PROCESSING FRAMEWORK

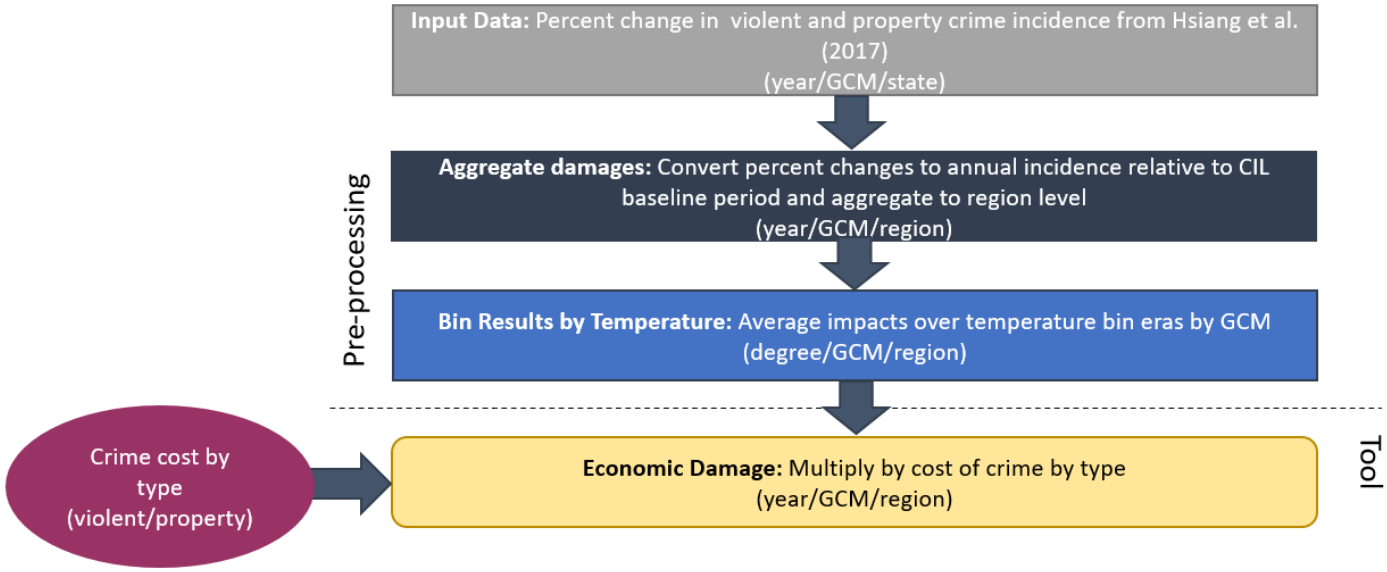

When FrEDI is run, the pre-processed by-degree crime functions are then applied to the input temperature scenario to calculate the unadjusted annual number of crimes based on the level of warming in each year of the input scenario. Lastly, the annual damages from both types of crime are monetized by multiplying these incremental changes in incidence by the region-specific, incidence-weighted cost of crime economic scalar estimates.

Limitations and Assumptions

- These projections of crime incidence do not account for future changes in population or other socioeconomic drivers. Because the incidence is not scaled with socioeconomic growth, it is likely that we underestimate future impacts. For reference, the standard CIRA data inputs imply that

population would grow by approximately 50%, and GDP would grow by about a factor of 5 over the 21st century.

- These projections use static values for the region-specific weighted costs of property and violent crime. It is possible that at least some components of the costs of property and violent crime could grow over time – for example a VSL for victims of murder, or the value of property damaged or stolen – but because the incidence is aggregated we are currently unable to assess the possible growth in these costs per incidence over time.
- For further discussion of the limitations and assumptions in the underlying sectoral model, please see Hsiang et al. (2017).

Vibriosis

Summary

UNDERLYING DATA SOURCES AND LITERATURE

Sheahan, M., Gould, C.A., Neumann, J.E., Kinney, P.L., Hoffmann, S., Fant, C., Wang, X. and Kolian, M. (2022). Examining the Relationship between Climate Change and Vibriosis in the United States: Projected Health and Economic Impacts for the 21st Century. *Environmental Health Perspectives*, 130(8). doi:https://doi.org/10.1289/ehp9999a.

This sectoral study estimates the health burden and the associated economic value in the CONUS resulting from changes in vibriosis cases due to climate change. Vibriosis is an illness contracted through food (typically raw seafood) and waterborne exposures to various Vibrio species. Vibrio is a bacterium that is prevalent in marine environments. Warmer water temperatures increase the abundance of Vibrio species in saltwater environments, and warmer air temperatures can increase the likelihood that efforts to keep harvested seafood cool up to the point of consumption may fail, leading to a higher risk of Vibrio infection.

The underlying study (Sheahan et al. 2022) uses CDC data on historical Vibrio infections and the severity of the resulting health effects, traces the infections to likely locations of exposure, and estimates the influence of environmental factors such as sea surface temperature on infection rates. The model of infection rates is then used to develop estimates of projected cases of vibriosis for future climate change scenarios. While the route of exposure is limited to marine coastal environments, the transport of seafood across the country means that infections can occur almost anywhere. Regional results reported in FrEDI are based on coastal exposure locations, not locations where seafood might be consumed. Damages are based on estimates of monetized direct medical costs, lost workdays, and changes in mortality outcomes. Lost workdays are monetized through estimated daily wage rate, and mortality outcomes through VSL.

For illustrative purposes, Figure B-20 shows the resulting damages by degree of warming for the mortality, direct medical cost, and lost days impact types by GCM, calculated using 2010 (figure A) and 2090 (figure B) socioeconomics (i.e., the endpoints of the socioeconomic scenarios).

FIGURE B-20. VIBRIO IMPACTS BY TEMPERATURE BIN DEGREE

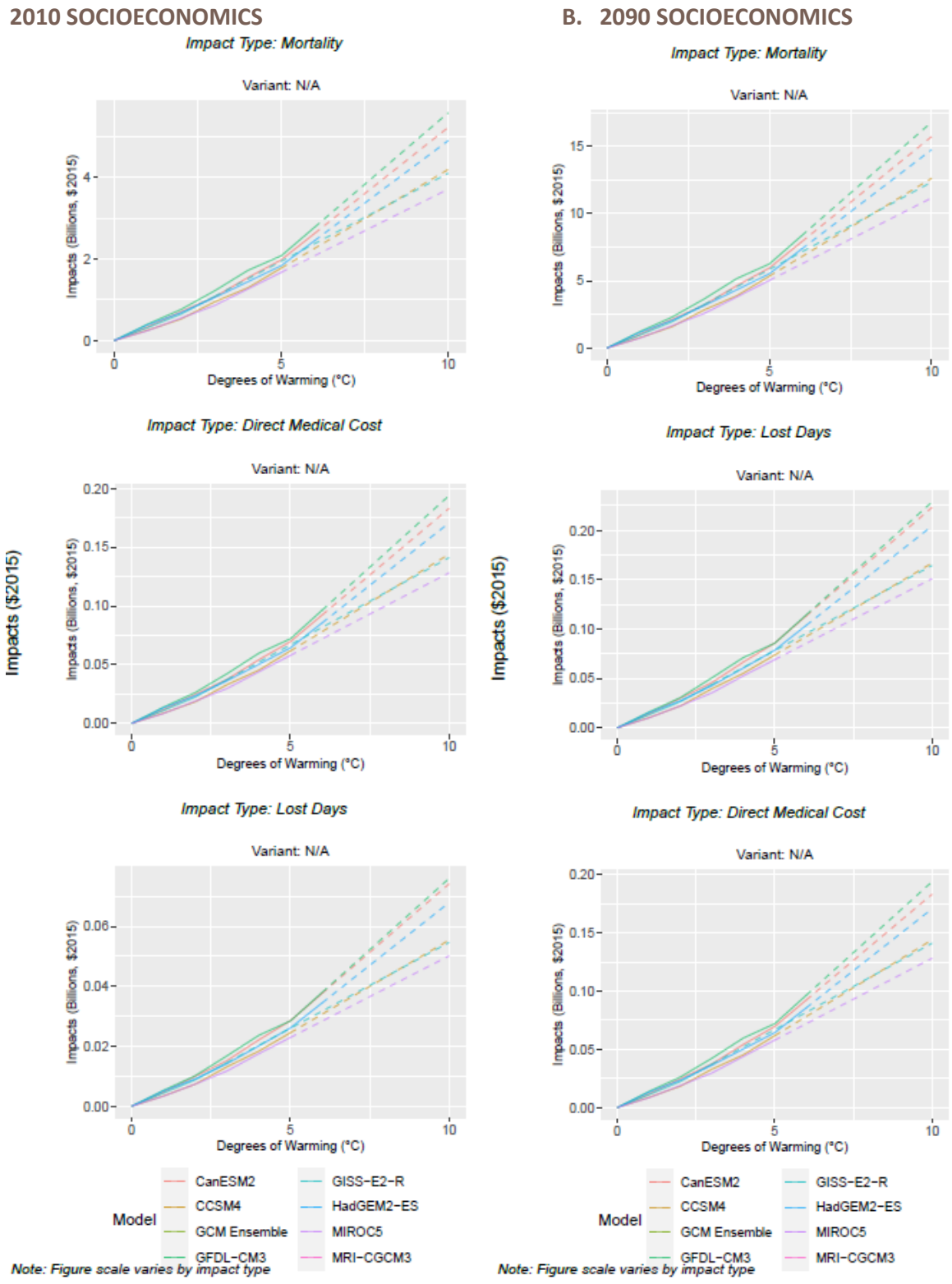

Processing steps

Processing steps are illustrated in **Figure B-20**. Original data provided by the Sheahan et al., (2023) study authors include the increases in health impacts (direct medical costs, lost days, or mortality counts) for affected populations at the county level from 2006 to 2099. To isolate the climate impacts in the first pre-processing step, baseline values (provided by study authors) are subtracted from these yearly values and summed to region level. Direct Medical Cost values are also deflated from 2018 dollars to 2015 dollars to align with FrEDI's default dollar years. In the second pre-processing step, regional impacts are binned by degree of CONUS temperature change for each GCM by averaging across the eleven-year windows where each GCM reaches each integer degree of CONUS warming relative to the baseline.

FIGURE B-20. VIBRIO DATA PROCESSING FRAMEWORK

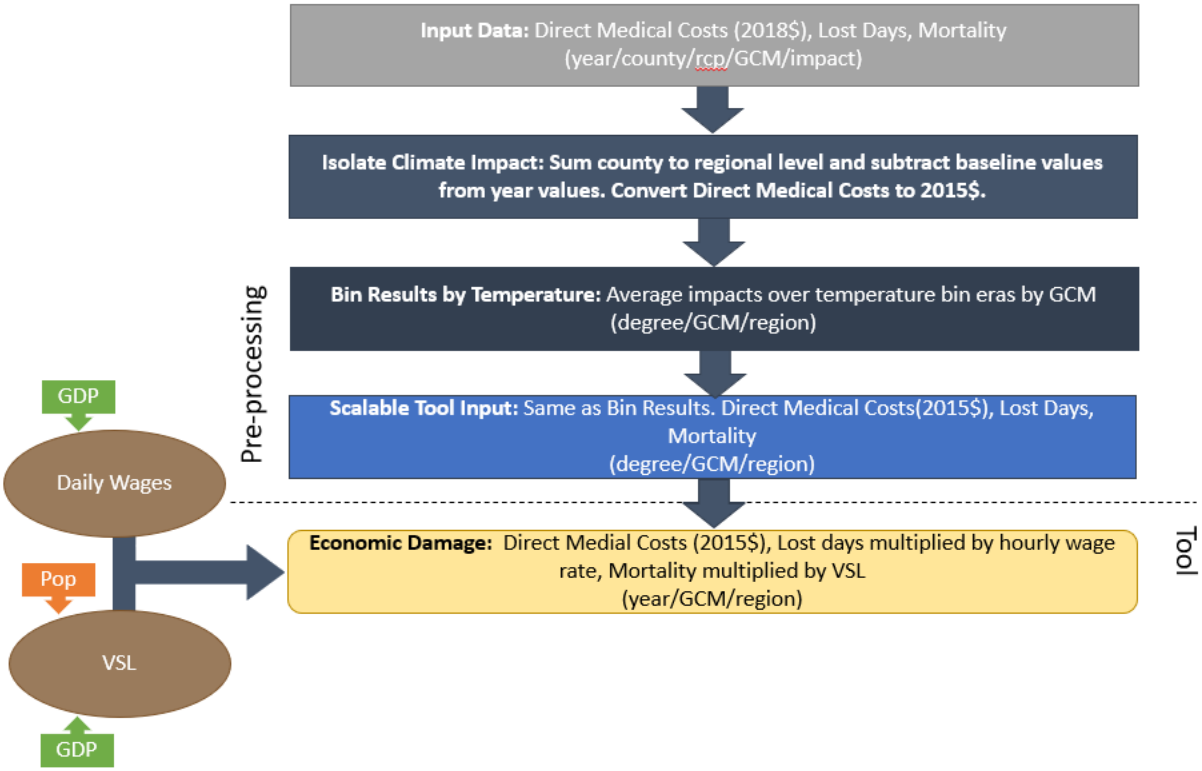

When FrEDI is run, the pre-processed by-degree impact functions are then applied to the input temperature scenario to calculate the unadjusted annual impacts based on the level of warming in each year of the input scenario. Note that population is not used in this calculation (see Limitations and Assumptions below). Lastly, annual mortality counts are monetized using the VSL, calculated at runtime from input GDP per capita (Eq. B-1) and lost days, which represent lost days of labor, are monetized using the daily wage rate scaled by user-input GDP per capita. Direct Medical Costs are already in dollar values and therefore only scale by the user-input temperature scenario.

Limitations and Assumptions

- The original study does not consider population growth in future case projections because the factors that drive vibriosis do not necessarily scale with population. Therefore, this processing does not provide per capita results to allow for population scaling.
- While the original study investigated the impact of changes in sea surface temperatures (related to GCMs) and vibriosis, this tool assumes changes in atmospheric temperature serve as a proxy for changes in baseline sea surface temperatures.
- For further discussion of the limitations and assumptions in the underlying sectoral model, see Sheahan et al. (2022).

Suicide

Summary

This sector addresses the impact of climate-driven changes in temperature and weather on suicide incidence for the population age 5 and older across CONUS using projections based on Belova et al. (2022).

UNDERLYING DATA SOURCES AND LITERATURE

Belova, A., Gould, C.A., Munson, K., Howell, M., Trevisan, C., Obradovich, N., and Martinich, J. (2022). Projecting the Suicide Burden of Climate Change in the United States. *GeoHealth* 6, no. 5. https://doi.org/10.1029/2021GH000580.

Mullins, J. T., & White, C. (2019). Temperature and mental health: Evidence from the spectrum of mental health outcomes. *Journal of Health Economics* 68, 102240. https://doi.org/10.1016/j.jhealeco.2019.102240.

The causative factors driving the association between temperature and suicide are not well understood, but evidence from other countries suggest that suicide by violent means is connected to elevated temperature, and hypothesized factors include sociological (e.g., increased alcohol use during heat waves), biological (e.g., effects on neurotransmitters such as serotonin which affect impulsivity and aggression), and psychological (e.g., temperature links to disinhibition and increased propensity for aggression and violence) components.[16]

Belova at al. (2022) assessed these effects using four different health impact function specifications developed primarily using results from Mullins & White (2019). Per the authors' recommendation, we use results from Belova et al. (2022) averaged across the four health impact function specifications. Changes in mortality are monetized by applying the GDP per capita adjusted VSL. Additional mental health effects from climate change have been suggested in the literature, but the scope of these quantitative results is limited to mortality from suicide. For illustrative purposes, **Figure B-21** shows the resulting damages by degree of warming by GCM, calculated using 2010 (figure A) and 2090 (figure B) socioeconomics (i.e., the endpoints of the socioeconomic scenarios).

[16] See Page, Lisa A., Shakoor Hajat, and R. Sari Kovats. "Relationship between Daily Suicide Counts and Temperature in England and Wales." *The British Journal of Psychiatry* 191, no. 2 (August 2007): 106–12. https://doi.org/10.1192/bjp.bp.106.031948.

FIGURE B-21. SUICIDE IMPACTS BY TEMPERATURE BIN DEGREE

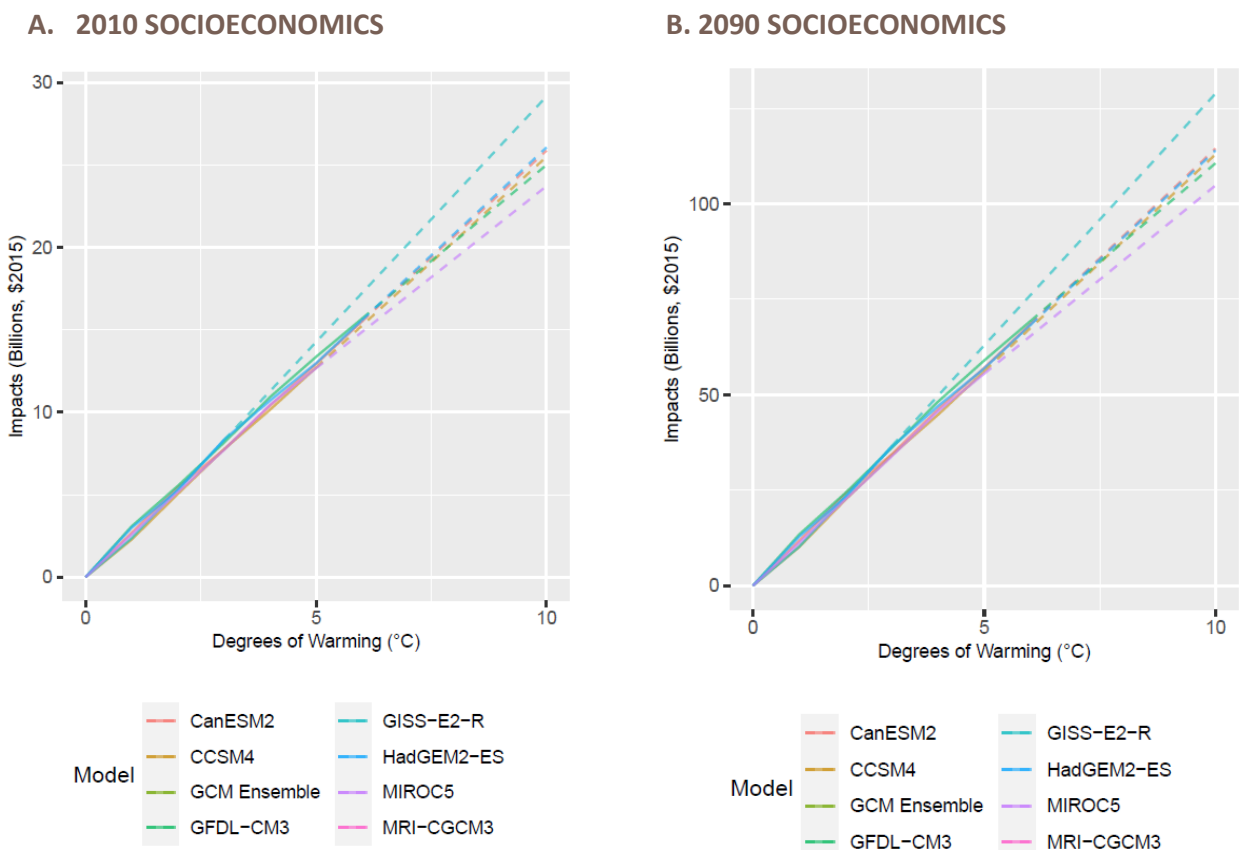

Processing steps

TABLE B-5. INCOMING DATA CHARACTERISTICS: SUICIDE

Data Features	Suicide Attributes
Evaluated Impacts	• Mortality: premature deaths per capita (physical) • Value of premature mortality (economic)
Variants	• None
Data Shape	• Integer degree (1-6) • Six GCMs (standard CIRA set) • County level • Age binned (5-24, 25-64, 65+)
Runs Provided	• With climate change, with and without population growth
Additional Data	• Population by age bin and county

Processing steps are shown in **Figure B-22**. The data provided by the Belova et al. (2022) study authors include baseline rates, populations, and the number of additional cases under RCP8.5 by GCM, county, age bin, and degree of warming for scenarios with and without population growth. We use the static population scenario for rate calculations and then apply scaling factors to account for demographic changes as

described below. While the authors also provided a distribution of impact results, FrEDI currently uses point estimates rather than the results of the Monte Carlo simulation.

In the first pre-processing step, populations and incremental additional case counts are aggregated to the state level by summing across age bins and counties. The case count is then divided by the impacted population (i.e., ages 5 and older) for each state to arrive at degree-binned future marginal incidence rates. Because these rates are only based on a subset of the total population (e.g., do not include all ages), a set of scalars is calculated during pre-processing to later adjust the user-input population when FrEDI is run. These scalars are calculated as the ratio of the 5+ population to the total population using the ICLUSv2 projections, which is the basis of FrEDI's default population scenario and the Belova et al. (2022) analysis.

An additional set of scalars also is calculated to account for dynamic demographic changes. The mortality projections from Belova et al. (2022) represent composite rates aggregated across age bins, and the underlying analysis includes implicit assumptions about how the relative weights of these age bins (and their corresponding incidence rates) change over time. For both the static and dynamic population scenarios provided by the authors, we calculate total incidence at the county level by multiplying the baseline rate by the population, adding the climate-attributable additional cases, and summing across age bins. We then sum case counts and populations to the state level and divide the total case count by population for each state to arrive at degree-binned future total incidence rates. Finally, we take the ratio of the dynamic population scenario rate to the static population scenario rate. Population is the only driver that varies between these two scenarios, so the ratio of the two represents the effect of demographic change on projected incidence rates. Both sets of scalars are calculated at the state level in all years for which we received data from the authors (the integer degree arrival years for the six included GCMs) and are used during FrEDI runtime to adjust calculated impacts.

FIGURE B-22. SUICIDE DATA PROCESSING FRAMEWORK

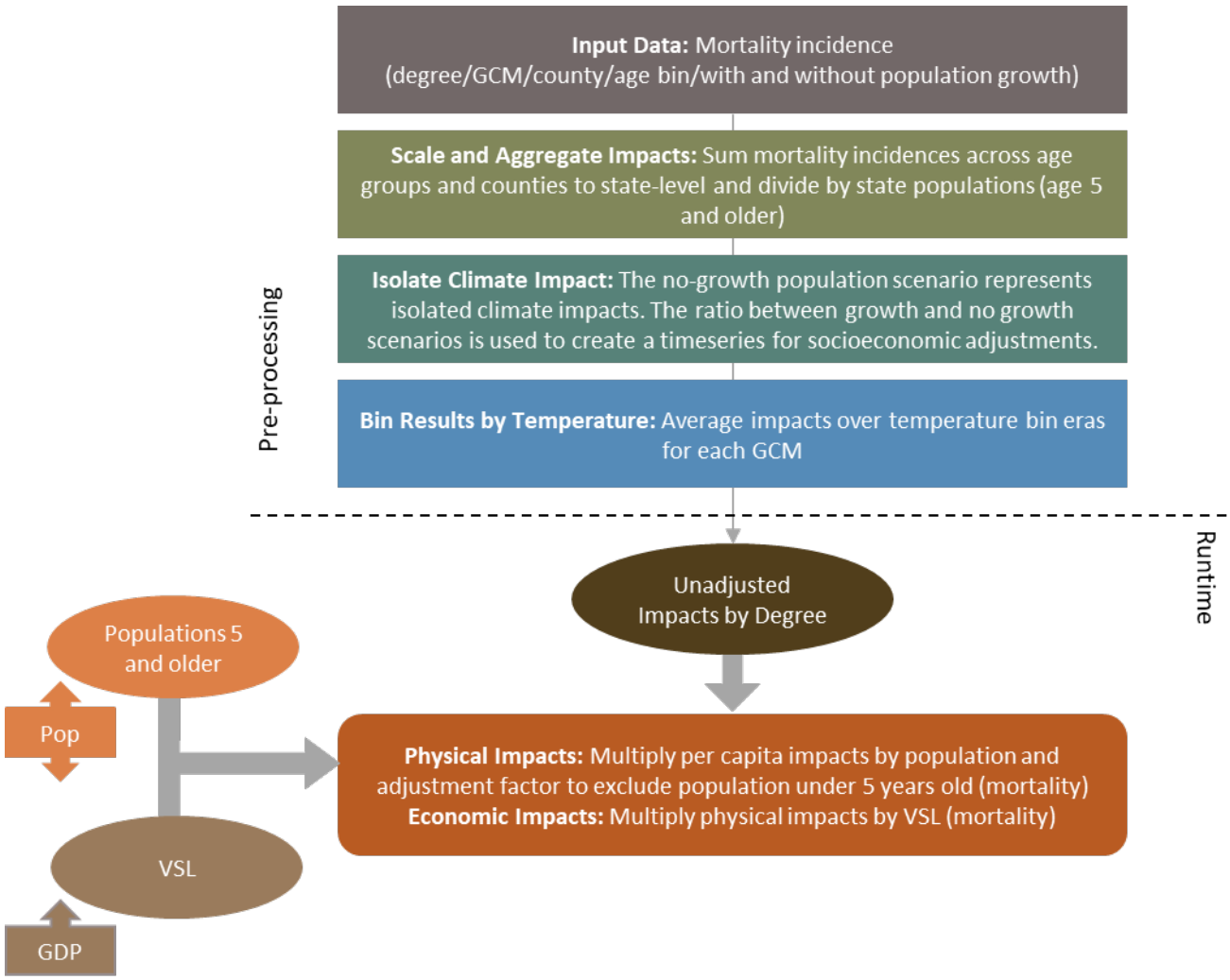

When FrEDI is run, the pre-processed by-degree per capita mortality functions are then applied to the input temperature scenario to calculate the unadjusted annual per capita impacts based on the level of warming in each year of the input scenario. The total annual physical mortality counts are then calculated by applying these annual per capita rates to the input population scenario, which are then scaled to account for changes in population demographics and to only include impacts to those age 5 and older. Lastly, annual mortality counts are monetized using the VSL, calculated at runtime from input GDP per capita (Eq. B-1).

Limitations and Assumptions

- There is some potential overlap in premature mortality of any type attributable to extreme heat (addressed in the Extreme Temperature, CIL Extreme Temperature, and ATS Extreme Temperature sectors) and suicide mortality attributed to high heat days in this sector. The effect is likely to be small because the "high heat day" metrics differ substantially, with a much lower threshold for high heat in the Belova et al. (2022) study used here.

- Based on communication with the authors of Belova et al. (2022), we use an average across the four impact function specifications here. Using an individual specification or a different subset of the four could alter estimates.
- These projections account for potential adaptation strategies only to the extent that they were implemented during the observation period of Belova et al. The potential for future adaptation efforts (e.g., expanded access to air conditioning, urban greening) and societal trends (e.g., increased recognition of mental health diagnoses and expanded access to mental health treatment) to reduce these impacts is not considered here.

B.3 Infrastructure Sectors

Coastal Properties

Summary

This sector study estimates future property value damages from combined sea level rise and storm surge in the CONUS, attributed to climate change.

UNDERLYING DATA SOURCES AND LITERATURE

Neumann, J. E., Chinowsky, P., Helman, J., Black, M., Fant, C., Strzepek, K., & Martinich, J. (2021). Climate effects on US infrastructure: the economics of adaptation for rail, roads, and coastal development. Climatic Change. https://doi.org/10.1007/s10584-021-03179-w

Lorie, M., Neumann, J. E., Sarofim, M. C., Jones, R., Horton, R. M., Kopp, R. E., Fant, C., Wobus, C., Martinich, J., O'Grady, M., Gentile, L. E. (2020). Modeling coastal flood risk and adaptation response under future climate conditions. Climate Risk Management, 29. Doi:10.1016/j.crm.2020.100233

Damages are estimated for all real properties (land and structure) in all coastal counties that contain land with a hydraulic connection to the ocean and containing property that is within 20 m elevation above sea level for the year 2000. Property values for potentially vulnerable structures and land are "market adjusted" assessed values that reflect 2017 property values for 302 counties along the CONUS coast – see Neumann et al. (2021) for details. Within the model, real property values appreciate over the century by GDP per capita projections.

The underlying damage simulation model includes cost estimates for no additional adaptation and two adaptation scenarios (reactive and proactive), as defined in the underlying study. Under the no additional adaptation scenario, properties are abandoned once inundated. Reactive adaptation loosely reflects structural adaptation options that can be adopted without collective action (e.g., elevation of structures and land near structures), while proactive adaptation includes consideration of options that likely require collective action (such as beach nourishment and construction of seawalls).[17] The model conducts a series of benefit-cost calculations at the level of a 150m x 150m grid cell to assess where and when adaptation could be cost-effective in mitigating property damage due to sea level rise and storm surge.

For illustrative purposes, **Figure B-23** shows the resulting damages overtime, by SLR scenario, for the three adaptation option variants included in FrEDI.

[17] The underlying study (Neumann et al. 2021) outlines the logic for classifying measures as reactive or proactive. The general concept is that reactive measures are either responsive to events (without foresight about future events) or can be undertaken without coordinated action between individuals and governments. Elevation, for example, is modeled at the individual property level in response to highly localized hazards, not as a collective action of municipal governments to modify building codes.

FIGURE B-23. COASTAL PROPERTIES IMPACTS BY SLR SCENARIO OVER TIME

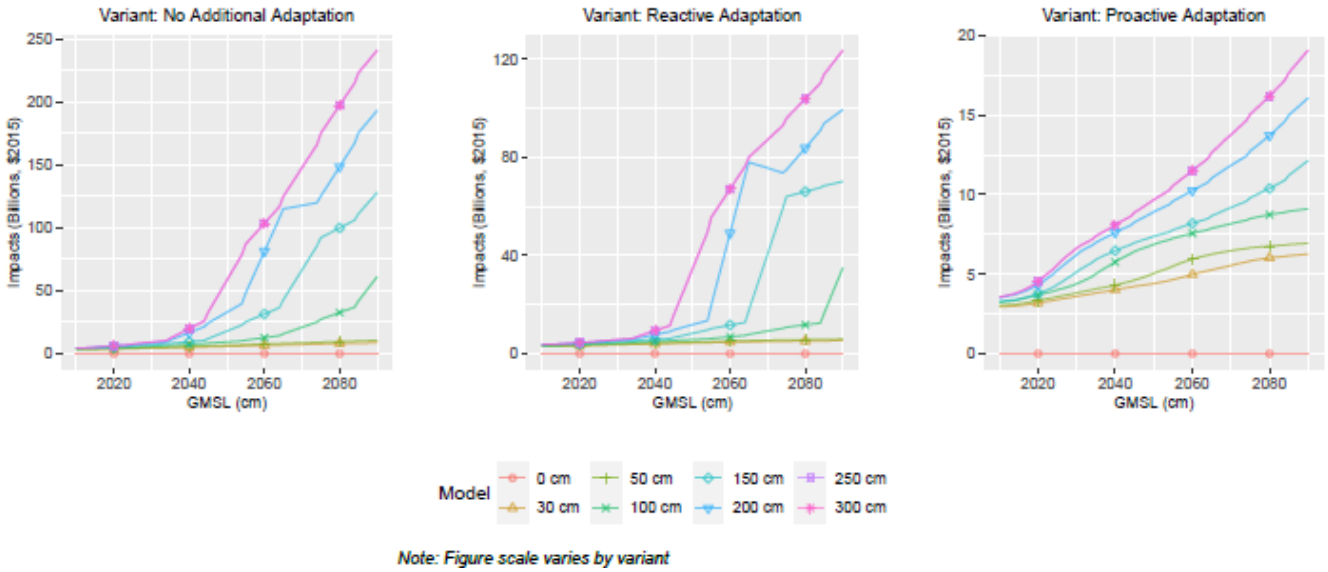

Note: Figure scale varies by variant

Processing steps

Processing steps are shown in **Figure B-24**. In the first pre-processing step, a trajectory of property damages that represent an 11-year rolling average of annual results from the underlying study are estimated for each sea level rise scenario, year, region, adaptation scenario, and for two static socioeconomic scenarios; 2010 and 2090. Residential and commercial properties, as well as energy infrastructure are considered when calculating potential damages in the underlying model. For this sector in FrEDI, the baseline is anchored at the year 2000, as the National Coastal Property Model (NCPM) starts with zero damages in this year. As with the temperature bin indexing, regional and local sea levels are mapped to GMSL based on the localized sea level rise projections from Sweet et al. (2017), which include effects such as land uplift or subsidence, oceanographic effects, and responses of the geoid and the lithosphere to shrinking land ice. When custom sea level rise scenarios are used as input in FrEDI, the relationship between GMSL and regional sea levels, and ultimately regional impacts, are mapped implicitly based on the underlying models.

As noted in the main report text, SLR is estimated separately from a reduced complexity model that incorporates the time- and trajectory-dependent qualities of SLR response to temperature. That implies that damages should be estimated along the trajectory using both the sea level height and the year that the sea-level height is reached (and therefore, that year's implicit socioeconomics).

FIGURE B-24. COASTAL PROPERTIES DATA PROCESSING FRAMEWORK

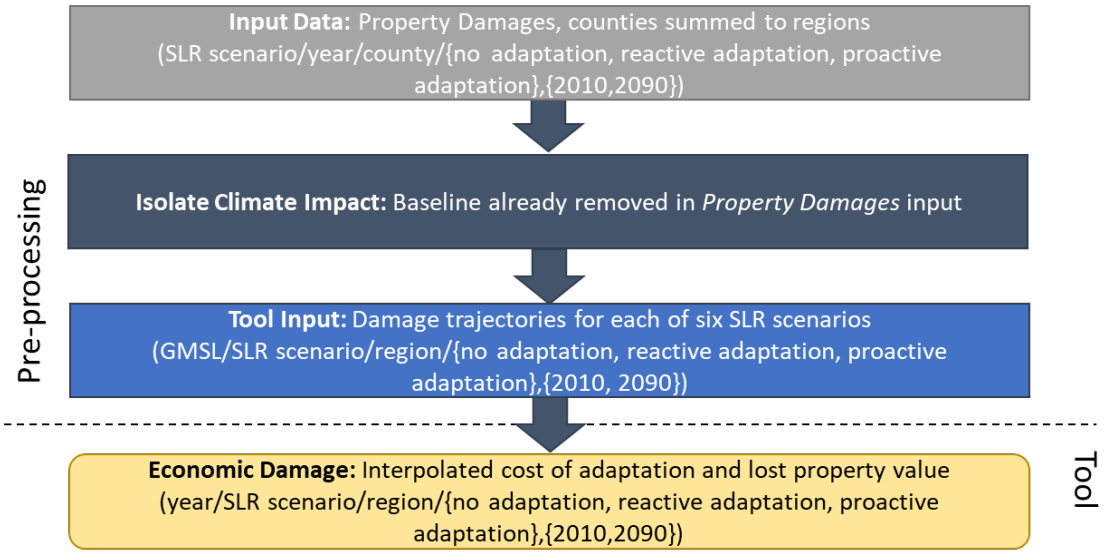

When FrEDI run, the damage trajectory is interpolated between the damage curves of the two underlying sea level rise scenarios that have sea level rise heights closest to the input scenario in any given year. For example, if the SLR trajectory reaches 175cm in 2080, the damage estimate would fall between the 150cm and 200cm scenarios for that year.

Limitations and Assumptions

- Damages are limited to land and structures within the study domain (i.e., flooding impacts to structures inland of 20m elevation are not quantified), and exclude the value of public infrastructure, which was not considered in the underlying sectoral study.
- Adaptation response decisions in the coastal zone are not typically made with strict cost-benefit decision rules, particularly at the local level. Other factors may include local zoning bylaws, future land use plans, the presence of development-supporting infrastructure, or proximity to sites with high cultural value. However, the analytical framework of this coastal property model provides a simple, benefit-cost decision framework that can be consistently applied for regional and national-scale analysis.
- The underlying study does not consider the effects of climate on storm surge activity (although impacts on wind damage are considered in a separate sector study included in the tool). The only non-climate change driven change to coastline considered was an increase in land and existing structure value over time.
- For further discussion of the limitations and assumptions in the underlying sectoral model see Neumann et al. (2021), Lorie et al. (2020), and USEPA (2017).

Transportation Impacts from High Tide Flooding

UNDERLYING DATA SOURCES AND LITERATURE

Fant, C., Jacobs, J. M., Chinowsky, P., Sweet, W., Weiss, N., Martinich, J. & Neumann, J. E. (2021). Mere nuisance or growing threat? The physical and economic impact of high tide flooding on US road networks. Journal of Infrastructure Systems. doi: 10.1061/(ASCE)IS.1943-555X.0000652

Summary

This sector study estimates the cost of delays to passenger and freight traffic on coastal roads in the CONUS that experience flooding due to combinations of high tides and sea level rise, as well as costs of adaptation in the form of infrastructure improvements.

Delay damages are in terms of passenger and freight vehicle-hours. These are monetized based on the value of travel time savings (VTTS) for passenger traffic, and the National Cooperative Highway Research Program's (NCHRP) inputs for cost of delay for freight traffic. Infrastructure improvements include building sea walls or elevating the elevation of the roadway surface. Infrastructure improvement costs include estimates of material, labor, and construction delays.

This sector in FrEDI considers three adaptation scenarios: no additional adaptation, reasonably anticipated adaptation, and direct adaptation. These adaptation scenarios differ from scenarios modeled for other infrastructure sectors. The no additional adaptation, reactive adaptation, and proactive adaptation scenarios of other infrastructure sectors are based on infrastructure development for an unchanging, current, or future climate in a given model time step. For this sector, the no additional adaptation scenario estimates costs of delays associated with flooding of roadways with the assumption that drivers do not re-route and instead wait until the roadway is clear to travel. The reasonably anticipated adaptation scenario assumes drivers re-route to avoid flooded roadways, with only slight delay due to increased travel time. This scenario also includes ancillary protection; in cases where flooded roadways are near properties that would be protected by sea walls or beach nourishment, this scenario assumes those roadways would also be protected and thus no longer flood.[18] In the direct adaptation scenario, where delay costs are high enough, roadways are either protected from flooding through construction of a sea wall or elevation of the road profile. For illustrative purposes, **Figure B-25** shows the resulting damages overtime by SLR scenario for the three adaptation variants available in FrEDI.

[18] Note that the including of ancillary protection of properties with sea walls in the "reasonably anticipated" category, consistent with the underlying Fant et al. (2021) study, may seem inconsistent with the classification of sea walls as "proactive" adaptation in the coastal properties sector. As outlined in the Fant et al. (2021) high-tide flooding paper, however, the impact of this potential inconsistency is slight - Figure 3 and accompanying text in that paper note that alternative routing reduces the no adaptation impacts by 77%, while the marginal additional impact of ancillary sea wall protection increases the total to an 80% reduction.

FIGURE B-25. HIGH TIDE FLOODING AND TRAFFIC IMPACTS BY TEMPERATURE BIN DEGREE

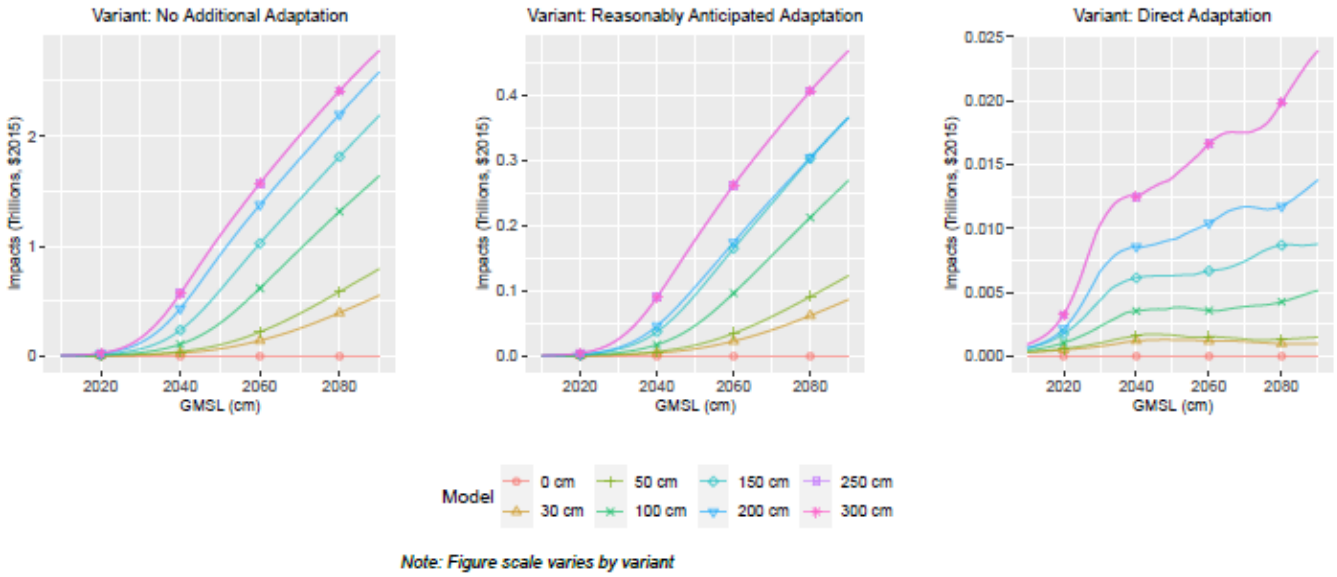

Note: Figure scale varies by variant

Processing steps

TABLE B-6. INCOMING DATA CHARACTERISTICS: TRANSPORTATION IMPACTS FROM HIGH TIDE FLOODING

Data Features	Transportation Impacts from High Tide Flooding Attributes
Evaluated Impacts	• Costs of delays and infrastructure improvements (economic)
Variants	• Direct adaptation • Reasonably anticipated adaptation • No additional adaptation
Data Shape	• Annual • Three adaptation scenarios • Six sea level rise scenarios • County level
Runs Provided	• With climate change, with socioeconomic growth
Additional Data	• None

Processing steps are shown in **Figure B-26**. Total traffic delay and adaptation costs at the county level are provided by the Fant et al. (2021) study authors. In pre-processing step one, these total costs are aggregated to the state level. These damages are available for all SLR scenarios, year, and adaptation scenario combinations. Annual damages are then calculated using the 11-year rolling average damages for each sea level rise scenario.[19] Similar to the Coastal Properties sector, this sector "zeroes out" in 2000, and thus has no baseline for which to adjust. This sector also relies on an interpolated damage estimation technique between results calculated in pre-processing for six SLR scenarios.

[19] This calculation utilizes an 11-year window when five years of data are available on either side of the central year. At the beginning and end of the time series, the window tightens to preserve balance around the central year.

FIGURE B-26. HIGH TIDE FLOODING AND TRAFFIC DATA PROCESSING FRAMEWORK

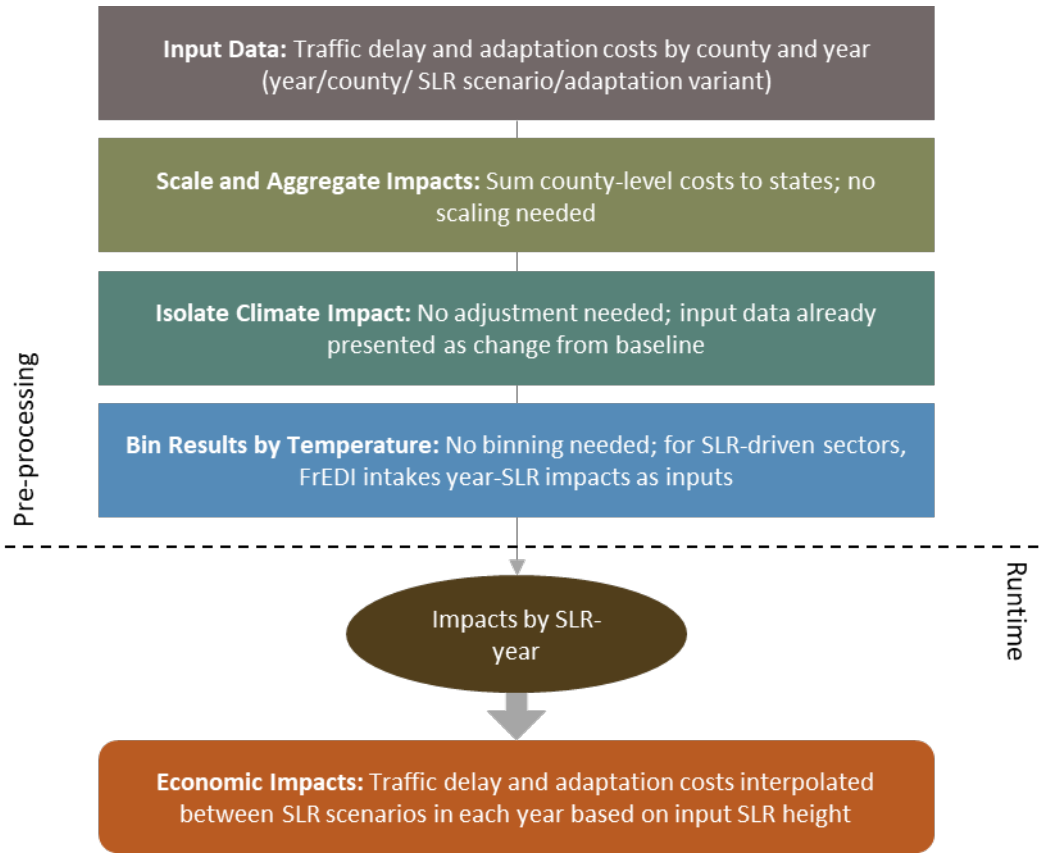

When the FrEDI R code is run, the damage trajectory is interpolated between the damage curves of the two underlying sea level rise scenarios that have sea level rise heights closest to the input scenario in any given year. For example, if the SLR trajectory reaches 175cm in 2080, the damage estimate would fall between the 150cm and 200cm scenarios for that year.

Limitations and Assumptions

- The underlying sectoral analysis is limited to road segments within the flood extent for the current minor flood level. This extent is expected to migrate further inland as sea levels rise. This analysis also omits consideration of impacts to underground roads.
- Flooding from rainfall or riverine flooding is not modeled and may exacerbate flood events or durations in the coastal zone if they occur simultaneously.
- Many direct adaptation options (e.g., hydrologic infrastructure) are not considered.
- The economic cost per hour of delay per passenger or freight vehicle is assumed to be constant over the century.
- For further discussion of the limitations and assumptions in the underlying sectoral model see Fant et al. (2021).

Rail

Summary

This analysis estimates repair, equipment, and delay costs to rail infrastructure due to rail track buckling or the risk of buckling in the CONUS associated with elevated temperatures. Damages are based on costs of repair, including equipment and labor, and delay costs. These costs are then scaled using total track miles in each state of CONUS.

UNDERLYING DATA SOURCES AND LITERATURE

Neumann, J. E., Chinowsky, P., Helman, J., Black, M., Fant, C., Strzepek, K., & Martinich, J. (2021). Climate effects on US infrastructure: the economics of adaptation for rail, roads, and coastal development. Climatic Change. https://doi.org/10.1007/s10584-021-03179-w

Chinowsky, P., Helman, J., Gulati, S., Neumann, J., & Martinich, J. (2019). Impacts of climate change on operation of the US rail network. Transport Policy, 75, 183-191. Doi:10.1016/j.tranpol.2017.05.007

The analysis is completed for each of three adaptation scenarios: no additional adaptation, proactive adaptation, and reactive adaptation. The no additional adaptation scenario incorporates no speed restrictions but results in a higher risk of track buckling associated with continued use of trains during high temperature events. Track buckling events require repairs that create delays. The reactive scenario considers reduced train speeds at higher temperatures to reduce likelihood of track buckling. The proactive scenario includes installation of temperature sensors to monitor probabilities of track buckling and modify train speeds as necessary (and therefore prevent delays associated with their unexpected need for repair). For illustrative purposes, **Figure B-27** shows the resulting damages by degree of warming for the three adaptation scenarios, by GCM, calculated using 2010 (figure A) and 2090 (figure B) socioeconomics (i.e., the endpoints of the socioeconomic scenarios).

FIGURE B-27. RAIL IMPACTS BY TEMPERATURE BIN DEGREE

A. 2010 SOCIOECONOMICS

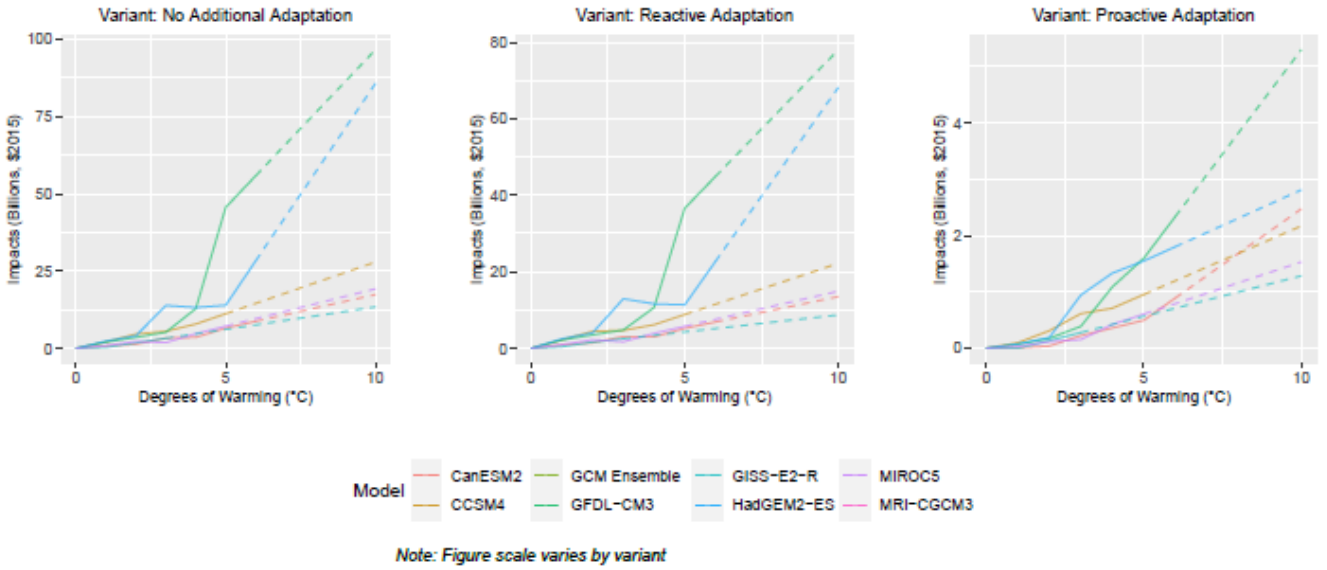

Note: Figure scale varies by variant

B. 2090 SOCIOECONOMICS

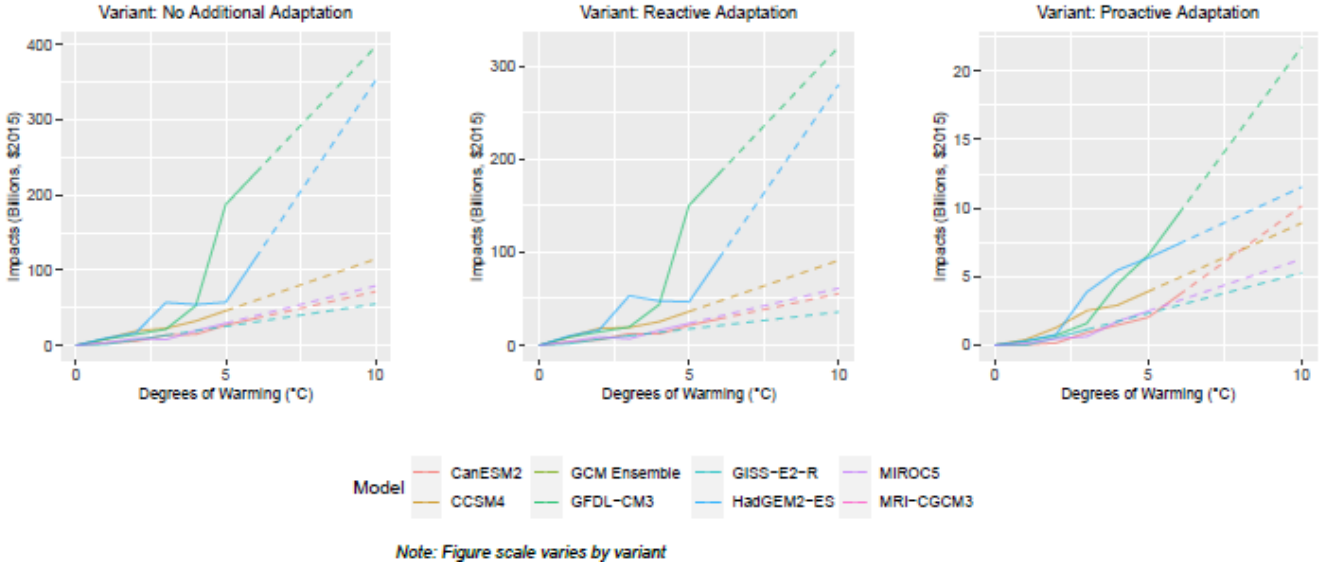

Note: Figure scale varies by variant

Processing steps

TABLE B-7. INCOMING DATA CHARACTERISTICS: RAIL

Data Features	Rail Attributes
Evaluated Impacts	• Rail Damage and Delay (economic)
Variants	• No Adaptation • Reactive Adaptation

Data Features	Rail Attributes
	• Proactive Adaptation
Data Shape	• Yearly projections 2006-2099 • Six GCMs (standard CIRA set) • ½ degree grid level
Runs Provided	• With socioeconomic growth and with climate change • With socioeconomic growth and without climate change (baseline runs; one baseline per adaptation scenario)
Additional Data	• Regional rail inventory • 2018 vintage ½ degree grid inventory

Processing steps are shown in

Figure B-28. The provided data from Neumann et al., (2021) reports damages at the Climatic Research Unit (CRU) ½ degree grid cell level. In the first pre-processing step, baseline costs from a reference scenario (i.e. costs under a no climate change scenario that include socioeconomic growth over the century) are subtracted for all adaptation scenarios to isolate the damages just due to climate change. There are unique baselines for each of the three adaptation scenarios. Across the three baselines, each 20-year period generally displays repeating patterns of year-to-year variation at different magnitudes. Thus, we take the mean of each 20-year period and subtract from its respective years' damages to sustain general trends in the baseline without being subjected to large variance year-to-year. In the second pre-processing step, net damages and track miles are then aggregated to the state level. The damages and track miles in grids that cross state lines are distributed relative to the percentage of grid area within each state. This impact model assumes that the spatial extent and distribution of rail infrastructure remains constant across the 21st century. In the next pre-processing steps, net damages are divided by total miles of rail within a state to produce damages per mile. Rail miles per state are developed by using a 2015 vintage ½ degree grid cell inventory[20] to determine state share of regional inventory and applying these weights to the regional inventory within FrEDI. Lastly, resulting annual net damages per mile are binned by degree of CONUS temperature change for each GCM by averaging across the eleven-year windows where each GCM reaches each integer degree of CONUS warming relative to the baseline.

[20] Bureau of Transportation Statistics (2015) National Transportation Atlas Databases – NTAD 2015, data available here: http://www.rita.dot.gov/bts/sites/rita.dot.gov.bts/files/publications/national_transportation_atlas_database/2015/index.html

FIGURE B-28. RAIL DATA PROCESSING FRAMEWORK

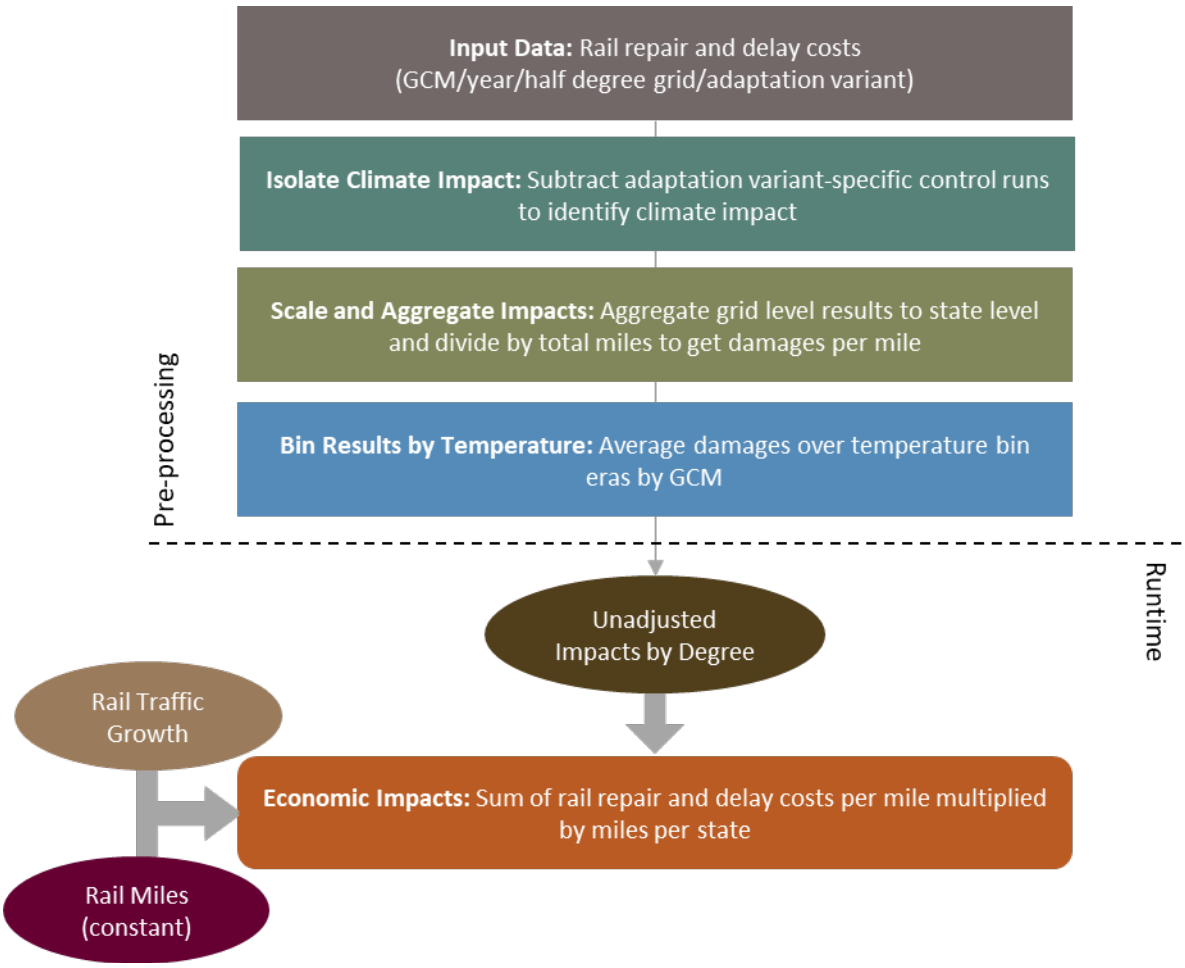

When FrEDI is run, the pre-processed by-degree impacts per mile functions are then applied to the input temperature scenario to calculate the unadjusted annual per mile impacts based on the level of warming in each year of the input scenario. Total damages are then calculated by applying these annual impacts per mile by the number of miles in a state, as well as a national socioeconomic growth scalar (with a 2010 base year). The scalar is calculated based on a ratio of a with and without growth scenario. Freight traffic represents 96 percent of rail traffic, and passenger traffic the remaining four percent.

Limitations and Assumptions

- The model assumes the number of rail miles is fixed and does not grow over time, though rail traffic over the existing rail network grows with a weighted average of population growth (for the passenger rail component) and economic growth (for the much larger freight rail component).
- Equipment, labor, and repair supply costs are assumed to remain constant.
- For further discussion of the limitations and assumptions in the underlying sectoral model see Neumann et al. (2021), Chinowsky et al. (2017), and EPA (2017).

Roads

Summary

This sector estimates the cost of road repair, user costs (vehicle damage), and road delays due to changes in road surface quality in the CONUS due to climate change (specifically changes in temperature, precipitation, and flooding).

UNDERLYING DATA SOURCES AND LITERATURE

Neumann, J. E., Chinowsky, P., Helman, J., Black, M., Fant, C., Strzepek, K., & Martinich, J. (2021). Climate effects on US infrastructure: the economics of adaptation for rail, roads, and coastal development. Climatic Change. https://doi.org/10.1007/s10584-021-03179-w

Neumann, J. E., Price, J., Chinowsky, P., Wright, L., Ludwig, L., Streeter, R., Jones, R., Smith, J. B., Perkins, W., Jantarasami, L., & Martinich, J. (2015). Climate change risks to US infrastructure: impacts on roads, bridges, coastal development, and urban drainage. Climatic Change, 131, 97-109. Doi:10.1007/s10584-013-1037-4

Damages are based on the cost of repairs and delays associated with either deteriorated road surfaces or road shutdowns to complete repairs, and delays are scaled by current period traffic, which in turn is adjusted for future changes in population (described further below). The per mile impacts are then multiplied by total state road miles and adjusted to reflect the likelihood of delay mitigation as proxied by an index of road density in each ¼ degree by ¼ degree grid cell, to produce a total damage estimate in a state.

Similar to the rail and coastal properties studies, the analysis models three adaptation scenarios: no additional adaptation, proactive adaptation, and reactive adaptation. In the no additional adaptation scenario, repairs to roads are limited to historic repair budgets; damages in this scenario are based on the cost of repairs to road surfaces, damage to vehicles associated with incompletely maintained roads, and delays associated with repairs to road surfaces or speed limitations attributed to poorly maintained roads.[21] Under the reactive adaptation scenario, repair budgets are increased to repair all damages in a given year to re-establish the pre-repair level of service. In the proactive scenario, roads are pre-emptively strengthened to prevent damage with consideration of future climate changes in the design and materials used for repair. Under the reactive and proactive adaptation scenarios, damages are based on the cost of repairs to road surfaces and the delays associated with repairs or speed limitations due to poorly maintained roads. The model considers three types of environmental stressors: temperature, precipitation, and flooding. Damages differ by road surface; road surfaces are either unpaved, paved, or gravel. This impact model runs at the quarter-degree grid cell level, and each grid cell is assigned adaptation-scenario specific budget for repairs.

For illustrative purposes, **Figure B-29** shows the resulting damages by degree for the three adaptation scenarios, by GCM, calculated using 2010 (figure A) and 2090 (figure B) socioeconomics (i.e., the endpoints of the socioeconomic scenarios). Note that the proactive adaptation results generally reflect a much lower damage estimate overall than no adaptation or reactive costs, but that in some scenarios the timing of those costs may be accelerated (and actually be triggered by relatively modest levels of warming) because

[21] The budget constraint in the no adaptation scenario can be thought of as a resilience threshold. For small amounts of warming, roads and their maintenance systems are adequate to meet increased stress. Once that resilience threshold is exceeded, costs increase quickly as road damage occurs.

of optimization of the capital cost of resilience investments and the high payoff to these investments in terms of avoiding future repairs and delays.

FIGURE B-29. ROADS IMPACTS BY TEMPERATURE BIN DEGREE

A. 2010 SOCIOECONOMICS

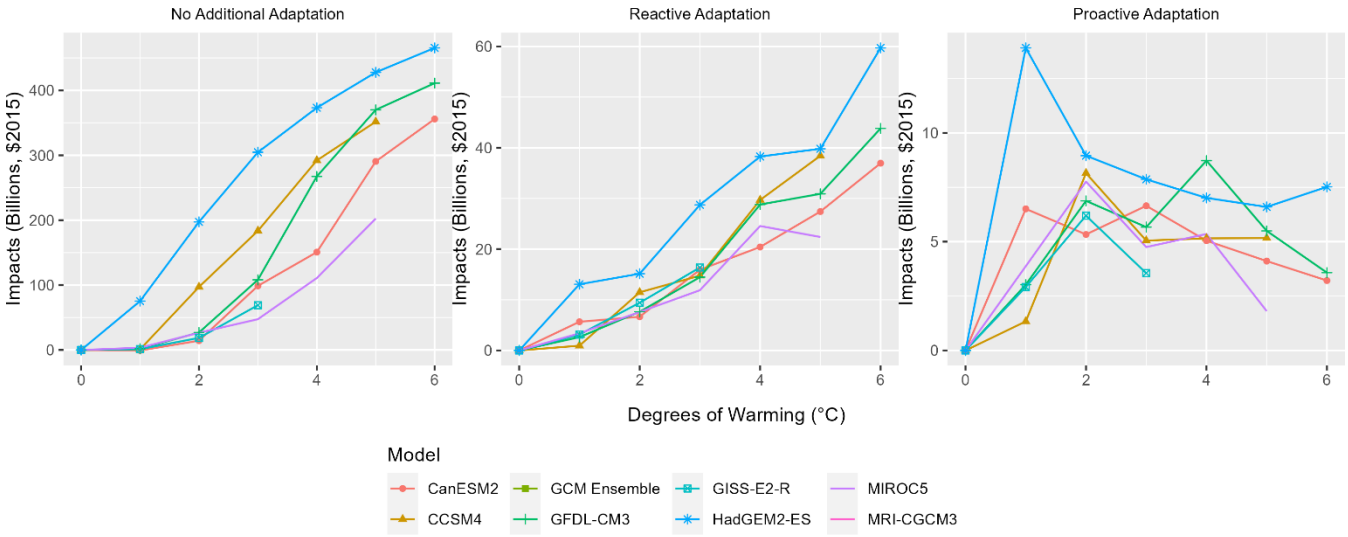

Note: figure scale varies by impact type

B. 2090 SOCIOECONOMICS

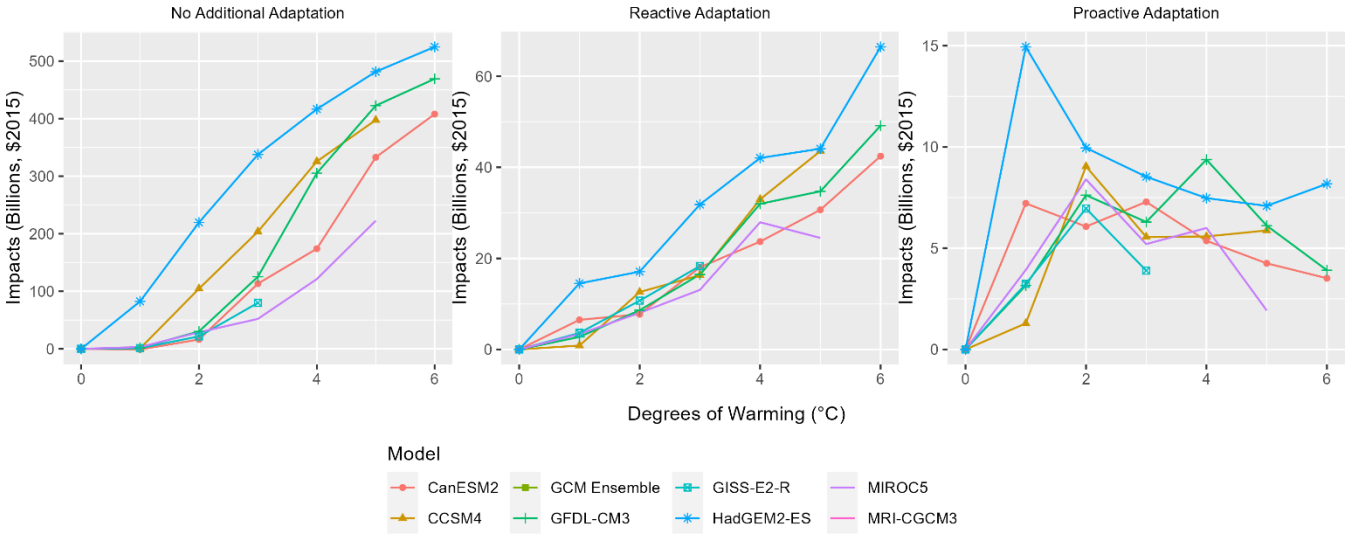

Note: figure scale varies by impact type

Processing steps

Processing steps are seen in **Figure B-30**. Quarter-degree resolution damages and road inventory data are provided by the Neumann et al., (2021) study authors and are allocated to each region. Grid cells that cross region lines are distributed proportionally by the percentage of area within each region. In the next pre-

processing step, the baseline is subtracted from projected damages to isolate damages associated with climate change for each GCM, year, and adaptation scenario combination. The No Adaptation and Reactive Adaptation Scenarios have the same baseline, a simple 20-year period repeated across time. We take the mean of this 20-year period and apply it to all Reactive and No Adaptation damages. The Proactive baseline is more complicated. It consists of 30 years of elevated but decreasing costs to begin the century, and from 2036 onwards is repeating 20-year period below Reactive and No Adaptation. This is meant to model the high initial investments in the Proactive scenario and their resulting lower costs later in the century. We take the mean of three 10-year periods to begin the century and apply the mean of 2036-2099 to all other values. In step 3, regional damages are binned by degree of CONUS temperature change for each GCM by averaging across the eleven-year windows where each GCM reaches each integer degree of CONUS warming relative to the baseline. Lastly, resulting damages by degree are divided by total miles of road within a state to produce damages in terms of dollars per mile per degree.

To account for additional repair due to increased traffic on damaged roads with increases in population, a population-dependent scalar is also calculated. The allocation of traffic by passenger and freight was not reported in the data provided by the underlying papers, and as the allocation of total damages between delay and repair cost is not provided, an aggregate scalar must be used to make the traffic adjustment. This scalar is based on the percent increase in damages across the century when the underlying model is run with population growth compared to a run with static population.

FIGURE B-30. ROADS DATA PROCESSING FRAMEWORK

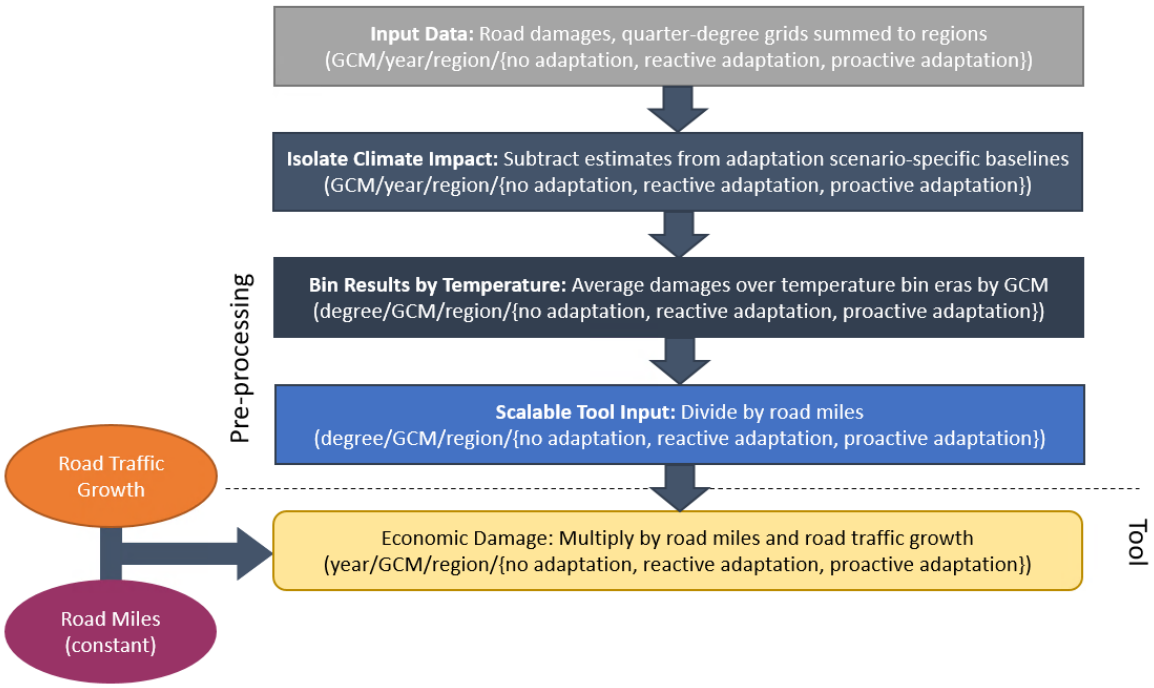

When FrEDI is run, the pre-processed by-degree damages per mile functions are then applied to the input temperature scenario to calculate the unadjusted annual impacts per mile based on the level of warming in

each year of the input scenario. Annual damages per mile are then scaled by region-level road miles and the socioeconomic scalar to account for changes in future population. For the proactive scenario, note that because repair under this scenario strengthens road surfaces pre-emptively, before damage occurs and with a planned road closure, delay times are approximately half the projected delays for no adaptation and reactive adaptation– see Neumann et al. (2021) for details.

Limitations and Assumptions

- The model assumes a fixed capital and maintenance expense budget, which is usually exhausted at some point under the no-adaptation scenario. This time dependency of the no adaptation scenario is difficult to eliminate in the data processing steps, which could bias the estimate up or down, depending on the speed of warming relative to the underlying scenarios. This bias is expected to be relatively small and the use of GCM average results minimizes this potential bias.
- Damages to vehicles associated with incompletely maintained roads are modeled only in the no adaptation scenario; the model assumes roads are completed repaired and thus vehicles receive no damage under the reactive and proactive adaptation scenarios.
- For further discussion of the limitations and assumptions in the underlying sectoral model see Neumann et al. (2021), Neumann et al. (2015), and EPA (2017).
- There is no adjustment made to the valuation of passenger and freight delay over time. While passenger delay could be adjusted with increases in average wage rate, freight delay is a more complicated amalgamation of lost time, fuel costs, and the wage rate for driver(s).

Asphalt Roads

Summary

This sector estimates the cost of asphalt road maintenance in the CONUS associated with climate change. This sector does not model any adaptation scenarios.

UNDERLYING DATA SOURCES AND LITERATURE

Underwood, B. S., Guido, Z., Gudipudi, P., & Feinberg, Y. (2017). Increased costs to US pavement infrastructure from future temperature rise. Nature Climate Change, 7, 704-707. Doi:10.1038/nclimate3390

Future impacts are quantified by comparing historical asphalt grades (values associating pavement temperature and performance) and those associated with future climate projections. This analysis includes four roadway types: interstates, national routes, state routes, and local roads. Impacts are based on the cost of maintaining the standard practice of material selection for asphalt road maintenance rather than employing proactive pavement adaptation. Costs per lane mile are multiplied by total state asphalt lane miles to produce a total damage estimate in a state. Note that this sector impact accounts for a subset of impacts in the FrEDI 'Roads' sector. Therefore, to avoid double counting, users should not add the asphalt road damages to those damages in the Roads sector. Note that asphalt lane miles are constant throughout the century, therefore only one set of impacts is shown in the figure. For illustrative purposes, **Figure B-31** shows the resulting damages by degree of warming by GCM.

FIGURE B-31. ASPHALT ROADS IMPACTS BY TEMPERATURE BIN DEGREE

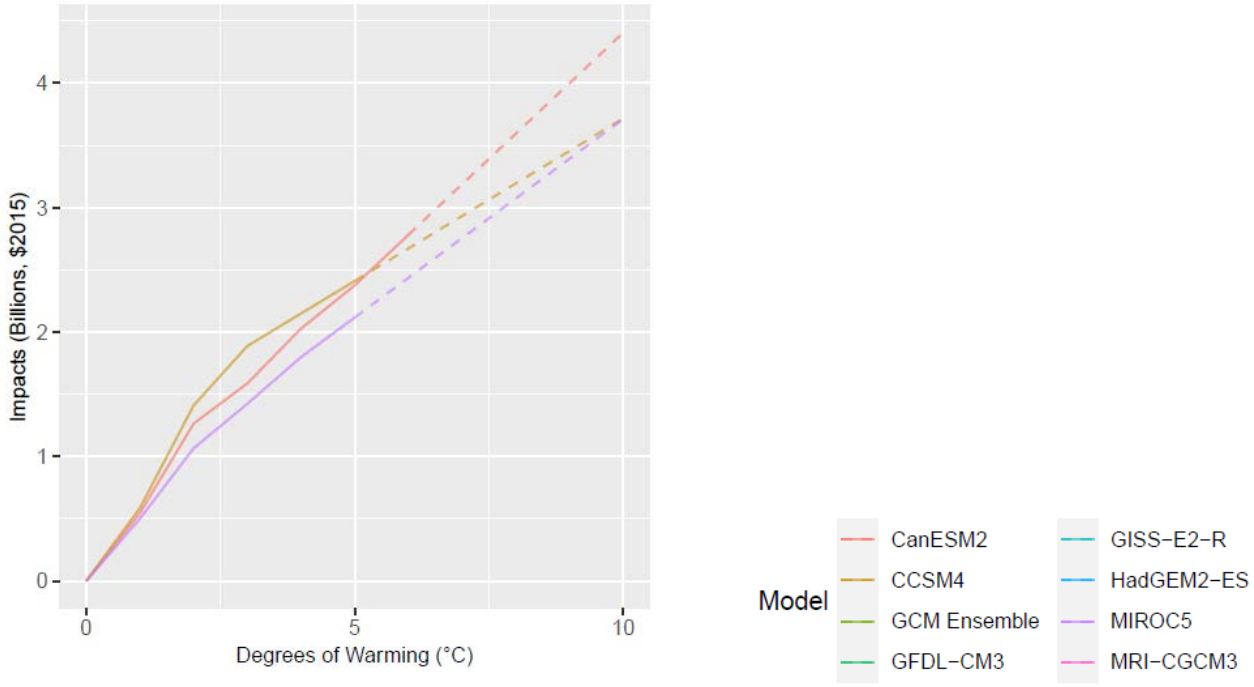

TABLE B-8. INCOMING DATA CHARACTERISTICS: ASPHALT ROADS

Data Features	Asphalt Roads Attributes
Evaluated Impacts	• Maintenance Costs (economic)[a]
Variants	• No additional adaptation
Data Shape	• 30-year era total costs • Three GCMs • By weather station
Runs Provided	• No socioeconomic growth and with climate change
Additional Data	• Lane Miles
Notes: a. Maintenance costs are meant to represent the costs of failing to update asphalt temperature grades over time.	

Climate Data Processing

This study sector relies on different climate data that additionally needs to be pre-processed for this sector to be included in FrEDI. Underwood et al. (2017) selected 19 climate models from CMIP5 from the archives of the Climate Analytics Group, three of which (CanESM2, CCSM4, and MIROC5) overlap with the suite of GCMs used in FrEDI. Although this study used the same GCMs, the bias correction and downscaling processes used by Climate Analytics Group differed from those used in the LOCA climate dataset (used in many of the FrEDI studies); therefore, new temperature bins are defined for the relevant new climate scenarios and related baselines. RCP8.5 results for these models are used for consistency with other FrEDI

sectors. Maximum and minimum daily temperature data for these three GCMs were processed in the 30-year periods employed by the study to determine future annual temperatures associated with the era-level GCM-specific asphalt road damage estimates available from the study. The temperature hindcast was subtracted from yearly projected temperature to identify GCM-specific integer degree arrival years that were used for temperature binning of impacts for this sector.

Processing steps

Remaining processing steps are seen in **Figure B-32**. In the first pre-processing step, the total asphalt road maintenance costs for three 30-year eras from the Underwood et al., (2017) study are summed to the state level and divided by the number of road miles in each state to derive state-level costs per mile. These impacts are available for all GCMs and states for three eras: 2010 (2010-2039), 2040 (2040-2069), and 2070 (2070-2099), as well as a baseline era, which are assigned to 1995 (1986-2005). In the next step, baseline impacts are subtracted from projected impacts for each GCM to arrive at maintenance costs associated with climate change for each era. Costs per mile associated with each era are then interpolated to derived annual costs, which are then binned by degree of CONUS temperature change for each GCM by averaging across the eleven-year windows (as described above) where each GCM reaches each integer degree of CONUS warming relative to the baseline.

FIGURE B-32. ASPHALT ROADS DATA PROCESSING FRAMEWORK

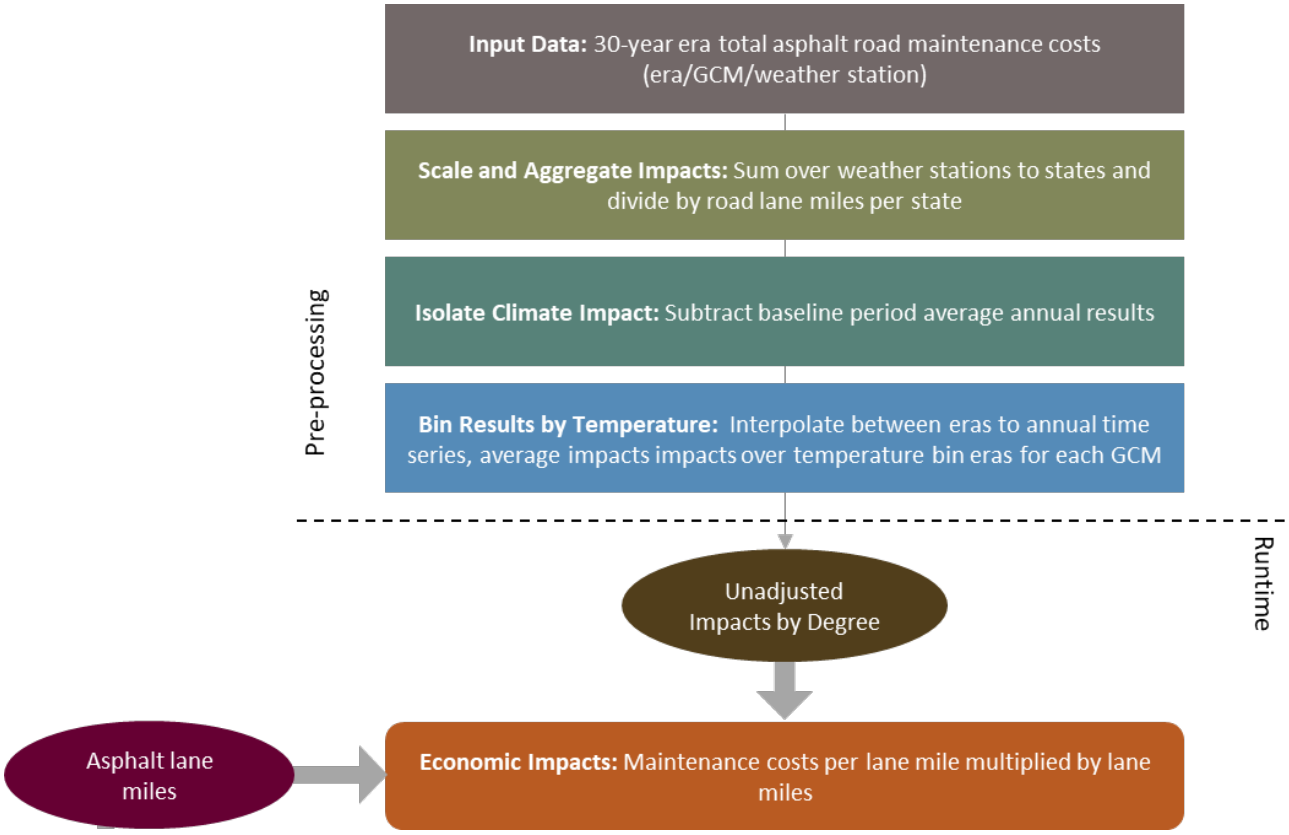

When FrEDI is run, the pre-processed by-degree costs per lane mile functions are then applied to the input temperature scenario to calculate the unadjusted annual costs per lane mile based on the level of warming

in each year of the input scenario. Total cost is then calculated by scaling these unadjusted results by the total lane miles in each state.

Limitations and Assumptions

- The underlying study uses a different set of climate projections (Climate Analytics Group) from most of the sectors that use LOCA, and a different baseline. While using a difference from the baseline and adjusting temperature arrival times is an attempt to correct any bias introduced, it is possible that these different climate projections and differences in the baseline create inconsistencies between this non-CIRA sector and other CIRA sectors.
- The underlying study includes a suite of 19 climate models, three of which are part of the CIRA suite of GCMs (CanESM2, CCSM4, and MIROC5). These three models reach warmer temperatures more quickly than the average across all 19 models in Underwood et al. (2017), and thus result in a higher average estimate of damages compared to the results presented in the paper. However, compared to the full suite of 38 CMIP5 GCMs, the three models are relatively close to the median temperature change values in 2090.
- The model references, but does not quantify, impacts of a proactive adaptation scenario. Therefore, uncertainty exists in how the modeled maintenance costs may be reduced due to adaptive actions or technologies.
- For further discussion of the limitations and assumptions in the underlying sectoral model see Underwood et al. (2017).

Urban Drainage

Summary

This sector study estimates the costs of proactive adaptation for urban drainage systems in 100 major coastal and non-coastal cities of the CONUS to meet future demands of increased runoff associated with more intense rainfall under climate change.

UNDERLYING DATA SOURCES AND LITERATURE

Price, J., Wright, L., Fant, C., & Strzepek, K. (2016). Calibrated Methodology for Assessing Climate Change Adaptation Costs for Urban Drainage Systems. Urban Water Journal, 13 (4), 331-344. Doi:10.1080/1573062X.2014.991740

Adaptive actions focus on the use of best management practices to limit the quantity of runoff entering stormwater systems and maintain current level of service (i.e., proactive adaptation to avoid damages), instead of expanding formal drainage networks of basins and conveyance systems. These best management practices generally include temporary storage above or below ground (e.g., bioswales, retention ponds), or infiltration (e.g., permeable pavement), and are based on EPA guidelines and construction cost estimates (see Price et al., (2016) for additional details).

Specifically, the analysis uses a reduced-form approach for projecting changes in flood depth and the associated costs of flood prevention under future climate scenarios, based an approach derived from EPA's Storm Water Management Model (SWMM). The approach assumes that systems are able to manage runoff

associated with historical climate conditions and estimates the costs of implementing the adaptation measures necessary to manage increased runoff due to climate change. Impacts are estimated in units of average adaptation costs per square mile for a total of 100 cities across the CONUS for three categories of 24-hour storm events (those with precipitation intensities occurring every 10, 25, and 50 years—metrics commonly used in infrastructure planning) and four future eras periods: 2030 (2020-2039), 2050 (2040-2059), 2070 (2060-2079), and 2090 (2080-2099). For illustrative purposes, **Figure B-33** shows the resulting damages by degree of warming by GCM.

FIGURE B-33. URBAN DRAINAGE IMPACTS BY TEMPERATURE BIN DEGREE

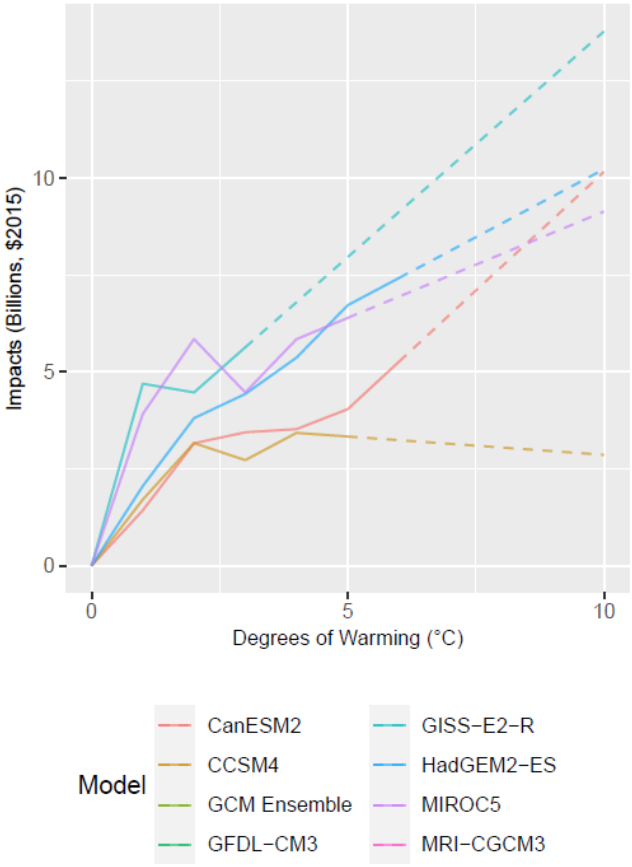

TABLE B-9. INCOMING DATA CHARACTERISTICS: URBAN DRAINAGE

Data Features	Urban Drainage Attributes
Evaluated Impacts	• Adaptation Costs (Economic)
Variant	• Proactive Adaptation
Data Shape	• Four 20-year eras (2030, 2050, 2070, 2090) • Five GCMs (standard CIRA set without GFDL) • By city • 10-year, 25-year, and 50-year storms
Runs Provided	• No socioeconomic growth and with climate change
Additional Data	• Land Area by city

Processing steps

Processing steps are seen in **Figure B-34**. The adaptation costs per square mile (weighted by area) for the 50-year storm for each GCM, city, scenario, and era combination are from Price et al. (2016). In the first step, these data are aggregated to the state level.[22] Unlike most other underlying studies, the Urban Drainage study does not produce an annual time series of results, due in part to the impact of extreme events which are not well-characterized at an annual scale. Therefore, in the next step, linear interpolation is used to create an annual time series of values for each GCM, scenario, and state combination for the period 1995-2099, using the known damage values at each of the four 20-year eras. Values are extrapolated for 2090-2099 using the linear trend observed between the 2070 and 2090 eras, and values for years prior to 2030 are estimated by using 1995 as a baseline year; i.e., impacts are assumed to be zero in 1995 and results are interpolated linearly between 1995 and 2030. Lastly, adaptation costs by state are binned by degree of CONUS temperature change for each GCM by averaging across the eleven-year windows (as described above) where each GCM reaches each integer degree of CONUS warming relative to the baseline.

FIGURE B-34. URBAN DRAINAGE DATA PROCESSING FRAMEWORK

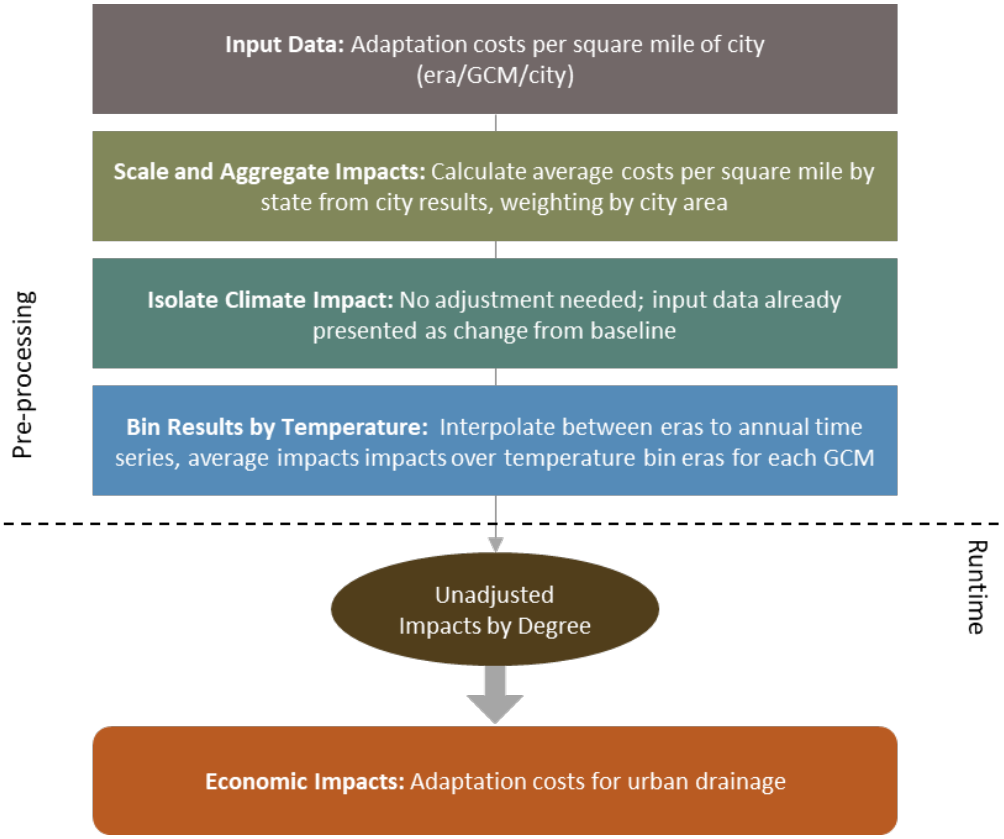

[22] For example, for a region with 2 cities, each with an area of 100 square miles, each city's area is divided by the sum of the areas, resulting in a proportion value of 0.5 for each city. This proportion value is then multiplied by each calculation of per-square-mile adaptation costs (calculated by storm, scenario, and year) to produce a weighted average adaptation cost per square mile. Note that the intensity/size of the 50-year storm varies with GCM, city, scenario, and era. The method yields changes in the absolute size of the storm over time and space, rather than the change in the frequency of the base period 50-year storm event.

When FrEDI is run, the pre-processed by-degree cost functions are then applied to the input temperature scenario to calculate the annual costs based on the level of warming in each year of the input scenario.

Limitations and Assumptions

- The underlying analysis assumes that the systems are able to manage runoff associated with historical climate conditions and estimates the costs of implementing the adaptation measures necessary to manage increased runoff due to climate change.
- Inclusion of all U.S. cities with stormwater conveyance systems would provide a more comprehensive characterization of future impacts. The underlying study is limited to 100 major U.S. cities. Therefore, the current estimates included for this sector represent underestimates of potential damages.
- For further discussion of the limitations and assumptions in the underlying sectoral model see Neumann et al. (2015), Price et al. (2016), and EPA (2017).

Inland Flooding

Summary

This sector study estimates the impact of riverine flooding in the CONUS attributable to climate change on property value.

UNDERLYING DATA SOURCES AND LITERATURE

Wobus, C.W., Porter, J., Lorie, M., Martinich, J., & Bash, R. (2021). Climate change, riverine flood risk and adaptation for the conterminous United States. Environmental Research Letters. doi: 10.1088/1748-9326/ac1bd7.

Wobus, C.W., Zheng, P., Stein, J., Lay, C., Mahoney, C., Lorie, M., Mills, D., Spies, R., Szafranski, B., & Martinich, J. (2019). Projecting Changes in Expected Annual Damages From Riverine Flooding in the United States. Earth's Future, 7(5), 516-527. Doi:10.1029/2018EF001119

The analysis uses change in expected annual damage (EAD) from flooding at each property in the United States under different temperature scenarios to value riverine flood impacts. The underlying data considers flooding for return intervals of two years through 500 years. Study authors calculate a frequency-loss curve for each property and integrate under the curve between flood frequencies of 0.0001 and 0.10 to calculate the EAD. The data excludes flooding events associated with urban drainage, quantifying only riverine floods instead. As a result, this sector does not account for all flooding events in cities and other urban areas; pluvial floods (associated with localized high rainfall events) are assessed in the *Urban Drainage* sector. The method applied estimates the baseline annual EAD using current structure characteristics (e.g., ground level floor elevation[23], replacement cost, market value), the

[23] These characteristics were made available to the study team by the First Street Foundation. Details of the dataset are provided in: First Street Foundation, 2020a. The First National Flood Risk Assessment: Defining America's Growing Risk. Available at https://assets.firststreet.org/uploads/2020/06/first_street_foundation__first_national_flood_risk_assessment.pdf

flood depths associated with baseline conditions for varying return periods[24], and depth-damage functions available from FEMA's HAZUS documentation.[25] The underlying study model provides estimates of projected property damage at multiple spatial scales – for this work, results were provided at the Census block group level; properties were grouped by Census block group and EAD values summed under baseline and future climate scenarios. Property values are held constant over the course of the century, and impacts are projected under a "no adaptation" scenario. -For illustrative purposes, **Figure B-35** shows the resulting damages by degree of warming for the average GCM ensemble.

FIGURE B-35. INLAND FLOODING IMPACTS BY TEMPERATURE BIN DEGREE

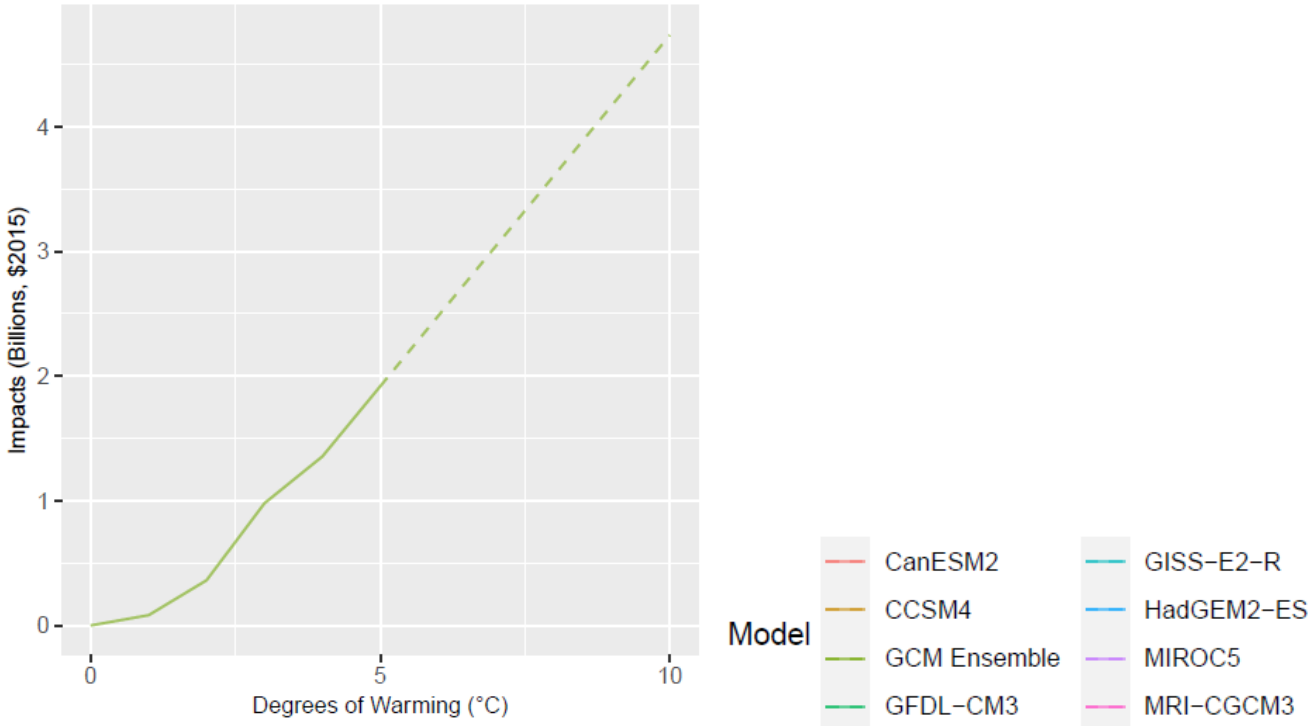

Processing steps

Processing steps are shown in Figure B-36. Wobus et al., (2021) study authors provided damages by degree by Census block group, as well as baseline EAD for the period 2001-2020. Impacts are averaged for one "GCM Ensemble", which includes fourteen models: ACCESS1-0, CanESM2, CESM1-CAM5, CMCC-CM, CSIRO-Mk3-6-0, FGOALS-g2, GFDL-CM3, HadGEM2-AO, HadGEM2-CC, HadGEM2-ES, IPSL-CM5B-MR, MIROC-ESM-

[24] Details of the "current climate" baseline flood risk modeling can be found in First Street Foundation, 2020b. First Street Foundation Flood Model: Technical Methodology Document. Available: https://assets.firststreet.org/uploads/2020/06/FSF_Flood_Model_Technical_Documentation.pdf

[25] FEMA, undated. Multi-hazard Loss Estimate Methodology: Flood Model Technical Manual. https://www.fema.gov/sites/default/files/2020-09/fema_hazus_flood-model_technical-manual_2.1.pdf

CHEM, MIROC-ESM, and NorESM1-M. In the underlying study, authors use the projected hydrology for each climate model to extract an annual maximum flow timeseries for a 20-year window centered on the year that the model reaches temperature thresholds of 1°C through 5°C above the 2001-2020 baseline.

In the first pre-processing step, block group damages are summed to regional damages. Next, the baseline EAD is subtracted from projected EAD by degree to isolate impacts attributable to climate change and values are deflated from 2020 dollars to 2015 dollars (FrEDI's default).

FIGURE B-36. INLAND FLOODING DATA PROCESSING FRAMEWORK

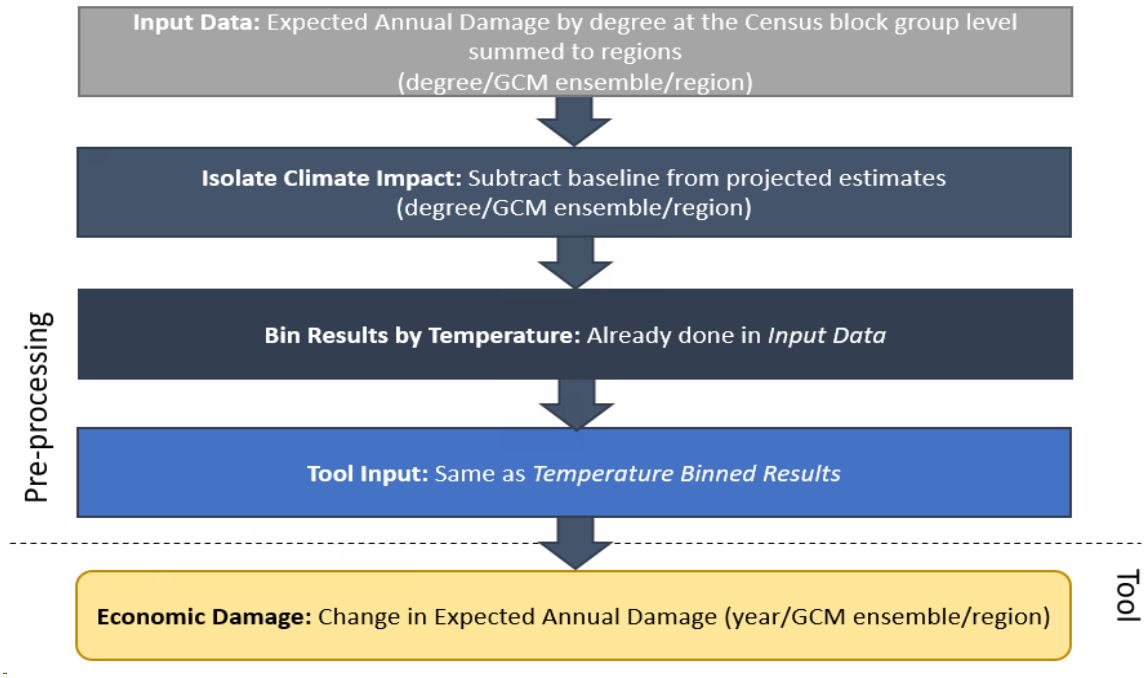

When FrEDI is run, the pre-processed by-degree damage functions are then applied to the input temperature scenario to calculate the total annual damages based on the level of warming in each year of the input scenario.

Limitations and Assumptions

- The analysis does not evaluate the potential for adaptation measures to mitigate flood risk at the property or community levels.
- The analysis does not account for changes in population and development within flood risk zones. Without a reasonable method to predict future floodplain development or policies governing development, these factors are held constant.
- This analysis relates increases in CONUS temperatures to changes in economic impacts of riverine floods. While climate science indicates that warming temperatures accelerate the hydrologic cycle, which in turn increase river flows, changes in near-surface temperatures do not necessarily characterize local or regional precipitation changes, or river flows, with a consistent signal. Local precipitation changes may also be correlated with other drivers that are not necessarily well

correlated with CONUS or regional scale temperature changes, e.g., the El Nino Southern Oscillation (ENSO). The study used here, however (Wobus et al., 2021) finds a monotonic trend of increases in the economic impact of floods at the regional scale (aggregated from the property level) as regional scale temperatures rise, supporting the relationship between U.S. regional temperature changes and flood impacts.

- For further discussion of the limitations and assumptions in the underlying sectoral model see Wobus et al. (2021) and Wobus et al. (2019).

Hurricane Wind Damage

UNDERLYING DATA SOURCES AND LITERATURE

Dinan, T., (2017). Projected increases in hurricane damage in the United States: the role of climate change and coastal development. Ecol. Econ. 138: 186–198. https://doi.org/10.1016/j.ecolecon.2017.03.034.

Congressional Budget Office (CBO). (2016). Potential Increases in Hurricane Damages in the United States: Implications for the Federal Budget. Washington, DC. June 2016

Marsooli, R. Lin, N., Emanuel, K., Feng, K. (2019). Climate change exacerbates hurricane flood hazards along US Atlantic and Gulf Coasts in spatially varying patterns. Nature Communications. https://doi.org/10.1038/s41467-019-11755-z

Summary

This sector study estimates the impact of changes in the frequency of hurricane strength wind damage to coastal properties in the CONUS. The results are primarily based on analysis by Dinan (2017), which projects hurricane damage from both wind and storm surge to properties in the Gulf and Atlantic coast states using a proprietary model developed by the firm Risk Management Solutions (RMS). Dinan (2017) projected changes in future hurricane frequency by hurricane category (Saffir-Simpson scale of Category 1 to Category 5) using a Monte Carlo aggregation of results from Emanuel (2013) for RCP8.5 and Knutson (2013) for RCP4.5.[26] The hurricane projections used in Dinan (2017) do not readily convert to an impact-by-degree warming indexing, so as part of processing this analysis instead relies on results from more recent Marsooli et al. (2019) study which provides change in return periods, maximum wind speed, and Category 5 storm frequency for the a late century period using an updated version of the Emanuel (2013) model, to project future hurricane activity by degree of warming for a set of GCMs. Further, because the detailed spatial and climate stressor specific results are not publicly accessible, we worked with Dinan, RMS, and other publicly available data to generate an estimate of damages attributable to climate change induced changes in wind damage to properties. -For illustrative purposes, **Figure B-37** shows the resulting damages by degree by GCM.

[26] See Emanuel, K., 2013. Downscaling CMIP5 climate models shows increased tropical cyclone activity over the 21st century. Proc. Natl. Acad. Sci. 110 (30), 12219–12224, and Knutson, T., et al., 2013. Dynamical downscaling projections of twenty-first-century Atlantic hurricane activity: CMIP3 and CMIP5 model-based scenarios. J. Clim. 26 (17), 6591–6617.

FIGURE B-37. HURRICANE WIND DAMAGE IMPACTS BY TEMPERATURE BIN DEGREE

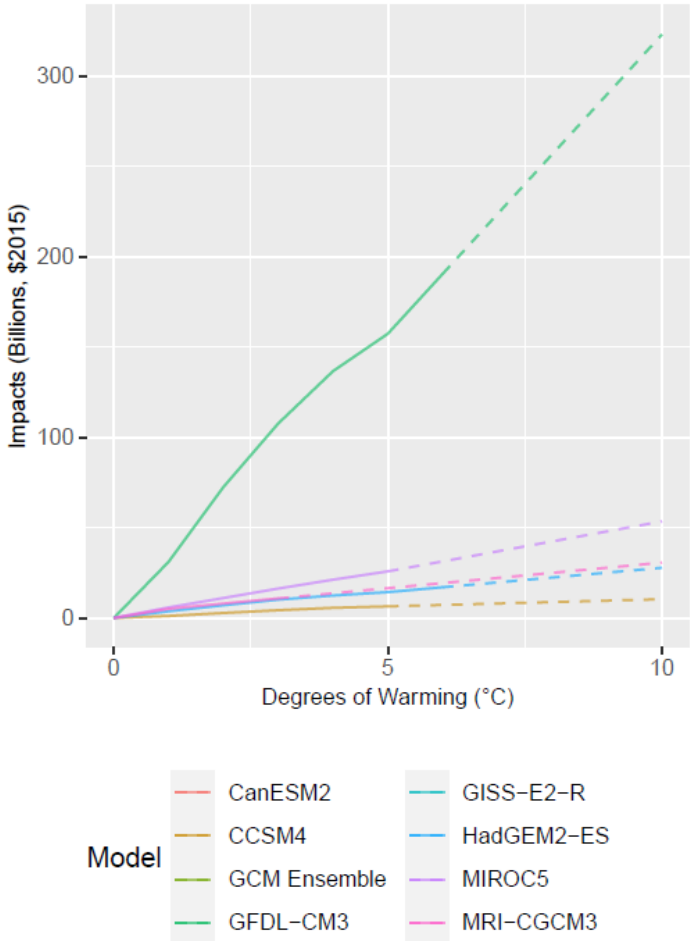

TABLE B-10. INCOMING DATA CHARACTERISTICS: HURRICANE WIND DAMAGE

Data Features	Hurricane Wind Damage Attributes
Impact Types	• Cost of hurricane wind damage to coastal properties (economic)
Variants	• No additional adaptation
Data Shape	• Single values representing baseline period (1980-2005) and projection period (2070-2095) • Five GCMs (CCSM4, GFDL-CM3, HadGEM2-ES, MIROC5, MRI-CGCM3) • County-level
Runs Provided	• No socioeconomic growth with climate change
Additional Data	• None

Processing steps

Processing steps are shown in **Figure B-38.** The first pre-processing step is to collect hurricane wind damage data from Dinan (2017), county level storm surge data from the National Coastal Property Model (NCPM), and wind profile change data from Marsooli et al., (2019).

The second pre-processing step is to estimate baseline and projected wind damages from these data. Baseline wind damage is calculated by parsing data on total hurricane damage by state from Dinan et al., (2017), reported in CBO (2016), into wind and storm surge components by state, using data on the ratio of wind to storm surge damage by state provided by the study authors (with permission from RMS). Wind damages by state are allocated to the county scale by using weights derived from the NCPM for county-level storm surge damage attributed to hurricanes in the year 2000 (base year with no SLR). This allocation method assumes that storm surge and wind damage are correlated but exclude some non-coastal inland counties which might be expected to incur wind damage (albeit with significant decay of wind speed relative to coastal counties).

Projected wind damages are then calculated using these baseline wind damages and projected wind profile changes. Wind profile changes are projected using estimates reported in Marsooli et al. (2019), which provides gridded estimates of the max wind speed and frequency of the 90th percentile event from an ensemble of simulated tropical cyclones for the Gulf and Atlantic Coasts for both the baseline of 1980–2005 to the future period of 2070–2095. The grid-cell results are spatially reaggregated to coastal counties. The future wind damages are then projected using ratios of future damage to baseline damage for each coastal county that employ a logistic function proposed by Emanuel et al. (2012) for the baseline and five of the six GCMs evaluated in Marsooli et al. (2019).[27] Although this study uses mostly CIRA GCMs, the bias correction and downscaling processes differed from those used in the LOCA climate dataset; therefore, new temperature bins are defined for the relevant new climate scenarios. These ratios are applied to the baseline damage estimated above, and baseline damages are subtracted to estimate future damages attributed to climate change. To interpolate between the baseline and projection, the baseline is assigned to 1986-2005 (FrEDI baseline) and the projection to 2070-2095, resulting in linear interpolation between 1995 and 2082. For extrapolation beyond 2082 the county-specific linear function is extended to 2099. Damages are then aggregated to the state level for each of the relevant GCMs and binned by degree of CONUS temperature change for each GCM by averaging across the eleven-year windows (as described above) where each GCM reaches each integer degree of CONUS warming relative to the baseline.

[27] MPI excluded due to data availability issues.

FIGURE B-38. HURRICANE WIND DAMAGE IMPACT PROCESSING FRAMEWORK

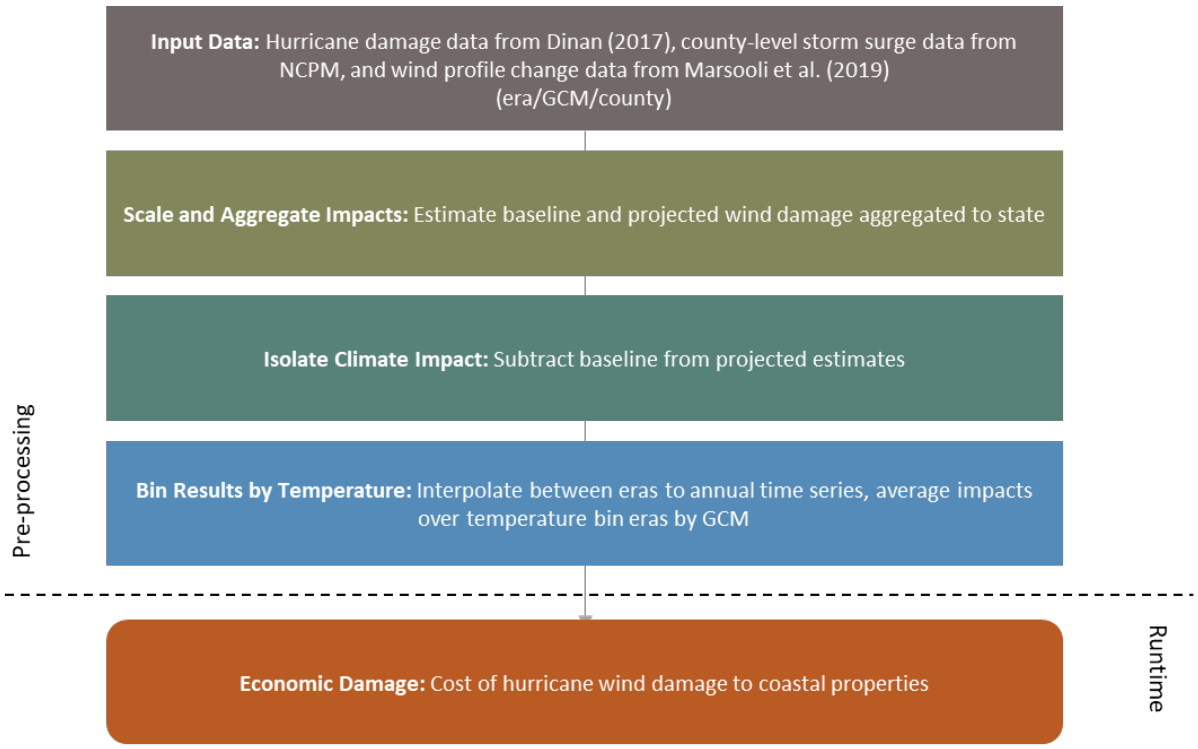

When FrEDI is run, the pre-processed by-degree cost of hurricane wind damage functions are then applied to the input temperature scenario to calculate the total annual costs based on the level of warming in each year of the input scenario.

The results indicate good agreement for four of the five models, with the fifth (GFDL) showing much higher damages than the other four. We considered applying skill weighting of the GCMs using weights provided in Marsooli et al. (2019) – the results using skill-weighting down-weight GFDL relative to other models, reducing the mean damages across all GCMs by about one-third – but the skill weights were calculated for wind speed rather than damage (damage is a non-linear logistic function of wind speed, capped at the high end by total structure value). The non-skill weighted results are used here for consistency with other sectoral analyses.

Limitations and Assumptions

- Hurricanes are relatively rare extreme events and are observed infrequently, which both limits the observed damage data on which estimates can be based and complicates estimates of projected hurricane activity. The Marsooli et al. (2019) study used here employs a well-regarded model of projected hurricane activity which provides results needed to estimate projected damages on a spatially disaggregated basis, but other models could yield different results.
- The underlying economic impact study relies on a proprietary model of hurricane wind and storm surge damages; the detailed county and scenario specific results from the model are not available

for use in the Framework. The published results are therefore disaggregated from publicly available total estimates into storm surge and wind using storm surge estimates from the Coastal Properties sector. This procedure ensures that damage estimates are not double-counted but introduces error and uncertainty in the estimates used here.

- Results from the underlying study were made available only at the state level, but analyses of projected storm surge damages are at the county level, and estimates of future hurricane activity are at a grid cell level. Adjustments made for spatial mismatches also introduce error and uncertainty in the estimates used here.
- This analysis interpolates linearly between the baseline period and late century (2070-2095) projection with no intermediate damage estimates, so mid-century values are less precise than other sectors.
- For further discussion of the limitations and assumptions in the underlying sectoral model see Dinan et al. (2017) and Marsooli et al. (2019).

B.5 Electricity Sectors

Electricity Demand and Supply

Summary

This sector estimates increases in system costs to the power sector in the CONUS. These system costs include capital, fuel, variable operation and maintenance (O&M), and fixed O&M costs.

UNDERLYING DATA SOURCES AND LITERATURE

McFarland, J., Zhou, Y., Clarke, L., Sullivan, P., Colman, J., Jaglom, W. S., Colley, M., Patel, P., Eom, J., Kim, S. H., Kyle, G. P., Schultz, P., Venkatesh, B., Haydel, J., Mack, C., & Creason, J. (2015). Impacts of rising air temperatures and emissions mitigation on electricity demand and supply in the United States: a multi-model comparison. Climatic Change, 131, 111-125. Doi:10.1007/s10584-015-1380-8

Increased costs are based on projected changes in demand for and supply of electricity across generation types. Effects on energy demand reflect the net impact of increased demand for residential, commercial, and industrial space cooling during summer/warmer months, and decreased demand for space heating during winter/cooler months. Effects on supply reflect the decreased production capacity of thermal power plants, and transmission capacity of the transmission system, associated with higher temperatures.[28] The complex interplay of supply and demand, coupled with forecast changes in fuel and energy production technology availability and prices, are modeled using the Global Change Assessment Model (GCAM-USA), a detailed service-based building energy model with a 50-state domain.

Costs are provided for a reference scenario, in which climate is held constant to the FrEDI baseline while socioeconomic variables are dynamic, and a projection run in which both climate and socioeconomic variables are changing. Estimates of costs with- and without-climate change are provided in five-year intervals. For illustrative purposes, **Figure B-39** shows the resulting damages by degree of warming by GCM, calculated using 2010 (figure A) and 2090 (figure B) socioeconomics (i.e., the endpoints of the socioeconomic scenarios).

[28] Note that the transmission system effects in this sector are separate from those modeled in the Electricity Transmission and Distribution Infrastructure sector.

FIGURE B-39. ELECTRICITY DEMAND AND SUPPLY IMPACTS BY TEMPERATURE BIN DEGREE

A. 2010 SOCIOECONOMICS **B. 2090 SOCIOECONOMICS**

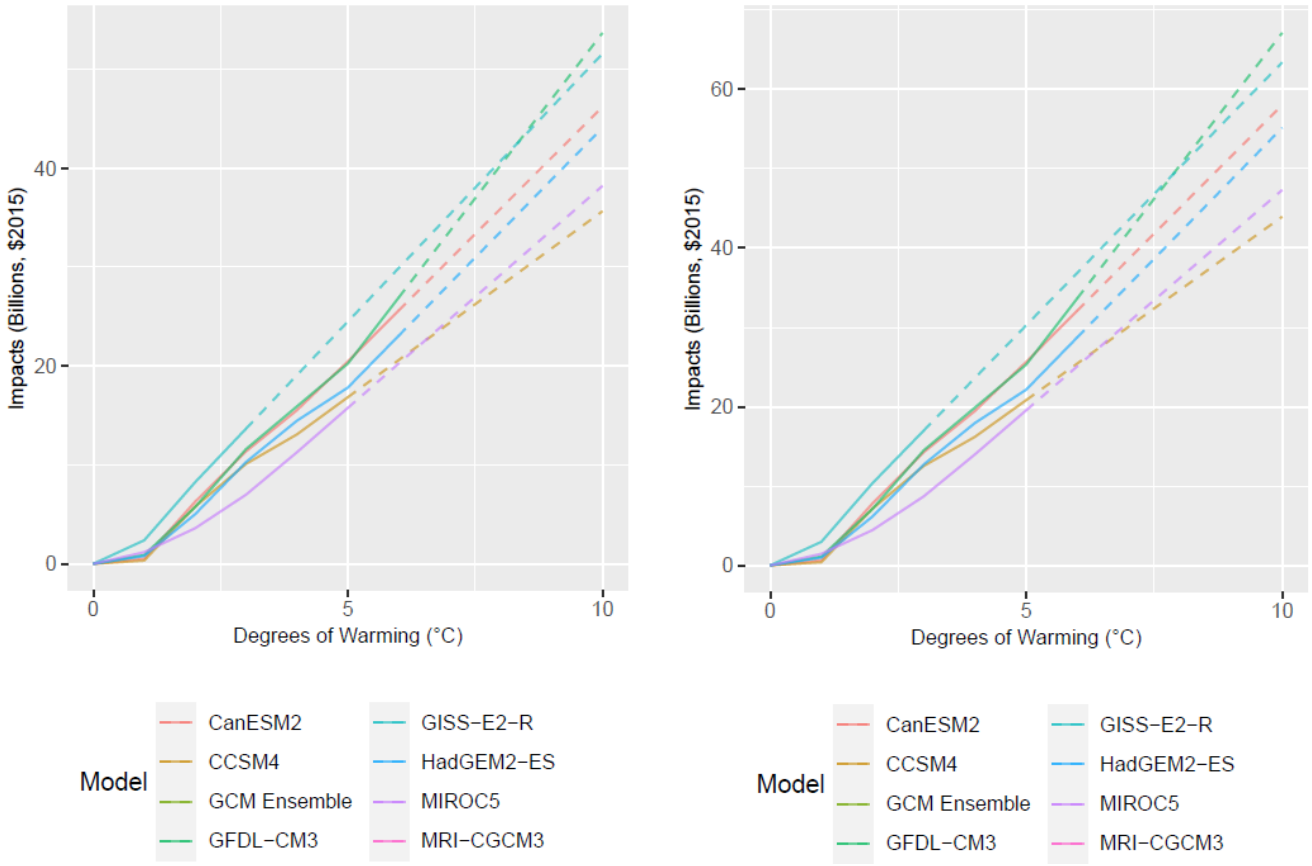

Note: figure scale varies by impact type

Processing steps

TABLE B-11. INCOMING DATA CHARACTERISTICS: ELECTRICITY DEMAND AND SUPPLY

Data Features	Electricity Demand and Supply Attributes
Evaluated Impacts	• Power Sector System Costs (economic)
Variants	• None
Data Shape	• 5-year intervals 2010-2100 • Six GCMs (standard CIRA set) • State-level
Runs Provided	• With socioeconomic growth and with climate change • With socioeconomic growth and without climate change (reference scenario)
Additional Data	• None

Processing steps for this sector are shown in **Figure B-40**. Data from the McFarland et al., (2015) study authors on the system costs for the power sector are provided for each GCM and a climate reference scenario for each state in 5-year intervals. In the first pre-processing step, annual operation and maintenance costs are interpolated between the 5-year interval data for both GCM projections and the reference scenario to create an annual trajectory. Next, the percent difference between the reference scenario and the GCM projected scenarios are calculated for each state-GCM-year combination. These percentages are then multiplied by their respective 2010 reference scenario value to calculate a damage trajectory that represents climate change with no socioeconomic growth. The resulting no-growth trajectory is then binned by degree of CONUS temperature change by averaging across the eleven-year windows where each GCM reaches each integer degree of CONUS warming relative to the baseline. To produce state level scalars for socioeconomic growth, each state's yearly reference scenario value is divided by its 2010 value to index the scalar to 2010. The scalar is then extrapolated to 2200 and 2300.

FIGURE B-40. ELECTRICITY DEMAND AND SUPPLY DATA PROCESSING FRAMEWORK

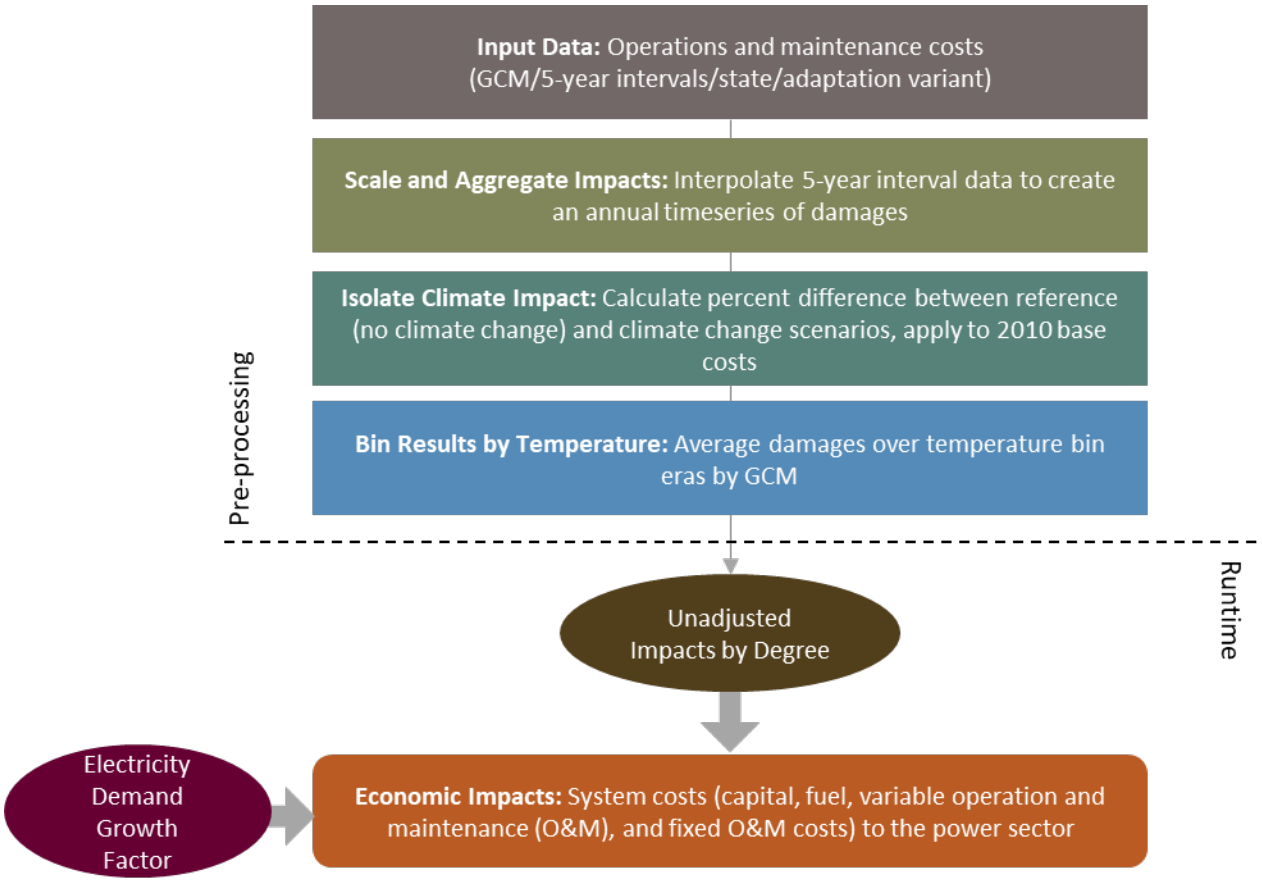

When FrEDI is run, the pre-processed by-degree system costs is then applied to the input temperature scenario to calculate the unadjusted annual system costs based on the level of warming in each year of the input scenario. These costs are then multiplied by the socioeconomic scalar for each given year to produce total cost estimates across the century.

Limitations and Assumptions

- Projected changes in heating degree days (HDD) and cooling degree days (CDD) are based on a temperature set-point of 65°F, a common convention that may lead to a conservative energy demand estimate.
- The temporal aggregation of the underlying electricity supply model is too coarse to assess the impact of extreme temperature events that occur on only the very hottest days of the year. As a result, the underlying study focuses on a single aspect of climate change: average ambient air temperature, and therefore omits effects of extreme temperature effects on peak demands and the loads required to meet those changes. Effects from future changes in the frequency and magnitude of extreme temperatures may stress electric power systems, and these economic risks are not captured in this study.
- For further discussion of the limitations and assumptions in the underlying sectoral model, see McFarland et al. (2015).

Electricity Transmission and Distribution Infrastructure

Summary

UNDERLYING DATA SOURCES AND LITERATURE

Fant, C., Boehlert, B., Strzepek, K., Larsen, P., White, A., Gulati, S., Li, Y., & Martinich, J. (2020). Climate change impacts and costs to U.S. electricity transmission and distribution infrastructure. Energy, 195. Doi:10.1016/j.energy.2020.116899

This analysis estimates damages to the electric transmission and distribution infrastructure in the CONUS due to climate change. This multi-dimensional analysis considers a wide range of climate stressors, including extreme temperature, extreme rain, lightning, vegetation growth, wildfire activity, and coastal flooding. Impact receptors include transmission and distribution lines, poles/towers, and transformers.

Monetized damages for this sector are the costs of repair or replacement of damaged infrastructure. The underlying impact study estimates damages under two infrastructure system scenarios: one with expansion of infrastructure associated with demand growth, and one with static infrastructure. Increases in demand growth may be due to population growth, or increased demand due climatic change — in particular, warmer temperatures increase usage of air-conditioning. The model identifies changes in performance and longevity of physical infrastructure, such as power poles and transformers, and quantifies these impacts in economic terms. While certain climate stressors do cause power outages which have associated direct and indirect economic costs, these damages are not included in damage estimates.

This analysis is based on three adaptation scenarios: proactive adaptation, reactive adaptation, and no additional adaptation. Repair costs are also allocated based on the activity being performed. These activities include transmission line capacity, wildfire repair, tree trimming, substation sea level rise, substation storm surge, wood pole decay, transmission transformer lifespan, and distribution transformer lifespan. For illustrative purposes, **Figure B-41** shows the resulting damages by degree of warming for the three adaptation scenarios, by GCM, calculated using 2010 (figure A) and 2090 (figure B) socioeconomics (i.e., the endpoints of the socioeconomic scenarios).

FIGURE B-41. ELECTRICITY TRANSMISSION AND DISTRIBUTION INFRASTRUCTURE IMPACTS BY TEMPERATURE BIN DEGREE

A. 2010 SOCIOECONOMICS

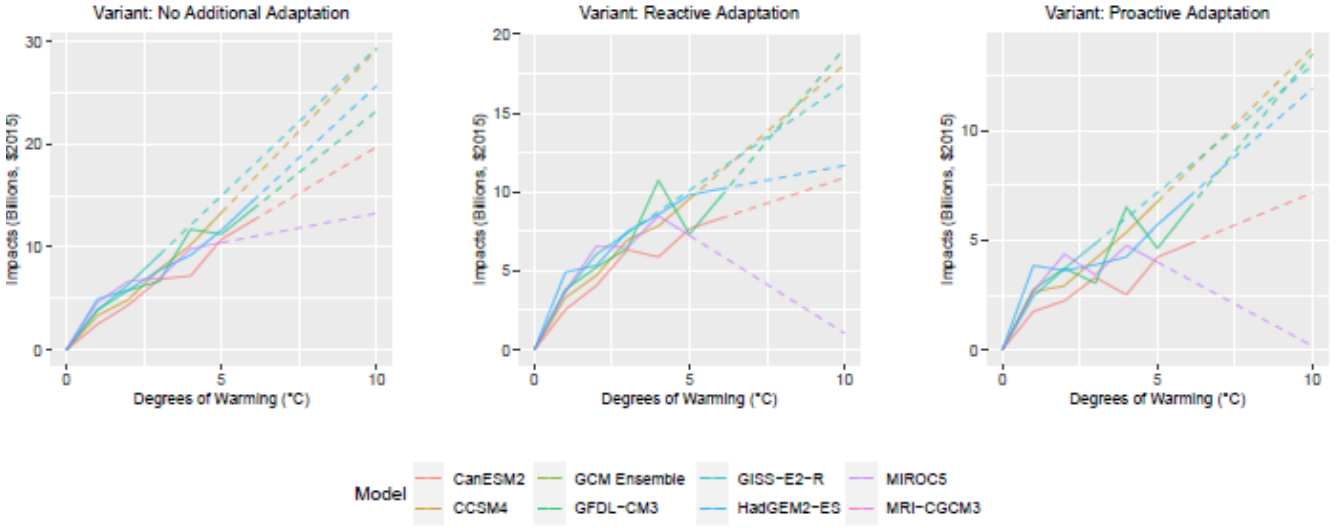

Note: Figure scale varies by variant

B. 2090 SOCIOECONOMICS

Note: Figure scale varies by variant

Processing steps

TABLE B-12. INCOMING DATA CHARACTERISTICS: ELECTRICITY TRANSMISSION AND DISTRIBUTION INFRASTRUCTURE

Data Features	Electricity Transmission and Distribution Infrastructure Attributes
Evaluated Impacts	• Costs of infrastructure replacement and repair (economic)
Variants	• Proactive adaptation • Reactive adaptation • No additional adaptation
Data Shape	• Year • Six GCMs (standard CIRA set) • Three adaptation scenarios • State level
Runs Provided	• Static infrastructure with climate change
Additional Data	• Infrastructure growth due to population change • Infrastructure growth due to climate change

Processing steps are seen in **Figure B-42**. The underlying impact model described in Fant et al. (2020) produces annual damage estimates for each infrastructure type, state, GCM, and adaptation scenario. The underlying study grows infrastructure with electricity demand increases due to climate change and population growth. In the first pre-processing step, to isolate demand growth associated with warming, damages associated with static demand are scaled by growth of demand attributable to warming.

After damages associated with climate driven infrastructure growth are calculated, results are aggregated for each GCM, year, and adaptation scenario. The costs are then binned by degree of CONUS temperature change for each GCM by averaging across the eleven-year windows where each GCM reaches each integer degree of CONUS warming relative to the baseline.

One additional set of scalars is calculated and included in FrEDI to account for infrastructure expansion to respond to increased demand from population growth.

FIGURE B-42. ELECTRICITY TRANSMISSION AND DISTRIBUTION INFRASTRUCTURE DATA PROCESSING FRAMEWORK

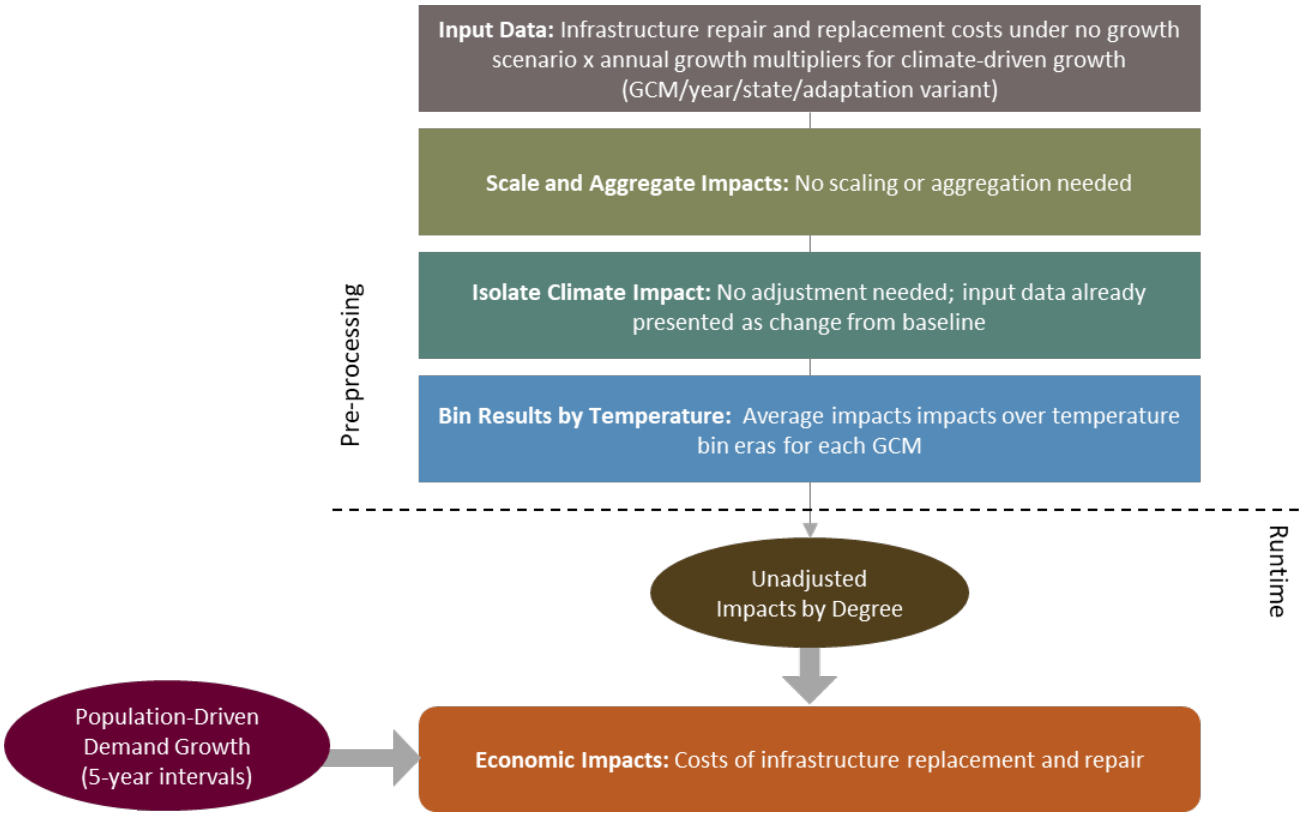

When FrEDI is run, the pre-processed by-degree cost functions are then applied to the input temperature scenario to calculate the unadjusted annual costs based on the level of warming in each year of the input scenario. Lastly, total annual costs are calculated by scaling the unadjusted costs by the climate-driven infrastructure growth and population-driven growth scalars. Thus, final damage estimates include expansion of electric grid infrastructure associated with a warming climate and with population growth. Note that because these damage estimates rely on an empirical relationship between damages with and without infrastructure growth in the underlying study's impact model, these damage estimates cannot be adjusted for custom input population trajectories.

Limitations and Assumptions

- The underlying study's impact model assumes that grid demand is controlled by population change and climatic factors; grid demand is assumed to not be influenced by economic growth. Future changes in the design and structure of electric grids are not considered in this study.
- One of the infrastructure types (Substation Damage from Sea Level Rise and Storm Surge) is not scaled by demand in the original study. Because the input data received from the authors was already aggregated across infrastructure types, all infrastructure types are scaled by demand in FrEDI. This has a minimal effect on the overall results because Substation Damage from Sea Level

Rise and Storm Surge accounts for the smallest portion of the damages among the final eight types considered in the original study.

- For further discussion of the limitations and assumptions in the underlying sectoral model, see Fant et al. (2020).

B.4 Ecosystems and Recreation Sectors

Water Quality

UNDERLYING DATA SOURCES AND LITERATURE

Fant, C., Srinivasan, R., Boehlert, B., Rennels, L., Chapra, S. C., Strzepek, K. M., Corona, J., Allen, A., & Martinich, J. (2017). Climate change impacts on US water quality using two models: HAWQS and US Basins. Water, 9(2), 118. Doi:10.3390/w9020118

Boehlert, B., Strzepek, K. M., Chapra, S. C., Fant, C., Gebretsadik, Y., Lickley, M., Swanson, R., McCluskey, A., Neumann, J., & Martinich, J. (2015). Climate change impacts and greenhouse gas mitigation effects on US water quality. Journal of Advances in Modeling Earth Systems, 7, 1326-1338. Doi:10.1002/2014MS000400

Yen, H., Daggupati, P., White, M. J., Srinivasan, R., Gossel, A., Wells, D., & Arnold, J. G. (2016). Application of large-scale, multi-resolution watershed modeling framework using the hydrologic and water quality system (HAWQS). Water, 8(4), 164. Doi:10.3390/w8040164

Summary

This analysis estimates damages in terms of the change in willingness to pay to avoid changes in water quality due to climate change. This analysis estimates climate change effects on water quality at the eight-digit HUC scale of the CONUS using the Hydrologic and Water Quality System (HAWQS) biophysical model. Note that the damages estimated for this sector only cover the change in value of recreation opportunities and do not include the value of health effects or other amenities associated with clean water.

HAWQS advances the functionality of the widely used and accepted Soil and Water Assessment Tool (SWAT), providing a platform for water quality modeling, primarily by minimizing the necessary initialization time. Originally developed by the U.S. Department of Agriculture (USDA), SWAT has been the core simulation tool for numerous U.S. national and international assessments of soil and water resources. The use of HAWQS over SWAT improves the ease of application to national scale analyses while still simulating a large array of watershed processes for a defined period of record.

The HAWQS model follows a broad modeling sequence: (1) the landscape phase, where the primary processes are climate, soil water balance, nutrient and sediment transport and fate, land cover, plant growth, farm management, and (2) the main channel phase, where the main processes are river routing, and sediment and nutrient transport through the rivers and reservoirs.

The HAWQS model projects changes in water quality parameters and simulated changes in river flow for five climate models under RCP8.5 and RCP4.5. These projections include future municipal wastewater treatment plant loadings (point source) scaled to account for population growth. Changes in overall water quality are estimated using changes in a Climate-oriented Water Quality Index (CWQI), a metric that combines multiple pollutant and water quality measures. Four water quality parameters (water temperature, dissolved oxygen, total nitrogen, and total phosphorus) are aggregated from the eight-digit HUC level to the Level-III Ecoregions, weighted by area.[29] Finally, a relationship between changes in the

[29] Designed to serve as a spatial framework for environmental resource management, ecoregions denote areas within which ecosystems (and the type, quality, and quantity of environmental resources) are generally similar. Ecoregions were originally created to support the development of regional biological criteria and water quality standards, and to set management goals for nonpoint source pollution.

CWQI and changes in the willingness to pay for improving water quality is used to estimate the economic implications of projected water quality changes. For more information on the approach and results for the water quality sector, please refer to Fant et al. (2017), Boehlert et al. (2015), and Yen et al. (2016). Specifically, impacts are estimated in the underlying study as per capita change in the willingness to pay to improve water quality for two future eras: 2050 (2040-2059) and 2090 (2080-2099). For illustrative purposes, **Figure B-43** shows the resulting damages by degree of warming by GCM, calculated using 2010 (figure A) and 2090 (figure B) socioeconomics (i.e., the endpoints of the socioeconomic scenarios).

FIGURE B-43. WATER QUALITY IMPACTS BY TEMPERATURE BIN DEGREE

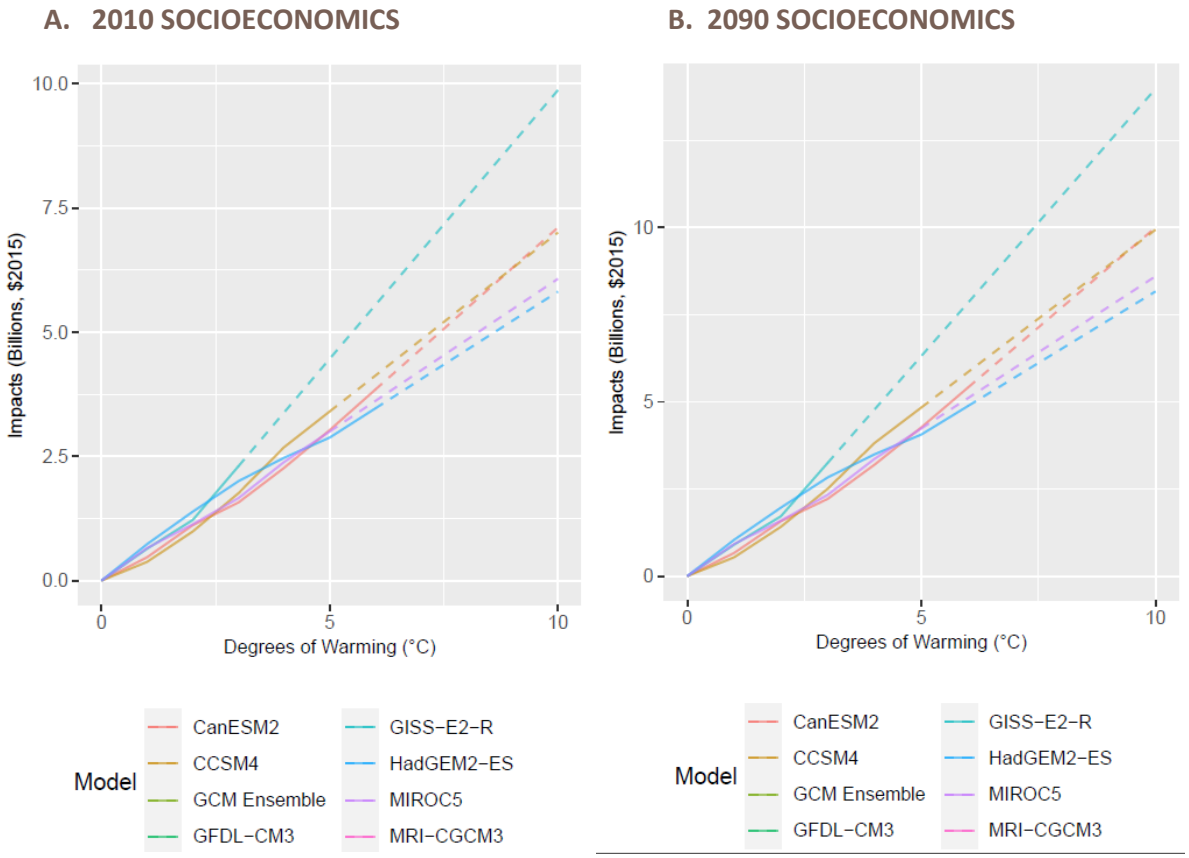

Processing steps

Processing steps are shown in **Figure B-44**. The per capita willingness to pay for each EPA Level 3 Ecoregion, GCM, and era combinations are from the underlying study. These climate change impacts are relative to a "control" scenario (one with socioeconomic growth and historical climate) to isolate the climate change impacts from the impacts of socioeconomic growth. In the first pre-processing step, these data are aggregated to the region level. Linear interpolation is then used to create an annual time series of values for each GCM and region combination for the period 1995-2099. Values are extrapolated for 2090-2099 using the linear trend observed between 2050 and 2090, and values for years prior to 2050 are estimated by using 1995 as a baseline year; i.e., impacts were assumed to be zero in 1995 and results are interpolated

linearly between 1995 and 2050. Finally, annual willingness to pay per capita rates are then binned by degree of CONUS temperature change for each GCM by averaging across the eleven-year windows where each GCM reaches each integer degree of CONUS warming relative to the baseline.

FIGURE B-44. WATER QUALITY DATA PROCESSING FRAMEWORK

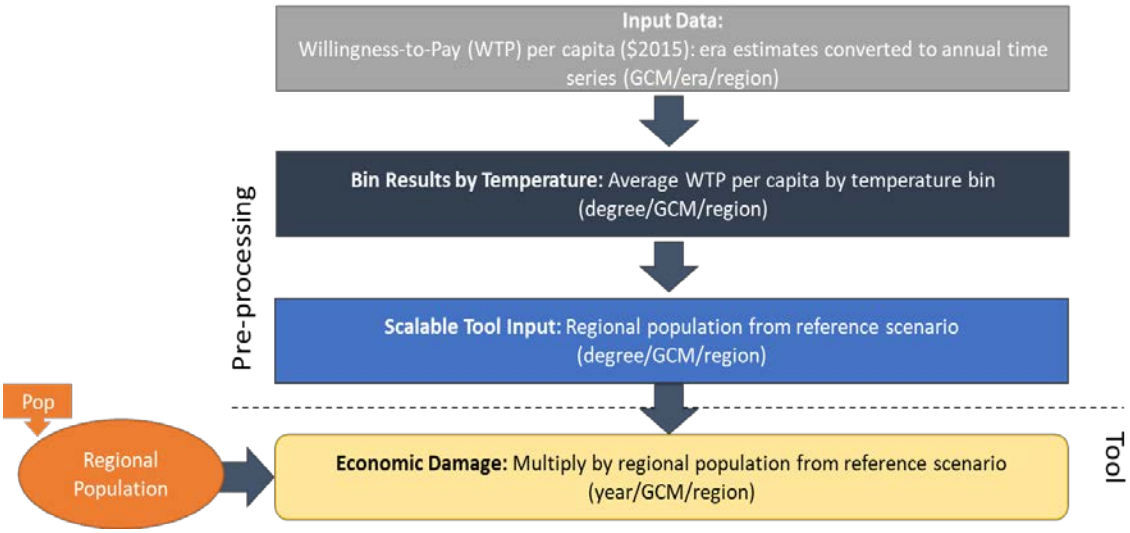

When FrEDI is run, the pre-processed by-degree per capita willingness to pay functions are then applied to the input temperature scenario to calculate the unadjusted annual WTP per capita values based on the level of warming in each year of the input scenario. The total damages are then calculated by applying these annual per capita rates to the input population scenario.

Limitations and Assumptions

- Decreases in water quality due to climate change will likely have adverse effects on human health and the environment, not represented in this section's results. For example, climate change impacts to water quality may affect ecological dynamics of freshwater systems, with cascading effects on ecosystem services and recreational opportunities.
- This analysis only considers four water quality parameters, and omits other constituents, such as sediment and heavy metals, that may be affected by changes in the climate system.
- The methods underlying the analysis do not consider the effects of climate change-induced extreme events on water quality, such as increased siltation and runoff following wildfire events.
- The analysis considers only a subset of all use/non-use values linked to water quality changes, therefore the damages reported here are likely underestimates of future impacts.
- By creating an annual time series for the period 1995 to 2100 based on values from 2050 and 2090 only, the temperature binning processing does not capture any non-linearities in the relationship between damages and temperature, particularly in the early years of the century.
- For further discussion of the limitations and assumptions in the underlying sectoral model, see Fant et al. (2017) and Boehlert et al. (2015).

Winter Recreation

Summary

This sector estimates lost revenue due to climate change to suppliers of three types of winter recreation occurring at 247 sites across CONUS: alpine skiing, Nordic skiing, and snowmobiling.

UNDERLYING DATA SOURCES AND LITERATURE

Wobus, C., Small, E. E., Hosterman, H., Mills, D., Stein, J., Rissing, M., Jones, R., Duckworth, M., Hall, R., Kolian, M., Creason, J., & Martinich, J. (2017). Projected climate change impacts on skiing and snowmobiling: A case study of the United States. Global Environmental Change, 45, 1-14. Doi:10.1016/j.gloenvcha.2017.04.006

Damages are based on the number of visits to winter recreational sites, entrance fees, and state-level average ticket prices. The model described in Wobus et al., (2017) was run using both 2010 and 2090 ICLUSv2 population. For illustrative purposes, **Figure B-45** shows the resulting damages by degree of warming for each recreation impact type by GCM, calculated using 2010 (figure A) and 2090 (figure B) socioeconomics (i.e., the endpoints of the socioeconomic scenarios).

FIGURE B-45. WINTER RECREATION IMPACTS BY TEMPERATURE BIN DEGREE

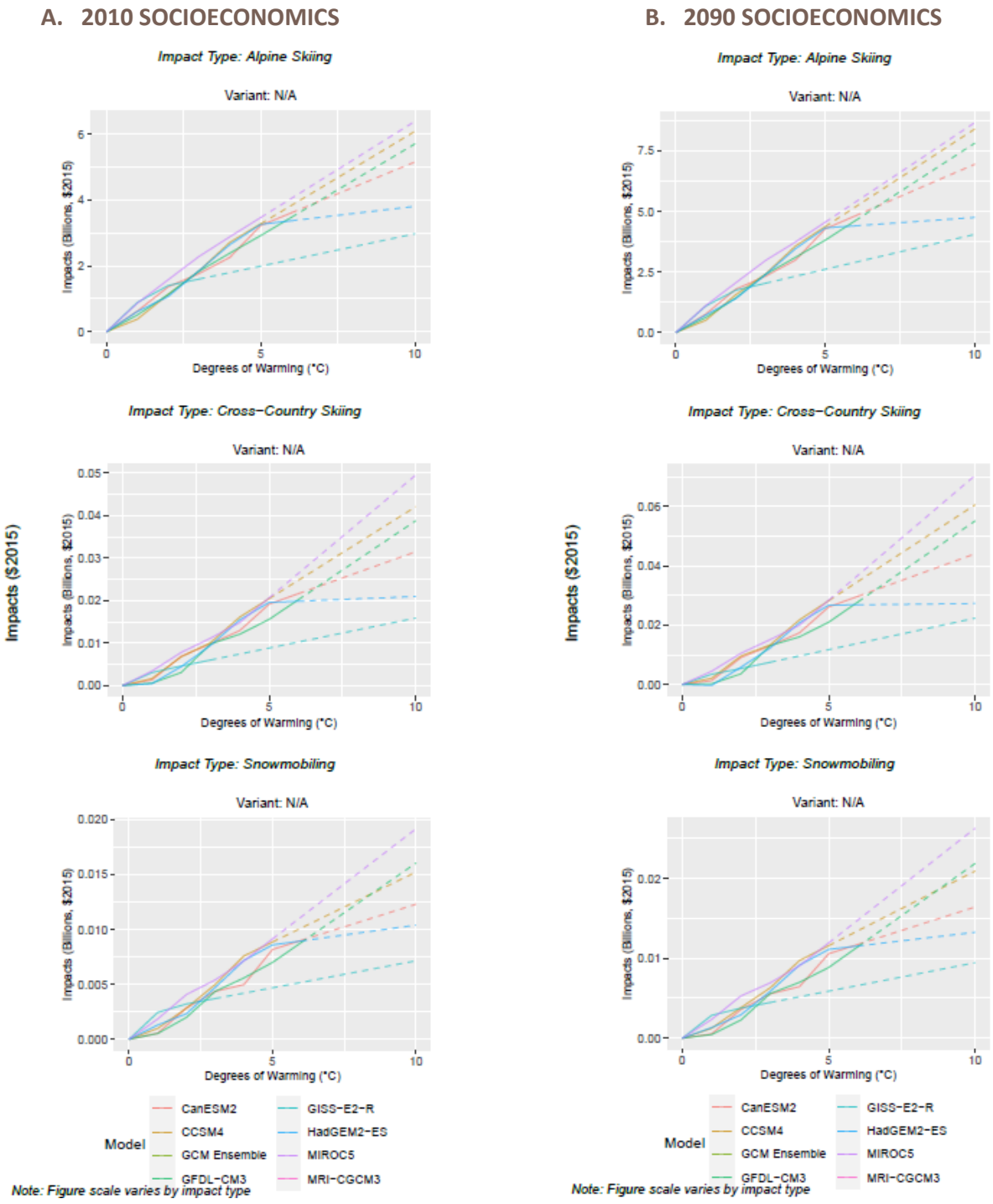

Processing steps

Processing steps are shown in **Figure B-46**. Lost ticket sales are available from Wobus et al., (2017) by degree across recreational activities (alpine skiing, Nordic skiing, and snowmobiling), GCMs, and regions, for both a 2010 and 2090 population. Climate impacts are already isolated from these data.

In the last pre-processing step, both the 2010 and 2090 regional estimates are divided by regional population to develop per capita estimates of forgone ticket sales for the three winter activities by degree of warming.

FIGURE B-46. WINTER RECREATION DATA PROCESSING FRAMEWORK

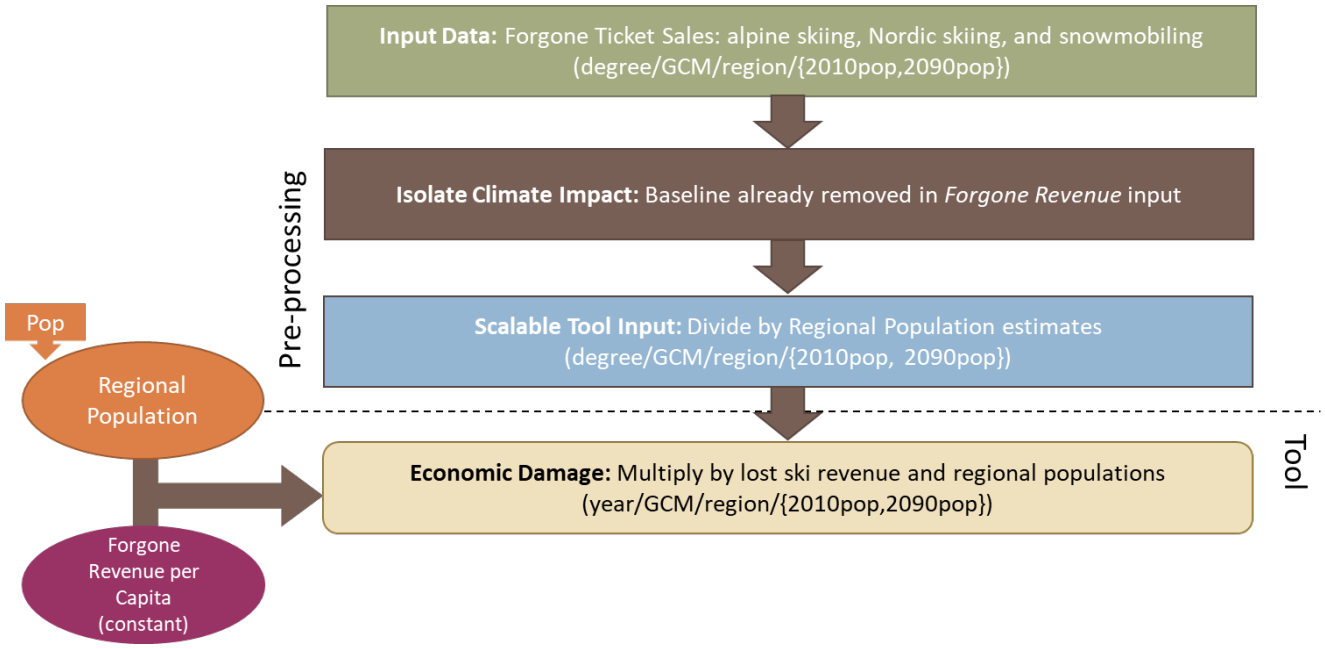

When FrEDI is run, the pre-processed by-degree per damage functions are then applied to the input temperature scenario to calculate the total annual lost revenue by region, GCM, and impact year.

Limitations and Assumptions

- The scope of winter recreation loss for the tool is derived only from analysis of the alpine skiing, Nordic skiing, and snowmobile sub-sectors of the industry. Potential losses to other winter recreation activities (e.g., tubing) are not quantified in this study.
- Potentially compensating adaptations from the lost opportunity to engage in winter recreation (for example, with other forms of outdoor recreation, or with indoor recreation) are not considered.
- For further discussion of the limitations and assumptions in the underlying sectoral model, see Wobus et al. (2017) and EPA (2017).

Marine Fisheries

Summary

UNDERLYING DATA SOURCES AND LITERATURE

Moore, C, Morley, J.W., Morrison, B., Kolian, M., Horsch, E., Frölicher, T., Pinsky, M.L., & Griffis, R. (2020). Estimating the Economic Impacts of Climate Change on 16 Major US Fisheries. Climate Change Economics, 12(1), 2150002. DOI: 10.1142/S2010007821500020

Morley, J.W., Selden, R.L., Latour, R.J., Frölicher, T.L., Seagraves R.J., & Pinsky M.L. (2018). Projecting shifts in thermal habitat for 686 species on the North American continental shelf. PLoS ONE, 13(5), e0196127.

This analysis estimates climate-driven changes in thermally available habitat for economically important commercial fish species in the CONUS based on methods described in Morley et al., (2018), and connects changes in fish species population with projected landings, valued using current ex vessel prices for individual species. The analysis first characterizes the potential economic impact of projected changes in the annual landings of 177 commercially harvested marine species from 2021 to 2100, based on the use of five general circulation models (GCMs) to project changes in each target species' thermally available habitat within the US Exclusive Economic Zone (EEZ). The Moore et al. (2020) paper from which these economic damage estimates are derived from then also includes estimates of the future welfare losses associated with changes in landings for a 16-fishery subset of fish species reflected in the estimates presented here, accounting for about 56 percent of current US commercial fishing revenues. We omit consideration of the welfare estimates because they are incomplete, and instead focus on the broader "screening analysis" results from the paper.[30] The screening analysis assumes constant prices through the 21st century, however, a key limitation discussed further below. The constant price assumption means that there is no socioeconomic adjustment for this sector. For illustrative purposes, **Figure B-47** shows the resulting damages by degree by GCM.

[30] As noted in the paper, to ensure welfare assessment would be analytically tractable, the authors limited its scope to 16 species that could be equally divided into four categories, each of which would contain commodities that the consumers might consider close substitutes. Given the limited number of species the analysis could consider, the authors also chose to focus, to the extent possible, on fisheries that account for the greatest share of current ex-vessel landings. While the welfare analysis provides additional insights about the potential for market adaptation to mitigate damages through seafood consumers substituting away from fish species that might be most affected by climate change, the welfare analysis unavoidably must examine only a subset of fisheries examined in the more comprehensive screening analysis.

FIGURE B-47. MARINE FISHERIES IMPACTS BY TEMPERATURE BIN DEGREE

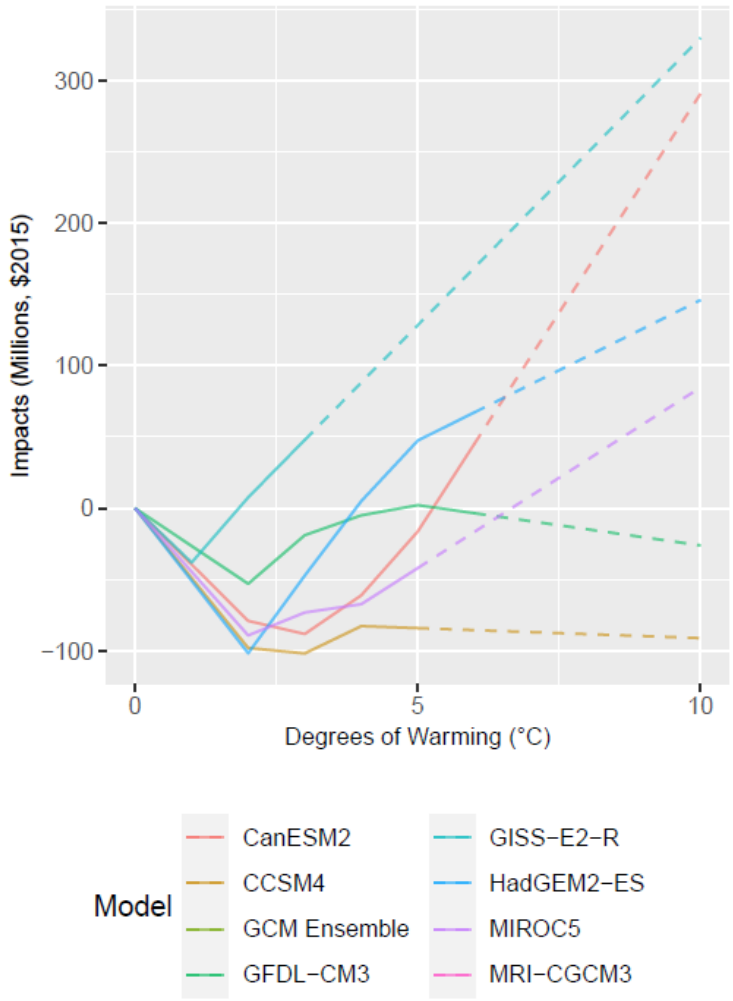

Processing steps

Processing steps are seen in **Figure B-48**. Annual marine fishery revenue data were obtained from the Moore et al., (2020) study authors, by GCM and state. In the first pre-processing step, results are binned by degree of CONUS temperature change for each GCM by averaging across the eleven-year windows where each GCM reaches each integer degree of CONUS warming relative to the baseline. In the second pre-processing step, the baseline estimates are subtracted from the by degree revenue data to isolate climate impacts. Because the original study used a later period baseline (2006-2017), results from four of the five GCM trajectories do not have data for the one-degree warming bin. One degree bin results are therefore generated by interpolating results between the baseline (zero degree) and the two-degree bin for these four GCMs.

FIGURE B-48. MARINE FISHERIES DATA PROCESSING FRAMEWORK

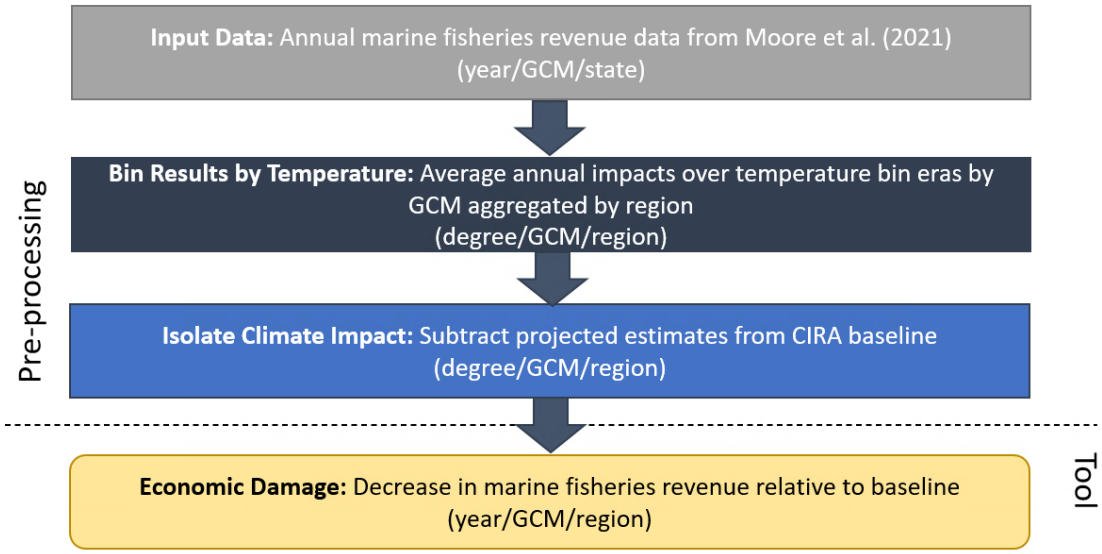

When FrEDI is run, the pre-processed by-degree lost revenue damage functions are then applied to the input temperature scenario to calculate the annual total lost revenue from marine fishereis, by GCM and region.

Limitations and Assumptions

- While the underlying study includes impacts for Southern Alaska fisheries, the analysis incorporated in FrEDI is limited to CONUS fisheries. In the 2007-2016 period, Alaska accounted for approximately one third of revenue from all fisheries, and almost 45% of the revenues from fisheries with habitat projections. The paper estimates that under RCP 8.5 climate change would reduce the annual value of ex vessel revenues by about 1.7% from baseline. These declines from baseline for Alaska fisheries are omitted from the FrEDI data, which does not include Alaska in the spatial domain.
- As noted above, the Moore et al. (2020) study includes a welfare analysis at national scale, for a subset of species. The results of the welfare analysis reflect both market adaptation though substitution effects, and changes in prices. The latter effect, which is characterized by large increases in ex vessel prices through the 21st century, appears to be a strong influence on the welfare estimates. Compared to the direct impacts in the screening analysis results, where prices are held constant, the welfare analysis yields results for the present value of damages that are two to three times larger, suggesting that the direct impact results incorporated in FrEDI are conservative.
- The Moore et al. (2020) and Morley et al. (2018) analyses exclude many factors that may influence species abundance and commercial landings, such as potential changes in primary productivity, species interactions, population dynamics, or fisheries management. In addition, because the approach focuses on potential changes in the landings of species that are already commercially harvested, it does not account for the possibility that an increase in the abundance of other species

could lead to the development of new fisheries. This type of development would help to offset potential losses in economic welfare attributable to a decline in the productivity of established fisheries.

- The species for which habitat projections are available account for nearly 80% of the average annual ex-vessel revenues on the East Coast. Coverage is somewhat lower in the other three regions, where the species for which habitat projections are available account for between 63% and 68% of the average annual revenue. These factors likely lead to underestimate of the total impact of climate change on fisheries.
- For further discussion of the limitations and assumptions in the underlying sectoral model, see Moore et al. (2020).

B.5 Labor Sector

Labor

Summary

UNDERLYING DATA SOURCES AND LITERATURE

Neidell, M., Graff-Zivin, J., Sheahan, M., Willwerth, J., Fant, C., Sarofim, M., & Martinich, J. (2021). Temperature and work: Time allocated to work under varying climate and labor market conditions. PLoS ONE 16(8): e0254224. https://doi.org/10.1371/journal.pone.0254224

The labor sector addresses economic damages from changes in total labor hours in the CONUS due to climate change. The analysis estimates changes in labor allocation, with both positive and negative responses in hours worked in weather-exposed industries (e.g., agriculture, construction, manufacturing). The study finds the relationship between temperature and hours worked is not significant during recession periods, and therefore projected losses are adjusted to account for the probability of recession. Damages are based on a physical measure of average hours worked by workers in high-risk industries, which is monetized in Neidell et al. (2021) by average wages across at-risk industries.[31] For illustrative purposes, **Figure B-49** shows the resulting damages by degree of warming by GCM, calculated using 2010 (panel A) and 2090 (panel B) socioeconomics (i.e., the endpoints of the socioeconomic scenarios).

[31] Hourly wages are based on average wages across at-risk industries: agriculture, forestry, fishing, hunting, mining, construction, and manufacturing.

FIGURE B-49. LABOR IMPACTS BY TEMPERATURE BIN DEGREE

A. 2010 SOCIOECONOMICS **B. 2090 SOCIOECONOMICS**

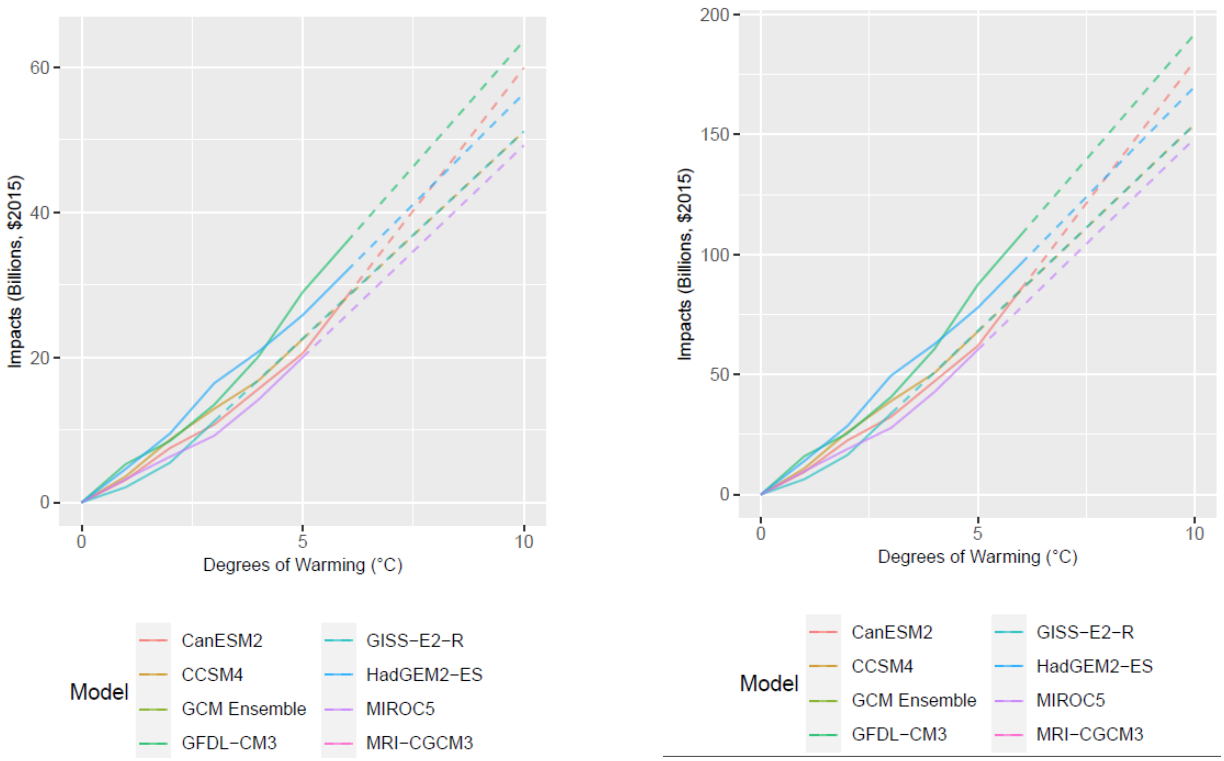

Processing steps

TABLE B-13. INCOMING DATA CHARACTERISTICS: LABOR

Data Features	Labor Attributes
Evaluated Impacts	• Lost hours among high-risk workers (physical) • Value of lost wages among high-risk workers (economic)
Variants	• No additional adaptation
Data Shape	• Year • Six GCMs (standard CIRA set) • State level
Runs Provided	• With climate change
Additional Data	• High-risk worker population • High-risk worker wage rate

Processing steps are shown in **Figure B-50**. Forgone labor hours for each year, GCM, and state are provided by the Neidell et al. (2021) study authors. These results already account for baseline hours lost, so no additional pre-processing is needed to isolate climate impacts. The next step divides these estimates by high-risk worker population to calculate lost hours per high-risk worker estimates. The population of high-risk workers varies by state but is assumed to remain constant over the century. Lastly, state-level lost hours per high-risk worker are binned by degree of CONUS temperature change for each GCM by averaging

across the eleven-year windows where each GCM reaches each integer degree of CONUS warming relative to the baseline.

FIGURE B-50. LABOR DATA PROCESSING FRAMEWORK

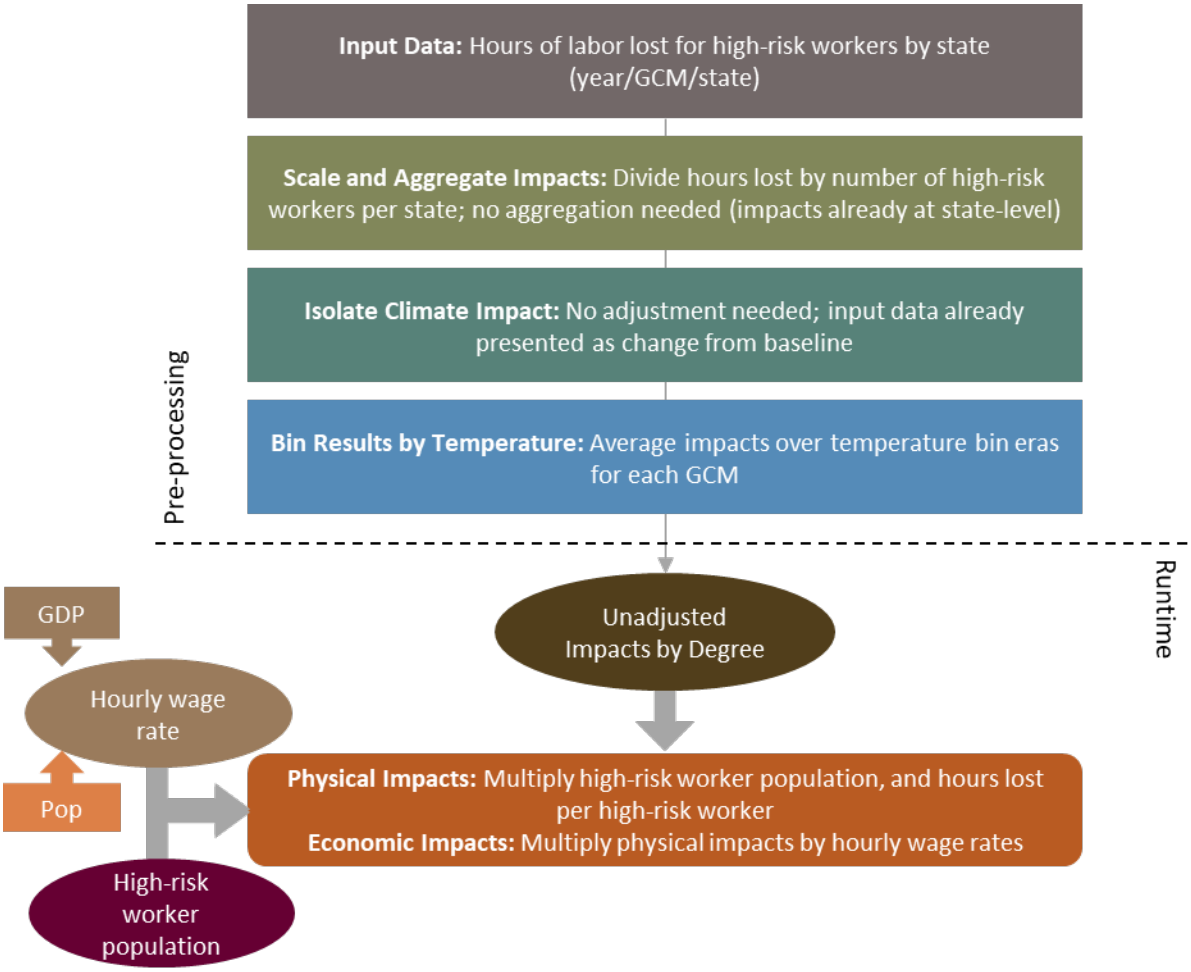

When FrEDI is run, the pre-processed by-degree lost hours per high-risk worker functions are then applied to the input temperature scenario to calculate the unadjusted annual hours lost per high-risk worker based on the level of warming in each year of the input scenario. The total labor hours lost are then calculated by applying these annual rates to the [32]Lastly, lost hours are monetized by multiplying the total annual hours lost by an average wage rate from the Bureau of Labor Statistics,[33] as is done in Neidell et al. (2021), inflated from 2010 values proportionally to GDP per capita growth. Therefore, the physical hours lost will

[32] This is a generic elasticity function that can be used in a time-series fashion, as used here, or for cross-sectional benefits transfers, as in the example in Masterman and Viscusi (2018), "The Income Elasticity of Global Values of a Statistical Life: Stated Preference Evidence", Journal of Benefit-Cost Analysis, 9(3):407-434. Note that the current default elasticity is 1.0, but can be set by the user as an input to the R code.

[33] U.S. Bureau of Labor Statistics. 2009. Table 2. Private industry by six-digit NAICS industry and government by level of government, 2009 annual averages: Establishments, employment, and wages, change from 2008. Available at: https://www.bls.gov/cew/publications/employment-and-wages-annual-averages/2009/tables/private-industry-by-six-digit-naics-and-government-by-level-of-government.pdf

not scale with changes in user-input population, but the monetized impacts will scale with wage rate, which is a function of user-input GDP per capita.

Limitations and Assumptions

- High-risk worker population is assumed to remain constant over the century. As discussed further in Neidell et al. (2021): "Information on the number of high-risk workers at the county level comes from the American Community Survey centered around 2010 (2008–2012 five-year estimates). We assume the number of high-risk workers will remain constant over time. This is because trends from the recent past, as well as near-term projections, suggest that while some industries defined as high-risk will reduce the number of workers they support, including agriculture and mining, and others have or will experience slight increases; on net the absolute number of high-risk workers has and is expected to remain roughly constant at least through 2029."
- This analysis does not evaluate the potential for new adaptations (behavioral or technological) by workers or employers to mitigate the effects of extreme temperatures on labor allocation. Adaptations present in the baseline period upon which the econometric analysis is based are assumed to be part of the modeled response to future temperature changes, however, new adaptation behaviors or technology are not evaluated.
- For further discussion of the limitations and assumptions in the underlying sectoral model see Neidell et al. (2021).

B.6 Agriculture Sector

CIL Agriculture

Summary

This sector addresses the impact of climate change on agricultural yields of key crops across all of CONUS. The Climate Impact Lab (CIL) Agriculture projections are drawn from functions estimating the effects of changes in temperature, precipitation, and CO_2 fertilization on yields of cotton, maize, soybean, and wheat. Temperature and precipitation response functions for wheat are based on research from Hsiang, Lobell, Roberts, and Schlenker (2013), and functions for cotton, maize, and soybean are drawn from Schlenker and Roberts (2009). CO_2

UNDERLYING DATA SOURCES AND LITERATURE

Hsiang, S., Kopp, R., Jina, A., Rising, J., Delgado, M., Mohan, S., Rasmussen, D.J., Muir-Wood, R., Wilson, P., Oppenheimer, M., Larsen, K., and Houser T. (2017). Estimating economic damage from climate change in the United States, *Science*, 356, 1362–1369.

Hsiang, S., Lobell, D., Roberts, M., and Schlenker, W. (2013). Climate and Crop Yields in Australia, Brazil, China, Europe and the United States. Available at SSRN: https://ssrn.com/abstract=2977571 or https://doi.org/10.2139/ssrn.2977571.

McGrath, J.M. and Lobell, D.B. (2013). 'Regional disparities in the CO2 fertilization effect and implications for crop yields', *Environ. Res. Lett.*, 8, 014054.

Schlenker, W. and Roberts, M.J. (2009). 'Nonlinear temperature effects indicate severe damages to U.S. crop yields under climate change', *Proc. Natl. Acad. Sci. U.S.A.*, 106, 15594–15598.

fertilization response functions for all four crops are based on estimates from McGrath and Lobell (2013).[34] Hsiang et al. (2017) use these functions to project future impacts on yields by GCM and RCP through the 21st century. Economic damages are based on changes from regional baseline production value averaged over 1990-2000 drawn from the USDA National Agricultural Statistics Service's (NASS) Quick Stats database. The currently available results include adaptation strategies only to the extent that they have been previously implemented in the study area. We anticipate that future revisions of FrEDI may incorporate a "with adaptation" variant that includes modelling of future adaptation behaviors and technologies specifically for maize. For illustrative purposes, **Figure B-51** shows the resulting damages by degree of warming for each impact type and for both variants (left and right plots), by GCM.

[34] Readers should note that the online version of McGrath and Lobell (2013) includes a link to Rosenthal and Tomeo (2013) and implies that Rosenthal and Tomeo "corrects" McGrath and Lobell. In fact Rosenthal and Tomeo is a complementary Perspective (commentary) article to McGrath and Lobell, and does not provide any correction of results or any results whatsoever.

FIGURE B-51. CIL AGRICULTURE IMPACTS BY TEMPERATURE BIN DEGREE

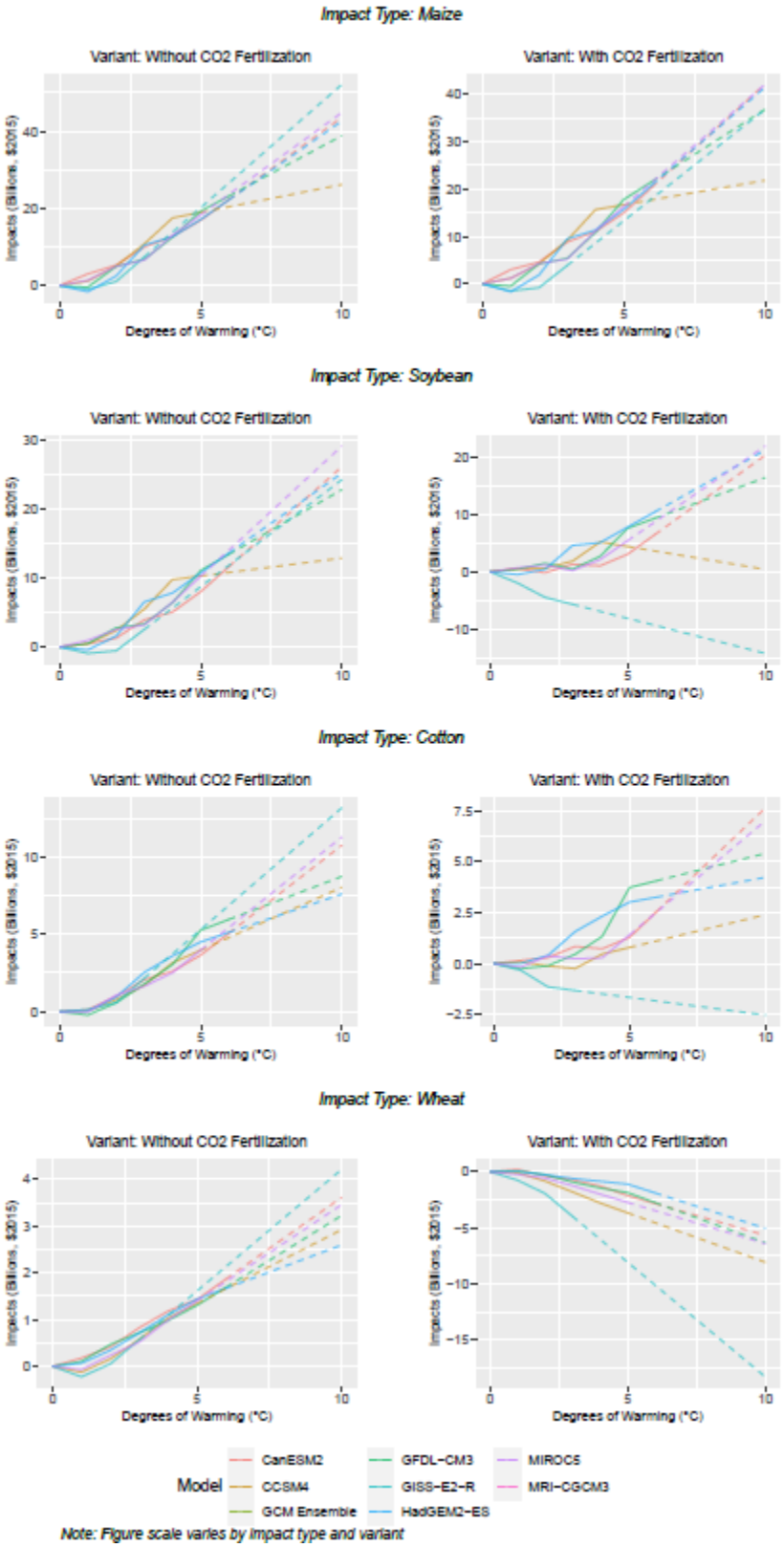

Note: Figure scale varies by impact type and variant

Processing steps

Processing steps are shown in **Figure B-52**. The Hsiang et al. (2017) study authors provide the percent change in yields of each crop under RCP8.5, by GCM, year, and state, as well as baseline yields by state and region averaged over the period 2000-2005. We interpret this 2000-2005 baseline in the underlying study as approximately consistent with the FrEDI baseline period. The authors provided a full distribution of impacts by degree, but this version of FrEDI uses the median estimates. In the first pre-processing step, the percent changes and baseline data by state are converted to absolute annual changes in yields and summed to the region level. In the second processing step, the region-level annual yield changes are binned by degree of CONUS temperature change for each GCM by averaging across the eleven-year windows where each GCM reaches each integer degree of CONUS warming relative to the baseline. In the third pre-processing step, temperature-binned absolute regional changes in yield are converted back to percent changes by dividing by regional baseline yields. Finally, regional percent changes in yields are scaled by the baseline production values from USDA NASS to give economic damage estimates.

FIGURE B-52. CIL AGRICULTURE DATA PROCESSING FRAMEWORK

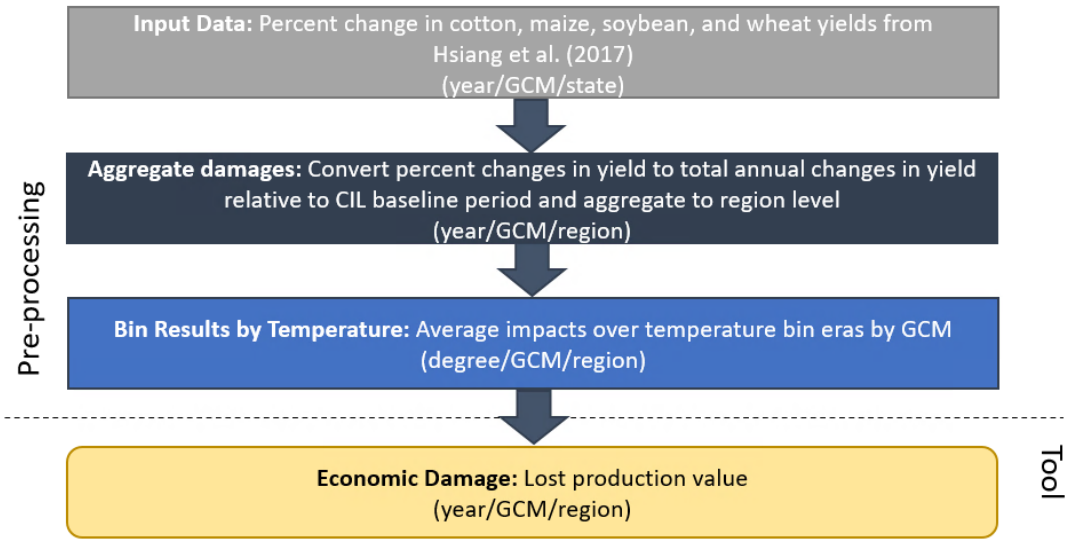

When FrEDI is run, the pre-processed by-degree percent changes in yield functions are then applied to the input temperature scenario to calculate the unadjusted annual percent changes in yields based on the level of warming in each year of the input scenario. Lastly, these are monetized by scaling the annual percent yield changes by the baseline production values from the USDA NASS to calculate the total annual lost production value.

Limitations and Assumptions

- The economic impacts presented are directly proportional to the underlying physical impacts and do not incorporate market effects on price due to projected changes in supply. For this reason, we

may underestimate future impacts. Work by Beach et al. (2015)[35] suggests that climate change may cause increases in crop prices overall, which supports the conclusion that we underestimate impacts.

- This study takes incomplete account of the impact of future potential changes in crop technology, energy and land use policies, and other interactions that could affect market outcomes. For the most part, these important factors affecting agricultural yield are not directly tied to changes in climate, but could be components of an adaptative response as climate change unfolds.
- The underlying study also omits some important aspects of climate change impacts to agriculture not directly tied to yield effects, including damages from extreme weather events, wildfire, and changes in weeds, pests, disease, and ozone damage. Collectively, these effects would likely result in larger yield losses than those estimated here.

For further discussion of the limitations and assumptions in the underlying sectoral model, please see Hsiang et al. (2017).

[35] Beach, R., Y. Cai, A. Thomson, X. Zhang, R. Jones, B. McCarl, A. Crimmins, J. Martinich, J. Cole, and B. Boehlert, 2015: Climate change impacts on US agriculture and forestry: benefits of global climate stabilization. *Environmental Research Letters*, **10**, doi: 10.1088/1748-9326/10/9/095004.

APPENDIX C | METHODS DETAILS

C.1 Global to CONUS Temperature Translation

One flexibility of FrEDI is its ability to generate impact estimates from either global or CONUS temperature input data. FrEDI contains a translation function, derived from global and CONUS temperatures from six CMIP5 GCMs used in many of FrEDI's underlying damage functions. **Figure C-1** plots the global and CONUS temperatures for the six GCMs, under RCP8.5, where each point represents an era (i.e., 2030, 2050, 2070, 2090) and GCM combination. All temperature changes presented are relative to the 1985-2006 baseline period.

FIGURE C-1. GLOBAL AND CONUS TEMPERATURES, RCP8.5

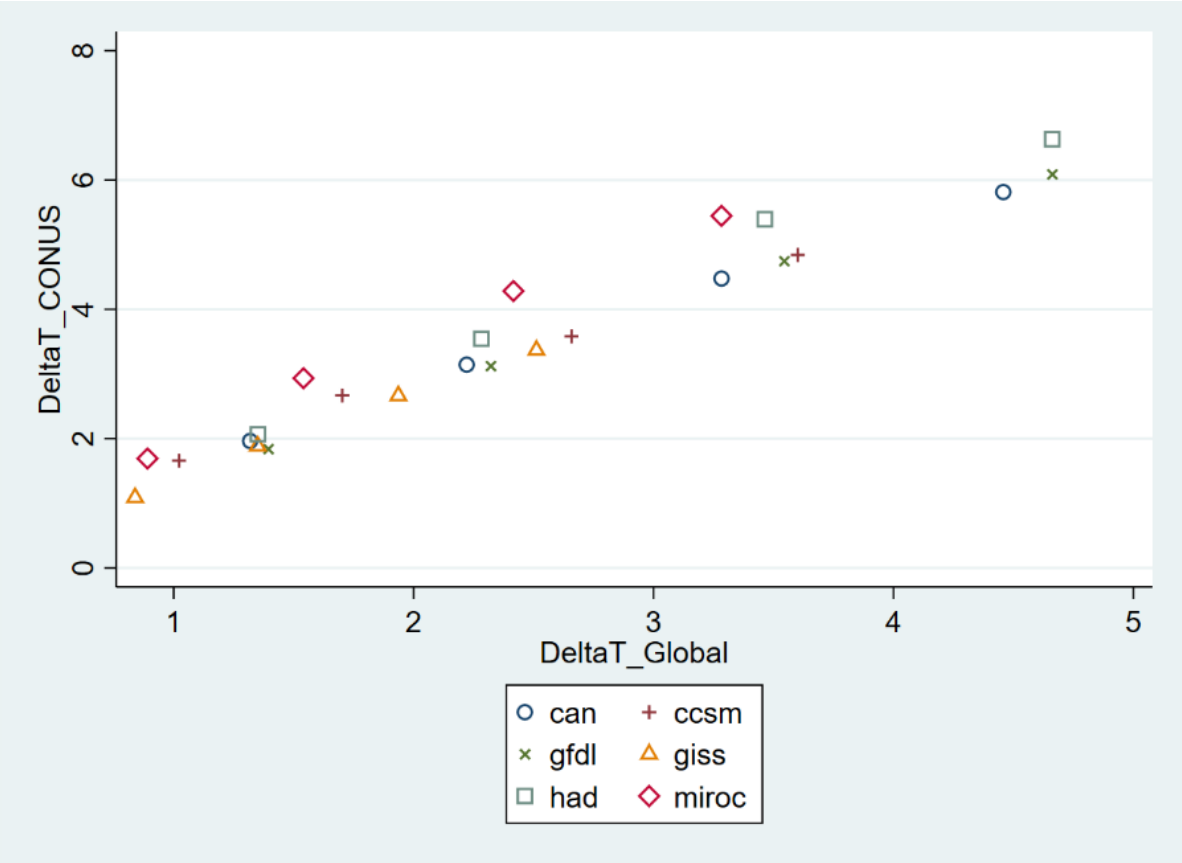

This plot shows global and CONUS temperatures for the six GCMs, under RCP8.5. Each data point is an era-GCM combination.

The relationship between CONUS and global temperatures is relatively stable across GCMs and over time, allowing us to use these available datapoints to develop a generalized relationship between global and CONUS temperature anomalies. The coefficients of this equation are as follows, in **Table C-1**.

TABLE C-1. CONUS TO GLOBAL TEMPERATURE TRANSLATION COEFFICIENT ESTIMATES

Regression estimates relating CONUS and global temperature changes, relative to a 1986-2005 baseline.

	ΔT_{CONUS}	
ΔT_{GLOBAL}	1.421	***
	(0.000)	
R-squared	0.990	
Adjusted R-squared	0.990	
N	24	

Standard errors listed below coefficients, in parentheses. * p<0.05; ** p<0.01; *** p<0.001

These coefficients are used to translate global temperature inputs into CONUS temperatures for binning indexing, however if a user inputs CONUS temperatures, the inverse of the formula can be used to generate global temperatures.

In general, relative to global temperatures, the use of national temperatures in FrEDI reduces scatter, improves fit, and allows better emulation of GCMs that might not have been used to generate the sector-specific damage functions. However, note that there are some sectors where an impact may be better associated with global rather than national temperatures, in the case where the impacts are a function of large-scale weather pattern or ocean circulation changes.

C.2 Calculation of global mean sea level

When a user provides FrEDI with an input temperature trajectory, but does not provide a custom sea-level rise trajectory, FrEDI calculates the projected sea-level rise at runtime from input amount of temperature change. To calculate global mean sea level from global mean temperature, we use a semi-empirical sea level model from Kopp et al., 2006. This model relates the rate of global mean sea level rise (dh(t)/dt) to global mean temperature at time T(t), an equilibrium temperature $T_e(t)$, and a small residual trend arising from the long-term response to earlier climate change Ø(t), relative to 2000 using equation 10 from Kopp et al., (2016).

$$\frac{dh(t)}{dt} = a * \left(T(t) - T_e(t)\right) + \emptyset(t) \qquad \text{(Equation C-1)}$$

In the equation above, $T_e(t)$ and Ø(t) are functions of time, where:

$$\frac{dT_e(t)}{dt} = \frac{(T(t) - T_e(t))}{tau_1} \qquad \text{(Equation C-2)}$$

$$\frac{d\emptyset(t)}{dt} = \frac{-\emptyset(t)}{tau_2} \qquad \text{(Equation C-3)}$$

The parameter values are estimated from the probability distributions of the semiempirical model parameters in Figure S5, and Dataset S1j, focusing on the posterior distribution calculated with the Mann et

al., (2009) temperature data set. We use the median parameter values across the distributions for this calculation. We used HadCrUT4 to determine the appropriate temperature offset between the actual temperature and the equilibrium temperature in 2000.

TABLE C-2. PARAMETER VALUES USED IN THIS ANALYSIS, FROM KOPP ET AL., 2016, MEDIAN AND 5TH AND 95TH PERCENTILES.

Parameter	Value	Units
$\emptyset(2000)$	0.14 (0.05, 0.29)	mm/yr
tau_1	174 (87, 366)	Year
tau_2	4175 (1140, 17670)	Year
a	4.0 (3.2, 5.4)	mm/yr/K
$T_e(2000)$	-0.05 (-0.12, 0.07)	K

Future versions of FrEDI may use several different approaches for addressing uncertainty. Some of these approaches include: using the parameter distributions in S1j using a Monte Carlo approach to sample the parameters distributions provided in Kopp et al., (2016), both Mann et al., (2009) and Marcott et al., (2013); calibrating $T_e(2000)$ and alpha parameters to emulate the range of sea level rise from AR6; and examine low-probability high impact outcomes such as the sea level rise projection including ice sheet instability from AR6 or the higher Sweet et al., (2017) scenarios. Some approaches (such as using the normal distributions for parameters or the alternate parameter set calibrated against Marcott et al. (2013)) will be straightforward, but others may be more challenging to implement. The semi-empirical approach was not designed to incorporate future sea level rise processes that were not observed in historical data such as ice sheet instability and may not be accurate for multi-century applications. We note that the user can supply FrEDI with exogenous global mean sea level rise scenarios instead of calculating them from global mean temperature.

References:

Hsiang, S., Kopp, R., Jina, A., Rising, J., Delgado, M., Mohan, S., Rasmussen, D. J., Muir-Wood, R., Wilson, P., Oppenheimer, M., Larsen, K., and Houser, T.: Estimating economic damage from climate change in the United States, Science, 356, 1362–1369, https://doi.org/10.1126/science.aal436 (2017).

Kopp, R. E. et al. Temperature-driven global sea-level variability in the Common Era. PNAS 113, E1434–E1441 (2016).

JGCRI/hector. GitHub https://github.com/JGCRI/hector/releases.

Mann, M. E. et al. Global Signatures and Dynamical Origins of the Little Ice Age and Medieval Climate Anomaly. Science 326, 1256–1260 (2009).

Marcott, S. A., Shakun, J. D., Clark, P. U. & Mix, A. C. A Reconstruction of Regional and Global Temperature for the Past 11,300 Years. Science (2013).

Met Office Hadley Centre observations datasets. https://www.metoffice.gov.uk/hadobs/hadcrut4/data/current/download.html.

Neumann, J. E., Chinowsky, P., Helman, J., Black, M., Fant, C., Strzepek, K., and Martinich, J.: Climate effects on US infrastructure: the economics of adaptation for rail, roads, and coastal development, Clim. Change, 167, 44, https://doi.org/10.1007/s10584-021-03179-w (2021).

Sweet, W. V. and Horton, R. and Kopp, R. E. and LeGrande, A. N. and Romanou, A. Climate Science Special Report: Fourth National Climate Assessment, Volume I. (U.S. Global Change Research Program, 2017).

Weitzman, M.: GHG Targets as Insurance Against Catastrophic Climate Damages, J. Public Econ. Theory, 14, 221–244 (2012).

APPENDIX D| SOCIAL VULNERABILITY MODULE

D.1 Overview

The main purpose of this module is to integrate the underlying data and analytical approach from EPA's Social Vulnerability Report[36] (hereafter referred to as the SV report) into the FrEDI tool. This allows users to explore how the impacts of climate change will be distributed among four population groups of concern: (1) individuals with low income (below two times the national poverty line), (2) those identifying as Black, Indigenous, or people of color (BIPOC), (3) those that are without a high school diploma, and (4) those that are 65 years of age or older. Analyzing impacts and disproportionality for specific racial and ethnic populations (e.g., Black or African American, Hispanic, Asian, etc.) within the BIPOC group has also been incorporated into the FrEDI module, consistent with data presented in the SV Report. Note that in contrast to the main sector calculations in FrEDI, the SV module estimates impacts sectoral for seven CONUS regions, to maintain consistency with the methodology in EPA's peer-reviewed SV Report.

D.2 Features of the module

The SV module assesses the disproportionate impacts of climate change under any user-defined scenario of temperature change across select sector categories. In order for consideration, the underlying sector study from the SV Report must first meet specific qualifications for technical feasibility.

1. **Fine spatial scale:** At least county-level results but preferably census tract.
2. **Per person impacts:** Easily converted to "physical" impacts per individual (for example, incidence per 100,000 for health impacts or damage ratios for flooding damage), ideally avoiding economic impacts because the burden of the same monetary cost is realized differently across individuals with, for example, different levels of income.

The sectors included in FrEDI-SV are listed in **Table D-1**, which also lists the impact estimated and whether a variant is included for the sector.

TABLE D-1. SECTORS CURRENTLY IMPLEMENTED IN FREDI-SV

Social Vulnerability Report Sector	Corresponding FrEDI-SV Impact Type	FrEDI-SV Metric of Impact	Spatial Scale	Default Adaptation scenario
Air Quality and Health	Air quality and new asthma cases (PM2.5 only)	New childhood asthma cases (age 0-17)	Tract	No Additional Adaptation
	Air quality and premature mortality (PM2.5 only)	Premature mortality (over age 65 only)	Tract	No Additional Adaptation

[36] https://www.epa.gov/cira/social-vulnerability-report

Social Vulnerability Report Sector	Corresponding FrEDI-SV Impact Type	FrEDI-SV Metric of Impact	Spatial Scale	Default Adaptation scenario
Extreme Temperature and Health[a]	Extreme temperature and mortality	Premature mortality (all ages)	Tract	No Additional Adaptation
Extreme Temperature and Labor	Extreme temperature and labor	Work hours lost	Tract	No Additional Adaptation
Temperature/Precip. and Traffic[b]	Roads: Temp/Precip and traffic	Hours of traffic delay	Tract	No Additional Adaptation
Coastal Flooding and Traffic	High tide flooding and traffic	Hours of traffic delay	Tract	Reasonably Anticipated Adaptation
Coastal Flooding and Property	Coastal flooding and property	Individuals threatened with total property loss	Block Group	No Additional Adaptation

Notes:
a. Based on the Mill et al. (2015) Extreme Temperature study.
b. Note that the impact of temperature and precipitation on road integrity and delays is not included in the main text of the social vulnerability report, but the method and results are described in detail in Appendix G of that report.

Briefly, the FrEDI-SV module uses damage functions (i.e., physical impacts by CONUS half-degree temperature increment) at the census tracts or block group level for each sector. Note that the impact metrics used in the SV module are physical measures, which are not included for all sectors in the main FrEDI code. For example, for the Coastal Flooding and Property category, the physical impact metric, individuals threatened with total property loss, aligns with the impact metric included in the SV report. In contrast, the Coastal Property impact metric used elsewhere in FrEDI is total monetized property damage or loss. The physical metric used in FrEDI-SV is designed to consider the likelihood of permanent home loss through repeated flood episodes causing damage and serves as an indicator of the most severe impacts of coastal flooding. Total property loss can be triggered by intense and repeated damage from storm surge or by permanent inundation from sea level rise. FrEDI identifies the annual expected damages to residential structures within a block group, and the property loss scenario considers properties which reach the 10 percent annual expected damage threshold – that is, total home loss is expected within a decade. This aligns with the assumption for a threat of abandonment in the underlying sector study for coastal property.[37]

The FrEDI-SV module also relies on demographic population information. While the SV Report did not consider population growth, total national population growth projections are included in the FrEDI-SV

[37] See Neumann, J. E., Chinowsky, P., Helman, J., Black, M., Fant, C., Strzepek, K., & Martinich, J. (2021). Climate effects on US infrastructure: the economics of adaptation for rail, roads, and coastal development. Climatic Change. https://doi.org/10.1007/s10584-021-03179-w

module so that it is consistent with the impacts derived from main FrEDI. The relative percent of each population group in each census tract are taken from current demographic patterns from the U.S. Census American Community Survey (ACS) dataset (2014-2018) (accessed via the IPUMS platform).[38] In the FrEDI-SV module, current demographic patterns are applied to projections of total national population growth (from ICLUS) and are held constant overtime because robust and long-term projections for local changes in demographics are not readily available. Therefore, FrEDI-SV does not consider how changes in future demographic patterns in the U.S. could affect risks to these populations.

As shown in **Table D-1**, the FrEDI-SV module is also designed with the capability to assess the impacts across different adaptation scenarios in each sector. The default adaptation assumption considered for most of the sectors in the FrEDI-SV module is a 'no additional adaptation' scenario, which current adaptation responses and human acclimatization to hazards are incorporated in the projection, but no additional planned adaptation investments are modeled beyond those already in place. For high tide flooding and traffic, a "reasonably anticipated" adaptation scenario is used as the default, which incorporates virtually costless and autonomous adaptation actions. As with the main FrEDI module, the ability to incorporate damage functions under different adaption assumptions depends on the data available in the underlying studies. Alternative adaptation scenarios currently included in FrEDI-SV include proactive adaptation scenarios for both roads and coastal property. In cases where alternative adaptation scenarios are included, which apply to sectors in the last three rows of **Table D-1**, those results are directly reported along with the default assumptions from the FrEDI-SV module.

D.3 Approach

This section describes the overall methodological approach behind the FrEDI-SV module, for a given set of climate scenarios (temperature trajectories).

Similar to the main FrEDI module, a series of pre-processing steps are first used to incorporate the underlying peer-reviewed studies from the SV report into a series of impact-temperature damage functions at the census tract level. In contrast with the main FrEDI module, which uses a database of state-aggregated impact-temperature functions from (mainly) six individual GCMs, the FrEDI-SV module uses impact-temperature relationship derived from the average across all six GCMs. This significantly reduces the processing time and database file size to compensate for the increased spatial detail in this module. When run in R, the FrEDI-SV module then uses this database of damage functions in the following steps:

1. Determine the physical impacts per population at the census tract level. With this, the R-code uses a linear interpolation between half degrees of warming from the input temperature trajectory.

[38] This analysis relied on the IPUMS platform to download ACS data through its National Historical Geographic Information System (NHGIS). The NGHIS codes for data this report relies upon are provided in Table 3, Appendix C of the SV Report. For the IPUMS platform see Manson S, Schroeder J, Van Riper D, Kugler T, and Ruggles S. IPUMS National Historical Geographic Information System: Version 15.0 American Community Survey 2014-2018a. Minneapolis, MN: IPUMS. 2020. http://doi.org/10.18128/D050.V15.0. Note that the NHGIS field codes in Table 3 are unique to IPUMS – ACS table numbers differ from the field codes shown in the SV report, but the data are identical.

2. Calculate aggregate impacts and populations at the regional and CONUS levels for both population groups of concern and reference populations. This is done by weighting the impacts at the census tract or block group by the respective population groups. Here is where we apply county-level population projections by applying county-level growth ratios to census tract or block group populations.
3. Calculate the variables used to calculate the disproportionality metrics (e.g., difference in risk, with and without adaptation (if available)), as used in EPA's SV Report and described in detail in the following section.

D.4 Disproportionality, difference in risk calculation

The following describes in more detail the steps taken to calculate the first disproportionality metric, the difference in risk. **Figure D-1** provides a visual representation of these steps.

FIGURE D-1.FIVE STEPS FOR ASSESSING THE DISPROPORTIONALITY OF IMPACTS ON SPECIFIC POPULATIONS

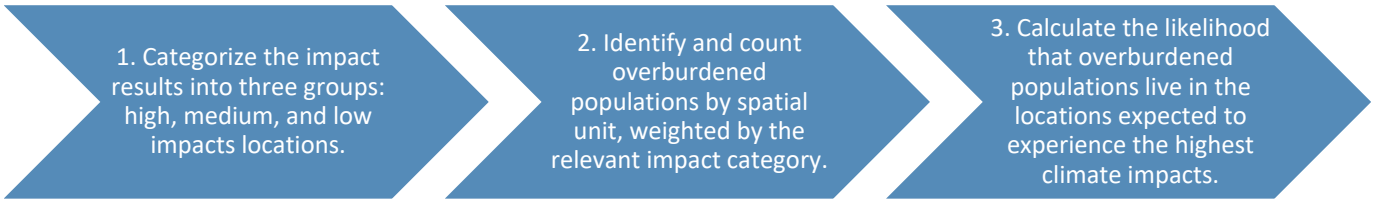

Step 1: Categorize the spatial data into three groups: high, medium, and low impact locations. We use the impacts per population (relative impacts or rates) to categorize climate impacts associated with a particular temperature trajectory by spatial unit (Census tracts or block groups) into three evenly sized groups, called terciles. The focus of the risk analysis is on the composition of populations found in the high impact group – where we are attempting to identify cases where specific populations are more likely to currently live in areas experience the largest impacts from climate change. Note that for coastal properties and high tide flooding, we only consider populations that live in coastal areas and are exposed to the coastal hazards of sea-level rise or storm surge during the 21st century projection period – we do not include inland areas.

Step 2: Identify and count specific populations by location. As discussed in the SV report, while we cannot observe exactly which individuals are exposed to the relevant climate hazard, we can overlay the results by location. For demographic patterns, we rely on data from the American Community Survey (2014-2018) at the Census tract or block group to (1) count the number of individuals in each population group of concern (sv_group) relative to reference population and then (2) weight the proportions by relevant climate hazard exposed population (e.g., children aged 0-17 years for childhood asthma). In the absence of projections

describing how detailed demographics will shift over the century, we assume the relative distribution of overburdened to non-overburdened populations is fixed at 2014-2018 levels.

Step 3: Calculate the likelihood that populations live in the locations expected to experience the highest climate impacts. We then model impacts and identify high impact areas. We define "high impact" as the census tract areas with the highest tercile of projected climate change impacts. Note that the spatial resolution of analysis varies by sector (e.g., census tract or block group), but is consistent within each analysis. Once we identify high impact areas, we identify the total population of interest and total remaining population in those same areas. From this, we calculate the likelihood of living in a high impact location, relative to the reference domain, for both population groups.

Step 4: Compare the likelihoods of population groups of concern and reference populations. The relative likelihoods described here are the result of comparing likelihoods of living in high impact areas for populations of interest relative to their reference population. These likelihoods are expressed relative to the reference population and are calculated at the national and regional level. The likelihood measures are separately calculated for each social vulnerability metric. These likelihood metrics can be interpreted as the degree to which climate impacts disproportionately affect population groups of concern relative to each reference population.

Table D-2 shows an example of the calculation of disproportionate risks of currently living in a location that is projected to experience the largest climate change impacts.

TABLE D-2. EXAMPLE CALCULATION OF DISPROPORTIONATE IMPACTS ON AN EXAMPLE POPULATION

Step	Values
1. Identify populations that impacted but who are and are not in a specific population group of concern	• Total population experiencing sectoral impacts: o 22 million people in specific group of concern o 93 million people in reference population
2. Identify high impact areas	• Within high impact census tracts: o 3.5 million people in group of concern o 14 million are in the reference population
3. Calculate the likelihood of living in a high impact area	• Likelihood of high impact: o 3.5/22 = 0.16: likelihood individuals in specific group are living in high impact areas o 14/93 = 0.15: likelihood individuals in the reference population are living in high impact areas
4. Compare likelihoods	• Group of concern likelihood / reference population likelihood = 0.160/0.147 = 1.09. o 1.09 - 1 = 9% difference in risk

D.5 Calculating impacts and rates by population groups

Below is the process for estimating the impacts for population groups of concern and reference populations for each temperature scenario, weighted average impact for CONUS and each region. In this case, "pop_weights" are the fraction of the population that are impacted, for example, people that are 17 or younger make up the childhood asthma population. Note that the equations below are for impacts by tract, which applies to most sectors but some sectors (coastal properties, for example) include impacts by census block group.

Total impacts by tract: Multiply impact by weighted populations in each population

impacts_sv_tract = rate_tract * sv_population_tract * pop_weights

impacts_ref_tract = rate_tract * ref_population_tract * pop_weights

Total impacts by region: Sum new asthma cases for each region (and CONUS) and each population

impacts_sv_region = Sum(impacts_sv_tract)

impacts_ref_region = Sum(impacts_ref_tract)

Average rates by region and CONUS

Impact_sv_region = impacts_sv_region / (sv_population_region * pop_weights)

Impact_ref_region = impacts_ref_region / (ref_population_region * pop_weights)

Total avoided cases for sv group, in scenario with policy action relative to baseline

Avoided_cases_sv_region = impacts_sv_region_policy - impacts_sv_region_baseline

D.6 Demographic data

Analyses in the FrEDI-SV module rely on demographic data from the five-year American Community Survey 2014-2018 (ACS). Where available, data are collected at the block group level or the census tract level. We rely on the IPUMS[39] platform to download ACS data through its National Historical Geographic Information System (NHGIS).

Population groups of concern included:

- **Low Income:** We define "low income" as populations living in households that have an aggregate income that is at most, twice the poverty threshold. ACS definitions for poverty thresholds are not geographically differentiated but do vary by household composition. Additional information on the definition of poverty thresholds can be found on the Census website.[40] In the SV module we

[39] IPUMS had previously been an acronym for Integrated Public Use Microdata Series, but not all of the data it accesses is public or is microdata, so since 2016 it has been known only by its acronym.
[40] https://www.census.gov/topics/income-poverty/poverty/guidance/poverty-measures.html

aggregate the estimates of population living in those households that fall into income to poverty threshold ratios below two.

- **BIPOC (ACS and the SV Report both use the term "Minority")**[41]**:** The ACS provides race and ethnicity information at the block group level. We define BIPOC as all racial and ethnic groups except white, non-Hispanic. The module relies on total population and white, non-Hispanic population to calculate BIPOC population at the block group spatial scale.
- **No High School Diploma:** The ACS tracks information on educational attainment – in this analysis we consider populations without a high school diploma to be a overburdened demographic. To estimate the number of people per block group with an educational credential of less than a high school diploma or equivalent, we rely on educational attainment data for the population 25 years or older.
- **65 and Older:** The module identifies people aged 65 or older as overburdened. We use age demographic information from the ACS to determine 65 and older populations at the block group level by aggregating population estimates for age groups provided by the ACS counting people 65 or older.

D.7 Outputs and Visualization

FrEDI-SV regional outputs (defined in **Table D-3**) can be used to assess: 1) absolute impacts on population groups of concern; 2) differences in risks (or exposure to hazards) across populations (a measure of disproportionality); and 3) the relative rates of impacts across different populations. Example uses of the FrEDI SV module are shown in Chapter 3 and discussed in detail below.

TABLE D-3. SV MODULE OUTPUT DATA DICTIONARY

Region	NCA region
svGroupType	Population group of concern category (e.g., 'sv_') or racial/ethnic group (e.g., 'race_')
driverUnit	Units of climate driver (centimeters of sea level rise or degrees Celsius of temperature)
driverValue	Value of climate driver relative to baseline
year	Year
impPop_ref	Number of impacted people in the reference population. Counts people who both live in a region where climate damages are assessed for the sector and fall into the population assessed by the sector (Labor: high-risk workers, Air Quality - Premature Mortality: age 65+, Air Quality - Childhood Asthma: age 17 and under, Coastal Properties: residents of the coastal zone, High Tide Flooding and Traffic: residents of the coastal zone, Extreme

[41] Consistent with other EPA reports, FrEDI-SV uses the abbreviation "BIPOC" (for Black, Indigenous, and people of color) to refer to individuals identifying as Black or African American; American Indian or Alaska Native; Asian; Native Hawaiian or Other Pacific Islander; and/or Hispanic or Latino. It is acknowledged that there is no 'one size fits all' language when it comes to talking about race and ethnicity, and that no one term is going to be embraced by every member of a population or community. The use of BIPOC is intended to reinforce the fact that not all people of color have the same experience and cultural identity. This report therefore includes, where possible, results for individual racial and ethnic groups. Note the SV report reported results for this group as attributed to a "minority" category. The results are the same here but the category title has been updated.

Region	NCA region
	Temperature: residents of 49 CONUS urban centers including 91 counties included in the underlying study, Mills et al. 2014, Roads: all people).
impPop_sv	Number of impacted people in the population group of concern. Counts people who both live in a region where climate damages are assessed for the sector and fall into the population assessed by the sector (Labor: high-risk workers, Air Quality - Premature Mortality: age 65+, Air Quality - Childhood Asthma: age 17 and under, Coastal Properties: residents of the coastal zone, High Tide Flooding and Traffic: residents of the coastal zone, Extreme Temperature: residents of 49 CONUS urban centers including 91 counties included in the underlying study, Mills et al. 2014, Roads: all people).
impact_ref	Total impact in the reference population (childhood asthma cases, mortality, hours of labor lost, hours of delay, or number of individuals threatened with total property loss, depending on sector)
impact_sv	Total impact in the population group of concern (childhood asthma cases, mortality, hours of labor lost, hours of delay, or number of individuals threatened with total property loss, depending on sector)
national_highRisk Pop_ref	Number of impacted people in the reference population living in tracts in the highest tercile of impacts nationally (subset of impPop_ref)
national_highRisk Pop_sv	Number of impacted people in the overburdened population living in tracts in the highest tercile of impacts nationally (subset of impPop_sv)
regional_highRisk Pop_ref	Number of impacted people in the reference population living in tracts in the highest tercile of impacts regionally (subset of impPop_ref)
regional_highRisk Pop_sv	Number of impacted people in the overburdened population living in tracts in the highest tercile of impacts regionally (subset of impPop_sv)
aveRate_ref	Impacts per person or per 100k people (depending on the sector) for the reference population
aveRate_sv	Impacts per person or per 100k people (depending on the sector) for the overburdened population
scenario	Name of user-provided climate scenario
variant	Adaptation scenario variant (e.g. with adaptation or without adaptation)

First, the FrEDI SV module outputs can be used to assess the risks (defined as the likelihood of living in areas projected to experience the largest impacts from climate change) for each population group of concern relative to those of the national impacted population, as follows:

$$Difference\ in\ Risk = \left(\frac{national\_highRiskPop_{SV}/national\_highRiskPop_{ref}}{impPop_{SV}/impPop_{ref}}\right) - 1 \qquad \text{(Equation D-1)}$$

These results are shown in the top panels of **Figure 8** in the main text and can be interpreted as: A specific population group (sv) is x% more likely to live in a location that is projected to experience the greatest impacts of climate change compared to the reference population.

Outputs from the FrEDI SV module can also be used to assess the relative rates of impacts between different population groups or individuals of different races and ethnicities, as well as differences in impact rates. These types of analyses can be done by comparing the 'aveRate_sv' and 'aveRate_ref' outputs for each group and sector from the SV module (example in bottom panels of Figure 9), which can be equivalently calculated from the impact [sv or ref]/impPop_[sv or ref] variables. Example results from this type of calculation are shown in the bottom panels of Figure 9.

To apply this calculation to a mitigation scenario and to calculate the relative benefits that will be experienced by different population groups, follow Equation D-2

$$Benefits\ Relative\ to\ the\ Ref.\ Population = \frac{baselineScenAvgRate_{SV} - policyScenAvgRate_{SV}}{baselineScenAvgRate_{ref} - policyScenAvgRate_{ref}} \quad \text{(Equation D-2)}$$

To calculate the extent to which disproportionate impacts may be exacerbated or mitigated under a temperature mitigation scenario, follow Equation D-3.

$$Change\ in\ Disproportional\ Impacts\ for\ Each\ Group\ between\ a\ Baseline\ and\ Policy\ Scenario = \frac{baselineScenAvgRate_{SV}}{baselineScenAvgRate_{ref}} - \frac{policyScenAvgRate_{SV}}{policyScenAvgRate_{ref}} \quad \text{(Equation D-3)}$$

Example results from these types of analyses are shown in Figure 14.

D.8 Comparison of FrEDI-SV to Underlying EPA (2021) Climate Change and Social Vulnerability Study

As noted in Section D.1, the FrEDI-SV module is based on methods and data developed for EPA's peer-reviewed Social Vulnerability Report.[42] To ensure that the module produces results consistent with those in the Social Vulnerability Report, we ran the FrEDI-SV module with similar inputs to those used in the report itself. This section provides a comparison of selected FrEDI-SV module results to results presented in the Social Vulnerability report for a hypothetical two-degree warming scenario.

The cross-consistency test presented here focuses on the Air Quality – Childhood Asthma sector results. **Table D-4** provides a comparison of one of the FrEDI-SV metrics, the total impacts in terms of cases of childhood asthma diagnoses, at two degrees of warming. As shown in the table, the differences between FrEDI-SV results and those presented in the SV Report are small. These small differences are largely driven by two factors:

1. Warming arrival time. Impacts in The SV Report were reported for degrees of mean global warming, while FrEDI-SV calculates impacts based on mean CONUS warming. **Table D-4** includes a comparison between the number of new childhood asthma diagnoses per year from climate-driven changes in air quality, predicted at 2°C global warming (SV Report) and the best match of 2°C global to CONUS

[42] https://www.epa.gov/cira/social-vulnerability-report

warming (FrEDI-SV). Differences in arrival time (i.e., year where 2°C is reached) between the global and CONUS projections cause minor discrepancies between the two impact estimates.

2. Changes in the distribution of sub-regional populations overtime. The SV Report used static population from the Bureau of the Census American Community Survey (ACS) centered on 2016 at the spatial scale appropriate for each sector (county, tract, etc.). FrEDI-SV, however, uses user-supplied regional population projections and disaggregates them to the county level using ratios calculated from ICLUSv2 projections (to downscale to state from region and then to county from state). These county-level ratios change over time with the ICLUS projections. The county populations are then further disaggregated to the tract level using static current-day ratios calculated from the same ACS data used in the SV report (tract/county). This second set of ratios is static and does not change over time.

TABLE D-4. COMPARISON OF PROJECTED CHANGES IN ANNUAL CHILDHOOD ASTHMA DIAGNOSES DUE TO CLIMATE-DRIVEN EFFECTS ON PM2.5

Comparison of results from FrEDI-SV module from FrEDIv3.4 (FrEDI-SV below) to results reported in EPA's Climate Change and Social Vulnerability report (SV Report – Table 3.3 on page 26), for 2 degrees of global warming (GMAT). Difference between the estimates is also shown.

Region	Number of New Childhood Asthma Diagnoses Per Year		
	2 Degree FrEDI-SV	2 Degree SV Report	Difference
Midwest	-1,100	-1,100	0
Northeast	520	450	70
Northern Plains	-69	-75	6
Northwest	120	130	10
Southeast	1,900	2,000	100
Southern Plains	50	40	10
Southwest	1,000	1,000	0
National Total	2,500	2,500	0

Note: All estimates rounded to two significant figures.

Figure D-2 shows the comparison of the **difference in risk** of currently living in a location projected to experience large changes in climate-driven changes in air quality, for overburdened populations relative to their reference populations at two degrees warming. Similar to the rates metric comparison in Table G-3, the results show good but not exact replication, owing to the previously mentioned differences in county and tract level populations. Differences between the results for the No High School Diploma category highlight a difference in methodological choice rather than a replication error. In FrEDI-SV, because the calculations for this endpoint measure impacts on children, the 65 and Older and No High School diploma groups are omitted. In the SV Report, the 65 and Older category was omitted, but the No High School Diploma category result was reported and discussed as a potential indicator of household overburdened status.

FIGURE D-2. COMPARISON OF DIFFERENCE IN RISK FOR CHILDHOOD ASTHMA DIAGNOSES DUE TO CLIMATE-DRIVEN EFFECTS ON PM2.5

Comparison of results from FrEDI-SV module from FrEDIv3.4 (Panel A below) to results reported in EPA's Climate Change and Social Vulnerability report (Panel B below – see SV Report – Figure 3.4 on page 27), for 2 degrees of global warming (GMAT).

A. FREDI-SV

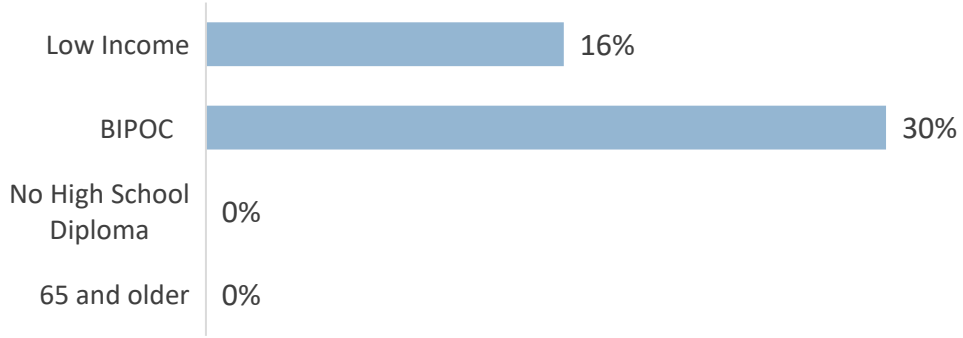

B. SV REPORT

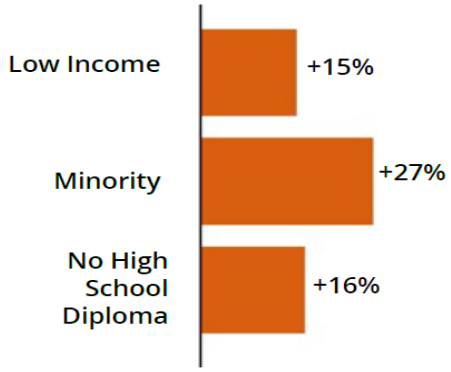

The tests highlight the population-driven differences discussed above. However, additional offline tests of FrEDI with external population inputs do provide an exact replication with the SV Report values, therefore confirming that while FrEDI-SV module uses the same treatment of regional population projections as the main module, it is consistent with the effect and relative patterns/magnitudes between regions and across scenarios when comparing to the SV report.

D.9 Guidance on interpreting results

It is important to note that while there is a growing body of literature revealing the abundance of historical and current disproportionate impacts from climate-driven hazards, FrEDI-SV does not include these historical (baseline) disproportionate impacts. FrEDI estimates the impacts of climate change relative to a baseline. In that process, the historical (or baseline) impacts are effectively a starting point for incremental analysis, and are controlled for in the projection results. The FrEDI-SV module also follows this approach, focusing on the disproportionality of climate change impacts relative to the baseline impacts. In doing so,

the historical disproportionality of impacts has also been removed and is not the focus of the module. For example, it has been shown that low-income communities are more at risk of both riverine (inland) and coastal flooding (e.g., Wing et al. 2022[43]). The impacts evaluated in the FrEDI-SV for flood risk to homes (both inland and coastal) exclude these historical disproportionate impacts by subtraction, and instead focus on where flood risks are increasing or decreasing compared to historical risk, and by how much. While baseline conditions can have an impact on the vulnerability to changes in flood risk, (e.g., a home in the current floodplain is more vulnerable to increases in flood occurrence or magnitude than a home outside the floodplain), changes in climatic conditions drive the *direction* (positive or negative) as well as magnitude of future change in flood risk.

For this reason, we encourage users of the FrEDI-SV tool to carefully examine the absolute risk results for the baseline scenario and policy scenarios applied in the module, as well as the incremental changes in risk, at both the national and regional scale, to best understand the dynamics of how risks to specific populations change over time. Careful consideration of the full range of results from FrEDI-SV can enhance the interpretation of results for policy analysts and decision-makers as well as for external and public constituencies who may be key audiences for these analyses.

[43] Wing, O.E.J., Lehman, W., Bates, P.D. et al. Inequitable patterns of US flood risk in the Anthropocene. Nat. Clim. Chang. 12, 156–162 (2022). https://doi.org/10.1038/s41558-021-01265-6

APPENDIX E | UPDATE REVISION LOG

This revision log provides a list of changes made to the peer-reviewed FrEDI documentation since the 2024 Peer-Review as EPA document EPA 430-R-24-001.

TABLE E-1. FREDI DOCUMENTATION REVISION LOG

Revision Date	Location of Revision in Documentation	Brief Description of Change and Rationale
		[to be filled in as edits to documentation are made after 2024 final publication]

FIGURE E-1. COMPARISON OF 2090 ANNUAL DAMAGES FOR GCAM REFERENCE SCENARIO ($BILLIONS)

Annual damages in 2090 by FrEDI version, for temperature changes from the GCAM reference scenario (ESC3) with FrEDI default GDP and populations. Results are intended to illustrate differences between code versions only. Differences in total values across versions are driven by an update in the default income elasticity for VSL growth (0.4 in FrEDI 3.4 and 1.0 in FrEDI 4.0), used for valuation in many health category sectors. A change in damage function extrapolation methodology causes a slight decrease in non-health impacts. Damages here reflect the sub-set of climate-related damages currently included within FrEDI and do not provide a comprehensive accounting of all climate-related damages to the U.S. This figure will be updated as new code versions are released.